ผลของเคอร์คิวมินต่อปฏิสัมพันธ์ระหว่างเม็ดเลือดขาวกับเอ็นโดทีเลียมในหนูแรทที่เกิดแผลกระเพาะอาหารจากยาต้านการอักเสบที่ไม่ใช่สเตียรอยด์

นางสาว สกลวรรณ ชูช่วย

วิทยานิพนธ์นี้เป็นส่วนหนึ่งของการศึกษาตามหลักสูตรปริญญาวิทยาศาสตรมหาบัณฑิต
สาขาวิชาสรีรวิทยา (สหสาขาวิชา)
บัณฑิตวิทยาลัย จุฬาลงกรณ์มหาวิทยาลัย
ปีการศึกษา 2552

EFFECT OF CURCUMIN ON LEUKOCYTE-ENDOTHELIUM INTERACTION IN RATS WITH NONSTEROIDAL ANTI-INFLAMMATORY DRUGS INDUCED PEPTIC ULCER

Miss Sakonwan Chuchuai

A Thesis Submitted in Partial Fulfillment of the Requirements
for the Degree of Master of Science Program in Physiology
(Interdisciplinary Program)
Graduate School
Chulalongkorn University
Academic Year 2009

Thesis Title	Effect of curcumin on leukocyte-endothelium interaction in rats with nonsteroidal anti-inflammatory drugs induced peptic ulcer
By	Miss Sakonwan Chuchuai
Field of Study	Physiology
Thesis Advisor	Associate Professor Duangporn Thong-Ngam, M.D.
Thesis Co-Advisor	Associate Professor Suthiluk Patumraj, Ph.D.

Accepted by the Graduate School, Chulalongkorn University in Partial Fulfillment of the Requirements for the Master's Degree

..... Dean of the Graduate School

(Associate Professor Pornpote Piumsomboon,Ph.D.)

THESIS COMMITTEE

..... Chairman

(Associate Professor Prakong Tangpraprutigul, Ph.D.)

..... Thesis Advisor

(Associate Professor Duangporn Thong-Ngam, M.D.)

..... Thesis Co-Advisor

(Associate Professor Suthiluk Patumraj, Ph.D.)

..... Examiner

(Associate Professor Pisit Tangkijvanich, M.D.)

..... External Examiner

(Bubpha Pornthisarn, M.D.)

สกลวรรณ ชูช่วย : ผลของเคอร์คิวมินต่อปฏิสัมพันธ์ระหว่างเม็ดเลือดขาวกับเอ็นโดทีเลียมในหนูแรทที่เกิดแผลกระเพาะอาหารจากยาต้านการอักเสบที่ไม่ใช่สเตียรอยด์. (Effect of curcumin on leukocyte-endothelium interaction in rats with nonsteroidal anti-inflammatory drugs induced peptic ulcer) **อ. ที่ปรึกษาวิทยานิพนธ์หลัก : รศ. พญ. ดวงพร ทองงาม, อ. ที่ปรึกษาวิทยานิพนธ์ร่วม : รศ.ดร. สุทธิลักษณ์ ปทุมราช, 104 หน้า.**

ยาต้านการอักเสบที่ไม่ใช่สเตียรอยด์ ทำให้เกิดผลข้างเคียงต่อระบบทางเดินอาหาร โดยเฉพาะแผลกระเพาะอาหาร เคอร์คิวมินเป็นสารออกฤทธิ์จากขมิ้นชัน ซึ่งมีฤทธิ์ต้านอนุมูลอิสระและต้านการอักเสบ การศึกษาครั้งนี้เพื่อหากลไกที่เป็นไปได้ของเคอร์คิวมินที่สามารถลดการเกิดแผล และการอักเสบของกระเพาะอาหารจากยาต้านการอักเสบที่ไม่ใช่สเตียรอยด์ในหนูแรท โดยทำการทดลองในหนูแรทเพศผู้สายพันธุ์ Spraque-Dawley แบ่งเป็น 3 กลุ่ม โดยกลุ่มควบคุม ได้รับน้ำมันมะกอก 0.5 มิลลิลิตร 30 นาทีก่อนได้รับ 5% $NaHCO^-_3$ 1 มิลลิลิตร จำนวน 2 ครั้ง เวลาห่างกัน 4 ชั่วโมง และกลุ่มยาต้านการอักเสบที่ไม่ใช่สเตียรอยด์ ได้รับน้ำมันมะกอก 0.5 มิลลิลิตร 30 นาทีก่อนได้รับยาอินโดเมธาซิน ขนาด 150 มิลลิกรัม/กิโลกรัม ซึ่งละลายใน 5% $NaHCO^-_3$ 1 มิลลิลิตร จำนวน 2 ครั้ง เวลาห่างกัน 4 ชั่วโมง และกลุ่มเคอร์คิวมินได้รับเคอร์คิวมินขนาด 200 มิลลิกรัม/กิโลกรัม ละลายในน้ำมันมะกอก 0.5 มิลลิลิตร 30 นาทีก่อนได้รับยาอินโดเมธาซินขนาด 150 มิลลิกรัม/กิโลกรัม ซึ่งละลายใน 5% $NaHCO^-_3$ 1 มิลลิลิตร จำนวน 2 ครั้ง เวลาห่างกัน 4 ชั่วโมง ทาง Intragastric หลังจากนั้น 8 ชั่วโมงครึ่งทำการศึกษาการเกาะติดของเม็ดเลือดขาวที่ผนังหลอดเลือดกระเพาะอาหาร เมื่อสิ้นสุดการทดลองเก็บตัวอย่างเลือด และชิ้นเนื้อกระเพาะอาหาร ผลการทดลองในกลุ่มยาต้านการอักเสบที่ไม่ใช่สเตียรอยด์ พยาธิสภาพของกระเพาะอาหารเกิดแผลกระเพาะอาหารและมีการอักเสบ พบระดับของไอแคมวันสูงขึ้น และมีการเกาะติดของเม็ดเลือดขาวที่ผนังหลอดเลือดสูงขึ้นอย่างมีนัยสำคัญทางสถิติเปรียบเทียบกับกลุ่มควบคุม และระดับของทีเอ็นเอฟแอลฟ่ามีแนวโน้มสูงขึ้น ส่วนกลุ่มเคอร์คิวมินพบการอักเสบกระเพาะอาหารดีขึ้น มีการลดลงของจำนวนแผล ลดระดับของไอแคมวันที่เพิ่มขึ้น และลดการเกาะติดของเม็ดเลือดขาวที่ผนังหลอดเลือด ระดับของทีเอ็นเอฟแอลฟ่ามีแนวโน้มลดลง สรุปผลการทดลองเคอร์คิวมินสามารถลดการเกิดแผลกระเพาะอาหารและการอักเสบจากยาต้านการอักเสบที่ไม่ใช่สเตียรอยด์ โดยลดระดับของไอแคมวัน และลดการเกาะติดของเม็ดเลือดขาวที่ผนังหลอดเลือด

สาขาวิชา..... สรีรวิทยา.....ลายมือชื่อนิสิต.....สกลวรรณ ชูช่วย.....

ปีการศึกษา..... 2552.....ลายมือชื่อ อ.ที่ปรึกษาวิทยานิพนธ์หลัก.....

ลายมือชื่อ อ.ที่ปรึกษาวิทยานิพนธ์ร่วม.....

4989197720 : MAJOR PHYSIOLOGY

KEYWORDS : NONSTEROIDAL ANTI-INFLAMMATORY DRUGS / CURCUMIN / GASTRIC MICROCIRCULATION / TNF-α / ICAM-1

SAKONWAN CHUCHUAI : EFFECT OF CURCUMIN ON LEUKOCYTE-ENDOTHELIUM INTERACTION IN RATS WITH NONSTEROIDAL ANTI-INFLAMMATORY DRUGS INDUCED PEPTIC ULCER. THESIS ADVISOR : ASSOC. PROF.DUANGPORN THONG-NGAM, M.D., THESIS CO-ADVISOR : ASSOC. PROF. SUTHILUK PATUMRAJ, Ph.D., 104 pp.

Nonsteroidal anti-inflammatory drugs induce gastric injury. Curcumin, the active ingredient of *Curcuma longa Linn.*, is a potent antioxidant and anti-inflammation. The present study determined the possible mechanism that curcumin could attenuate gastric injury induced by nonsteroidal anti-inflammatory drugs in rats. Male Sprague-Dawley rats were divided into three groups. Control group was fed olive oil 0.5 ml 30 minute prior to 5% $NaHCO^-_3$ 1 ml at time 0^{th}, 4^{th} hr. NSAIDs group was fed olive oil 0.5 ml 30 minute prior to indomethacin (150 mg/kg BW day twice day) dissolved in 5% $NaHCO^-_3$ 1 ml at time 0^{th}, 4^{th} hr. Pretreatment group was fed curcumin 200 mg/kg BW dissolved in olive oil 0.5 ml 30 minute prior to indomethacin 150 mg/kg BW dissolved in 5% $NaHCO^-_3$ 1 ml at time 0^{th}, 4^{th} hr. After 8^{th} hours 30 min, the leukocyte adherence of post-capillary venule in stomach was studied by intravital fluorescence microscopy then rats were sacrificed. The serum and stomach samples were collected at the end of the study. The stomach histopathology in indomethacin group showed multiple erosions with mild to moderate inflammation. Serum of ICAM-1 level and leukocyte-endothelium interaction increased significantly when compared with control group. Pretreatment with curcumin group resulted in decreasing the elevation serum of ICAM-1 level and leukocyte-endothelium interaction. In conclusion, curcumin could attenuate gastric injury induced by nonsteroidal anti-inflammatory drugs through the reduction of ICAM-1 level and leukocyte-endothelium interaction of gastric microcirculation.

Field of Study : Physiology Student's Signature Sakonwan Chuchuai

Academic Year : 2009 Advisor's Signature

Co-Advisor's Signature

ACKNOWLEDGEMENTS

I would like to express my sincere gratitude to my advisor, Associate Professor Duangporn Thong-Ngam and my co-advisor, Associate Professor Suthiluk Patumraj for their excellent instruction, guidance, encouragement, and constructive criticism which enable me to carry out my study successfully.

I am deeply beholden to Assistant Professor Naruemon Klaikeaw for histopathological examination.

Furthermore, my grateful is extended to members of the thesis committee for their valuable comments and the correction of this thesis.

Finally, I am thankful to my family and my friends for their loves and supports during this educational experience.

This study had a financial support from Grant of Ratchadaphiseksomphot, Faculty of Medicine, Chulalongkorn University, Bangkok, Thailand.

CONTENTS

PAGE

THAI ABSTRACT……iv

ENGLISH ABSTRACT……v

ACKNOWLEDGEMENTS……vi

CONTENTS……vii

LIST OF TABLES……ix

LIST OF FIGURES……x

LIST OF ABBREVIATIONS……xii

CHAPTER I INTRODUCTION……1

CHAPTER II THEORY AND LITERATURE REVIEW……4

-The stomach ……4

-Blood supply……6

-Gastric circulation……6

-Nonsteroidal anti-inflammatory drugs ……8

-Pharmacokinetics……11

-Pathogenesis……11

-Leukocyte-endothelial cell adhesion……14

-Cyclooxygenase (COX)……15

-Tumor necrosis factor-alpha(TNF-α)……17

-Intercellular adhesion molecule-1 (ICAM-1)……18

-Mechanisms expression of adhesion molecules……19

-Curcumin (diferuloylmethane)……22

-Animal Models of NSAIDs-Induced gastric Injury……30

CHAPTER III MATERIALS AND METHODS……40

-Reagents……40

-Animal preparation……41

-Experimental Protocols……41

-Data Collection……42

-Data Analysis……54

CONTENTS

PAGE

CHAPTER IV RESULTS……55

CHAPTER V DISCUSSION AND CONCLUSION……78

REFERENCES……84

APPENDICES……96

-APPENDIX A……97

BIOGRAPHY……104

LIST OF TABLES

TABLE PAGE

1 Summary of infiltration of inflammatory cells and erosion in all groups (model 1).....31

2 Summary of infiltration of inflammatory cells and erosion in all groups (model 2).....33

3 Summary of infiltration of inflammatory cells and erosion in all groups (model 3).....36

4 ELISA data (TNF-α).....50

5 ELISA data (ICAM-1).....53

6 Summary of infiltration of inflammatory cells and erosion in all groups.....62

7 Summary of Mean leukocyte adhesion in all groups 66

8 Summary of Mean leukocyte adhesion in all groups 67

9 Summary of Mean leukocyte adhesion in all groups 69

10 Hemodynamic.....71

11 ELISA (TNF-α).....72

12 Summary of serum of TNF-α 73

13 ELISA (ICAM-1).....75

14 Summary of serum of ICAM-1.....76

LIST OF FIGURES

FIGURE PAGE

1 Anatomy of stomach ……..……..……..4

2 Structure of gastric wall ……..……5

3 Blood supply of the stomach……..…..6

4 Schematic representation of microvasculature in gastric wall ….……..…..8

5 NSAIDs classification ……..…….....9

6 Mechanism of nonsteroidal anti-inflammatory drugs ……..…….....10

7 Mechanism of nonsteroidal anti-inflammatory drugs (COX inhibitor)……..…….....11

8 Local effect of NSAIDs induced gastric ulcer ……..……...12

9 Nonsteroidal anti-inflammatory drugs induced gastric injury ……..……..……..…….....13

10 Steps in the recruitment of leukocytes in postcapillary venules……..…..15

11 Comparison of the domain structures of PGHS-1/COX-1 and PGHS-2/COX-2……..16

12 Schematic of regulatory COX-1 and COX-2 gene promoters……..…..17

13 TNF-receptor and ligand……..…….....18

14 Structure and regulation of the ICAM-1 promoter……..……..19

15 Mechanisms the expression of adhesion molecules……..…..21

16 Chemical structure of curcumin……..……..25

17 Regulation transcription of NF-κB ……..……..27

18 Absorption and metabolism of curcumin……..29

19 Histopathology of stomach were fed indomethacin in normal saline……..…..32

20 Histopathology of stomach were fed indomethacin in 5% sodium bicarbonate.....34

21 Histopathology of stomach were fed IMN in 5% sodium bicarbonate (continue).....35

22 Histopathology of stomach were fed IMN in 5% sodium bicarbonate twice day.....37

23 Histopathology of stomach were fed IMN in 5% sodium bicarbonate twice day.....39

24 Diagram of experimental design……..……42

LIST OF FIGURES (continue)

FIGURE PAGE

25 Study of leukocyte- endothelium interaction on gastric microcirculation……..45

26 Intravital fluorescent microscopy and instruments……..46

27 Image analysis……..47

28 Standard curve of TNF-α……..50

29 Standard curve of ICAM-1……53

30 Histopathology in control group……..57

31 Histopathology in NSAIDs group……58

32 Histopathology in NSAIDs group (continue)……59

33 Histopathology in curcumin group……..60

34 Histopathology in curcumin group……..61

35 Intravital microscopic in control group……..63

36 Intravital microscopic in NSAIDs group.....64

37 Intravital microscopic in curcumin group.....65

38 Mean leukocyte adhesion.....68

39 Mean leukocyte adhesion.....70

40 Standard curve of TNF-α……..72

41 Serum TNF-α level.....74

42 Standard curve of ICAM-1……..75

43 Serum ICAM-1 level.....77

LIST OF ABBREVIATIONS

AP-1	Activator protein-1
BW	Body weight
^{o}C	Degree Celsius
cm	Centimeter
CVs	Collecting venules
DBP	Diastolic blood pressure
ELAM-1	Endothelial-leukocyte adhesion molecule-1
ELISA	Enzyme-linked immunosorbent assay
eNOS	Endothelial nitric oxide synthase
ERK	Extracellular signal-regulated kinase
g	Gram
G	Gravity
H_2O_2	Hydrogenperoxide
H&E	Hematoxylin and Eosin
HR	Heart rate
ICAM-1	Intercellular adhesion molecule-1
IκB	NF-κB inhibitor
IKK	NF-κB inhibitor-kinase
IL	Interleukin
ip	Intraperitoneal injection
JNK	c-Jun N-terminal kinase
kg	Kilogram
LPS	Lipopolysaccharide
m	Meter
MA	Muscle arteriole
MAP	Mean arterial blood pressure

LIST OF ABBREVIATIONS (Continue)

MC	Muscle capillary
MEK	Mitogen-activated protein kinase/Extracellular signal-regulated kinase
mg	Milligram
mmHg	Millimeter of mercury
MTA	Mucosal terminal arterioles
MV	Muscle venules
NF-κB	Nuclear factor-kappa B
O^-_2	Superoxide radical
OH^-	Hydroxyl radical
O.D.	Optical density
PCVs	Postcapillary venules
PGE_2	Prostaglandin E_2
pg/ml	Picogram per milliliter
ROS	Reactive oxygen species
SD	Standard deviation
SA	Small arteries
SBP	Systolic blood pressure
SMA	Submucosal arterioles
SMV	Submucosal venules
SOD	Superoxide dismutase
SV	Small veins
TNF-α	Tumor necrosis factor-alpha
µl	Microliter
µm	Micrometer

CHAPTER I

INTRODUCTION

Background and Rationale

The use of salicylates in therapeutic practice early in the 20th century gave rise to anecdotal reports of their side effects on the stomach, and these have remained an important feature of the use of anti-inflammatory analgesics since that time. Substantial evidence collected over that past 25 years from clinical studies, both patient trials and retrospective surveys, have indicated that chronic use of aspirin and nonsteroidal anti-inflammatory drugs (NSAIDs) gives rise to serious iatrogenic effects in the gastrointestinal (GI) tract. These include the development of haemorrhage and ulcers in a significant proportion of the patient population. Major epidemiological studies have documented the increasing of serious gastropathy over the period since the nonaspirin NSAIDs were introduced into clinical practice (Fries et al., 1989; Langman et al.,1994).

The continued world-wide growth on the use of these products for analgesic and anti-inflammatory utilities has led to substantial problems over 100000 hospitalizations and 17000 deaths per year in the US alone have been estimated. The financial significance of such side-effects on health care budgets is therefore enormous, while the clinical risk of serious side-effects from these NSAIDs is an important factor in long term therapy, especially in the elderly. Moreover, even the use of low dose aspirin for cardiovascular protection, which is becoming ever more popular, is associated with an elevated risk of bleeding and ulceration in the gut (Brendan, 2002).

A study published in 1969 showed that aspirin induces topical injury in the dog stomach (Davenport, 1969). Subsequently, Fromm (Fromm, 1987) reported that acidic NSAIDs can directly damage the gastric epithelium by intracellular accumulation of these drugs in an ionized state, an occurrence known as ion trapping. However, the fact that enteric- coated formulation, pro-drugs or systemic administration of NSAIDs did not reduce the frequency of gastroduodenal ulcerations implies a minor role for topical injury (Kelly et al., 1996). There might be other mechanisms by which NSAIDs induce topical injury. Lichtenberger and colleagues (Lichtenberger et al., 1995) showed that

NSAIDs reduce the hydrophobicity of the mucus gel layer by changing the action of surface active phospholipids. By preassociating an NSAIDs with zwitterionic phospholipids, the complex has proved to restore the mucus hydrophobicitty and reduce acute gastric injury, without losing its effectiveness (Lichtenberger et al., 1995).

Since Vane's discovery (Vane, 1971) in 1971 that NSAIDs act by the inhibition of prostaglandin synthesis, there is substantial evidence that the ulcerogenic effect of an NSAIDs correlates well with its ability to suppress prostaglandin synthesis (whittle, 1981; Rainsford and Willis, 1982). Endogenous prostaglandins regulate mucosal blood flow, epithelial cell proliferation, epithelial restitution, mucosal immunocyte function, mucus and bicarbonate secretion and basal acid secretion (Wallace, 1997). Inhibition of prostaglandin synthesis probably weakens the gastric mucosal defence to resist luminal irritants. Although inhibition of prostaglandin synthesis is a major mechanism in the ulcerogenic effect of NSAIDs, it is not the only factor. Mice with defective gastric prostaglandin synthesis did not spontaneously develop gastric ulceration (Langenbach et al., 1995).

Results from animal studies show strong evidence that neutrophil adherence to the endothelium of gastric microcirculation is critical in NSAIDs injury (Wallace et al., 1990). Neutrophil adherence damages the mucosa by liberating oxygen-free radicals, releasing proteases, and obstructing capillary blood flow. NSAIDs might induce the synthesis of tumour necrosis factor- alpha (TNF-α) and leukotrienes, (Appleyard et al., 1996; Rainsford, 1983) and these inflammatory mediators stimulate neutrophil adherence by up-regulation of adhesion molecules (Andrews et al., 1994).

Curcuma, a genus in the plant family of Zingiberacea,is the biological source for curcuminoids, including curcumin. Curcuma longa, the yellow tuberous root that is referred to as turmeric, was taken from India to Southeast Asia. It possesses a broad range of pharmacological activities including antioxidant, anti- carcinogenic and anti-inflammatory effects (Toda et al., 1985). There are currently limited studies investigating the effect of curcumin on NSAIDs- induced gastric mucosal injury in the part of gastric microcirculation.

Research Questions

Can curcumin attenuate leukocyte-endothelium interaction in gastric microcirculation and change histopathology with nonsteroidal anti-inflammatory drugs-induced gastric injury in rats?

Research Ojectives

1. To study the effects of curcumin on leukocyte-endothelium interaction in gastric microcirculation with nonsteroidal anti-inflammatory drugs- induced gastric injury in rats.
2. To study the effects of curcumin on serum TNF-α level with nonsteroidal anti-inflammatory drugs- induced gastric injury in rats.
3. To study the effects of curcumin on serum ICAM-1 level with nonsteroidal anti-inflammatory drugs- induced gastric injury in rats.
4. To study the effects of curcumin on histopathological changes with nonsteroidal anti-inflammatory drugs- induced gastric injury in rats.

Hypothesis

Curcumin has an attenuating effect on leukocyte-endothelium interaction of gastric microcirculation, serum TNF-α level, serum ICAM-1 level and changes histopathology with nonsteroidal anti-inflammatory drugs induced gastric injury in rats.

Expected Benefit and Application

Experimental data would give known effects of curcumin on leukocyte-endothelium interaction in gastric microcirculation, serum TNF-α level, serum ICAM-1 level and changes histopathology with nonsteroidal anti-inflammatory drugs induced gastric injury in rats and applied for treatment in patients with NSAIDs induced gastric injury.

CHAPTER II

THEORY AND LITERATURE REVIEW

The stomach

The stomach (Figure 1) is a J-shaped tube, with two openings, lining between the esophagus and the duodenum. The lesser curvature of the stomach extends the short distance from the esophagus to duodenum along the medial to superior aspect, while the greater curvature extends the longer distance on the lateral to inferior aspect. The stomach has distinct anatomical subdivisions that have functional differences. First, the cardia is a small area presently inside the cardiac opening. Next, the fundus and body (corpus) are the main parts of the stomach. The fundus consists of the dome of the stomach. They secrete hydrochloric acid and enzymes involved in the digestion of food such as pepsinogen. Last, the pyloric region is subdivided into antrum, pyloric cannal, and pyloric sphincter. This region occupies the distal end of the stomach is responsible for mucus, gastrin, and pepsinogen secretion (Thomson et al., 1992). The antrum contains cells that sense pH and secrete hormones (such as somatostatin and gastrin) that regulate acid production in the fundus.

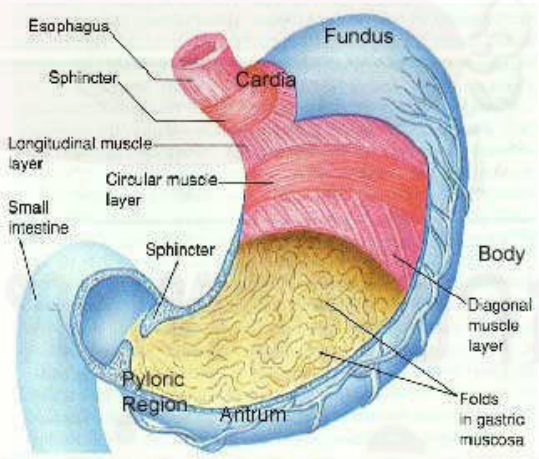

Figure 1 Anatomic structure of stomach : The body part of the stomach was used to observe leukocyte- endothelium interaction in gastric microcirculation. (http://missinglink.ucsf.edu/lm/IDS_106_UpperGI/Upper%20GI/stomach.htm)

The wall of the stomach has four layers (Figure 2) consisting of mucosa, submucosa, muscularis propria, and serosa.

The mucosa, surface of the stomach, is made up of epithelium and surrounding connective tissues called the lamina propria. The epithelium contains different types of cells which secrete compounds to aid digestion and stomach protection. The lamina propria contains the supporting framework, such as capillary network and nerve fibers, for the epithelial cells.

The submucosa is consists of the loose connective tissues in which are embedded lymphatic vessels, blood vessels, and scattered mononuclear cells including mast cells.

The muscularis propria is composed of three layers of smooth muscles: the outer-lumen longitudinal muscles, middle circular muscles, and inner-lumen oblique muscles. The nerves and ganglion cells are located between the outer longitudinal and middle circular muscle layers.

The serosa is a thin covering of loose connective tissues with blood vessels, lymphatic vessels, and nerve fibers. This layer is contiguous with the omentum and ligaments attaching the stomach to spleen and liver.

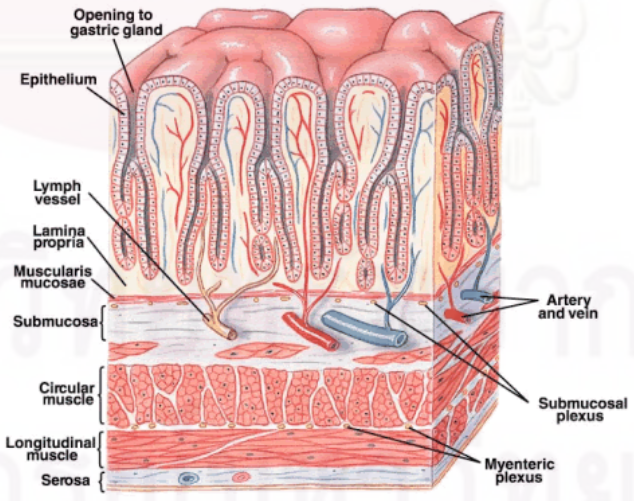

Figure 2 Structure of gastric wall

(www.mybodyindex.com/m-stomach.php)

Blood supply of the stomach

The postcapillary venules (PCVs) of the stomach selected in this study are located on the muscle.

The stomach has rich network of anastomosing vessels derived from the various branches of the celiac trunk and originated from the anterior surface of the thoracic aorta just below the aortic hiatus. The celiac trunk is a short vessel that divides into three arteries (Figure 3): the left gastric artery, the splenic artery and the common hepatic artery. Each of these parts supplies a portion of the stomach. The left gastric artery supplies the fundus and left superior portion of the lesser curvature. The splenic artery gives rise to the short gastric arteries that serve to the fundus and body along the greater curvature of the stomach. Moreover, the right and left gastroepiploic arteries also form an anastomosis along the greater curvature. Last supplier, the common hepatic artery gives rise to the gastroduodenal artery and the right gastric artery that contribute the inferior lesser curvature of the stomach.

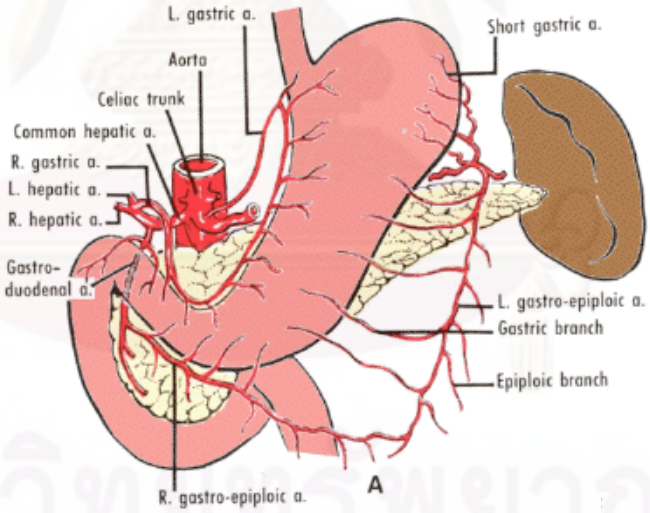

Figure 3 Blood supply of the stomach

Gastric circulation

The circulation of the gastric wall has arrangement, which has branching hierarchy and relative dimensions. The posterior branch of the left gastric artery gives rise to series of long vessels supplying the posterior corpus. These vessels pierce the

external muscle layers at the lesser curvature near the cardia and run under the muscle coat in the superficial submucosa radially toward the greater curvature. These small arteries (SA) is (89± 2.1 μm) form the main submucosal arteriole-arterial anastomotic plexus or primary arcade of submucosal arterioles (SMA1). In turn, these vessels form smaller and smaller branches, which interconnect with each other and the parent vessels forming a secondary (SMA2) and a tertiary (SMA3) arcade of submucsal arterioles. The SMA3 gives rise to small mucosal terminal arterioles (MTA) which run perpendicularly through the muscularis mucosae and, on entering the mucosa, divide into the hexagonal mucosal capillary plexus. Collecting veins (CVs) run perpendicularly through the mucosa. Within the deeper mucosa they drain into the venous anastomosis, which, on entering the muscularis mucosae, gives rise to the secondary arcade of submucosal venules (SMV2). Interestingly, CVs were larger in diameter (36.4 ± 1.1 μm) than the deeper mucosal venous anastomosis (31.5 ± 1.3 μm) or the initial part of SMV2. The SMV2 enter the primary arcade of submucosal venules (SMV1), which follow the same course as the primary arterioles and return blood to the small veins (SV). The SV run parallel with SA, penetrated the external muscle layers, and leave the superficial submucosa (Peti-Peterdi et al., 1998).

Therefore, PCVs (15-25 μm) collect blood from muscle capillary and drain it into MV. Like other veins, there are leukocyte adhesion and fenestration during inflammation. These structures were selected to investigate the leukocyte-endothelium interaction induced by nonsteroidal anti-inflammatory drugs.

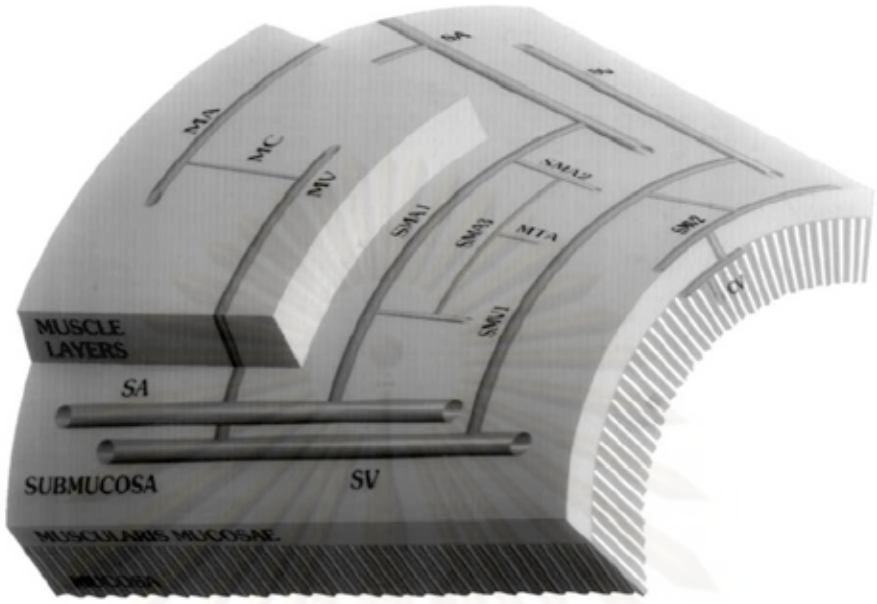

Figure 4 Schematic representation of microvasculature in gastric wall: Blood vessels were identified numerically according to their branching order and vascular hierarchy: small artery (SA), submucosal primary (SMA1), secondary (SMA2), and tertiary (SMA3) arterioles, mucosal terminal arteriole (MTA), collecting venule (CV), submucosal secondary (SMV2) and primary (SMV1) venules, muscle arteriole (MA), capillary (MC), and venule (MV), and submucosal small vein (SV). Common input and output of muscle and mucosal circulations are SMA1 and SMV1 (Peti-Peterdi et al., 1998).

Nonsteroidal anti-inflammatory drugs (NSAIDs)

Nonsteroidal anti-inflammatory drugs (NSAIDs) are the most commonly used drugs in inflammatory diseases, since they are effective in management of pain, fever, redness, edema arising as a consequence of inflammatory mediator release (Ferreira, 2002; Mitchell and Warner, 1999). Studies have show that both therapeutic and side effects of NSAIDs are dependent on cyclooxygenase (COX) inhibition (Warner et al., 1999). It has been suggested that COX-2 inhibition is responsible for the therapeutic effects of NSAIDs, while COX-1 inhibition causes the gastrointestinal side effects (Patrignani, 2000; Xie et al., 1991).

NSAIDs can be grouped in four categories:

1. Selective COX-1 inhibitors, such as aspirin
2. Non-selective COX inhibitors: a number of the NSAIDs examined exhibit COX-1/COX-2 IC_{50} ratio between 0.5 and 3.0 such as indomethacin
3. Relatively selective COX-2 inhibitors, such as diclofenac with COX-1/COX-2 IC_{50} ratio of 10-20
4. Highly selective COX-2 inhibitors comprising three experimental compounds with COX-1/COX-2 IC_{50} ratio of 140-250 and rofecoxib with the ratio>400 (Patrignani, 2000).

Tab. 1. COX isoform selectivity assessed in the whole blood assays *in vitro* by cyclooxygenase inhibitors (Reprinted with permission of Elsevier Ltd., [60])

Inhibitor	COX-1/COX-2 IC_{50} ratio	
Aspirin	0.01	
S-Indobufen	0.043	Selective COX-1 inhibitors
Valeryl Salicylate	<0.24	
Ibuprofen	0.50	
Naproxen	0.56	
S-Ketoprofen	0.61	
Flurbiprofen	1.00	Non-selective COX inhibitors
Sodium Salicylate	1.03	
6-MNA[a]	1.49	
Indomethacin	1.90	
Piroxicam	3.12	
Meloxicam	11.16	
Nimesulide	17.69	Relatively selective COX-2 inhibitors
Diclofenac	18.90	
SC-58125	143.30	
NS-398	168.00	Highly selective COX-2 inhibitors
L-745,337	246.00	
Rofecoxib	410.00	

[a] 6-MNA is the active metabolite of nabumetone

Figure 5 NSAIDs classification: selective COX-1 inhibitors, non-selective COX inhibitors, relatively selective COX-2 inhibitors and highly selective COX-2 inhibitors (Patrignani, 2000).

It is well-know that therapy with COX inhibitors is associated with a number of side effects including gastrointestinal erosions. Such critical adverse reactions are highly dependent on COX-1 inhibition (Burdan et al., 2004). The most common side effect of NSAIDs is gastrointestinal (GI) toxicity. Gastrointestinal toxicity has been attributed to the inhibition of the COX-1 mediated generation of the cytoprotective prostanoids, such as prostaglandin PGE_2 and PGI_2. GI system damage may very from hidden blood loss to ulcer perforation (Bjorkman, 1999).

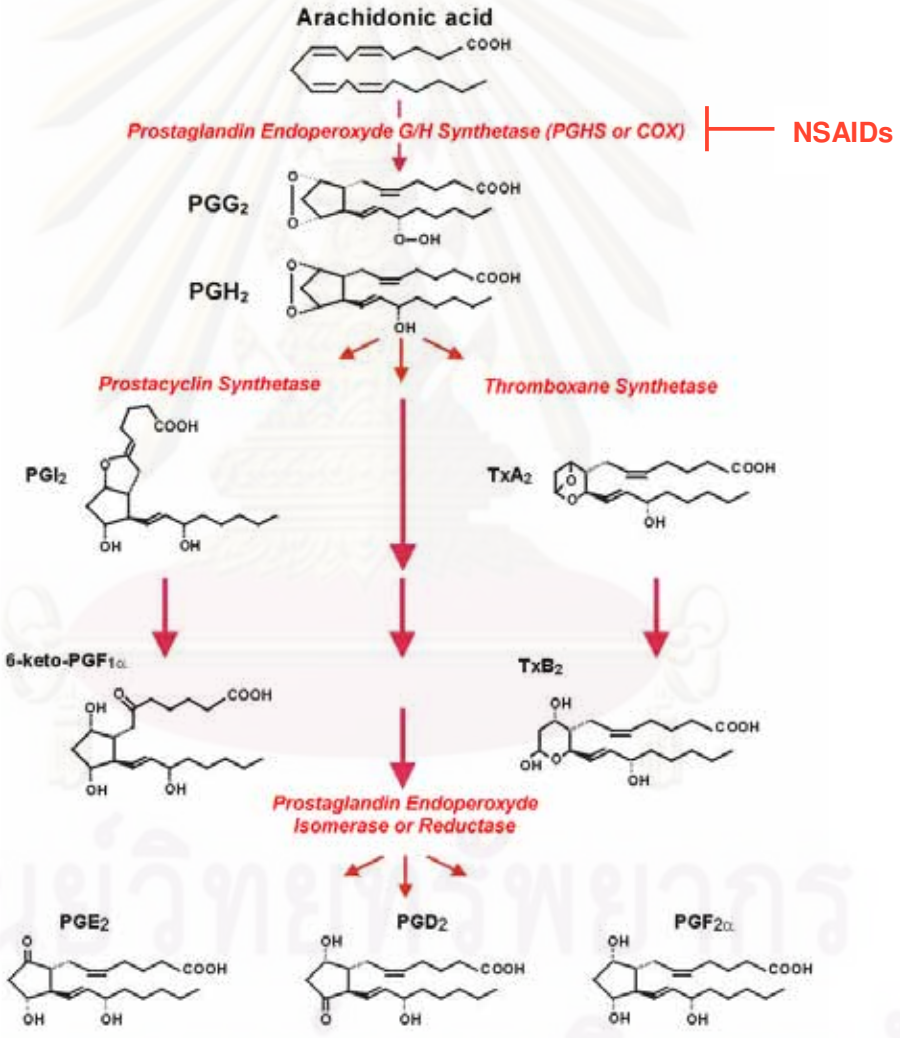

Figure 6 Mechanism of action: nonsteroidal anti-inflammatory drugs

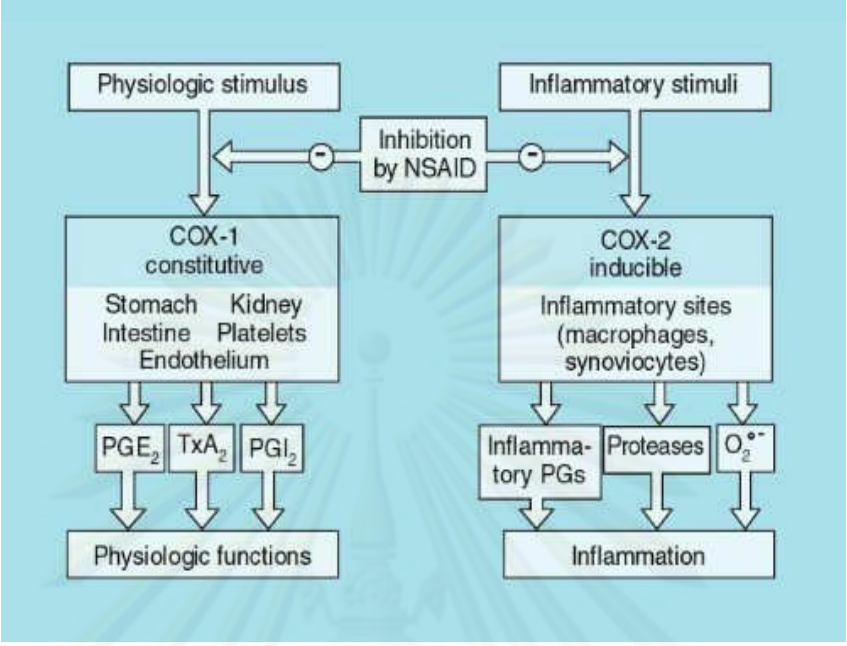

Figure 7 Mechanism of action: nonsteroidal anti-inflammatory drugs (COX inhibitors)

Pharmacokinetics

Most nonsteroidal anti-inflammatory drugs are weak acids, with a pKa of 3-5. They are absorbed well from the stomach and intestinal mucosa. They are highly protein-bound in plasma (typically >95%), usually to albumin, so that their volume of distribution typically approximates to plasma volume. Most NSAIDs are metabolized in the liver by oxidation and conjugation to inactive metabolites which are typically excreted in the urine, although some drugs are partially excreted in bile. Metabolism may be abnormal in certain disease states, and accumulation may occur even with normal dosage.

Pathogenesis of NSAIDs induced gastric injury

Nonsteroidal anti-inflammatory drugs (NSAIDs) are among the most commonly prescribed drugs worldwide. It is a well-known phenomenon that NSAIDs cause gastric mucosal damage resulting in outcomes ranging from nonspecific dyspepsia to ulceration, upper gastrointestinal (GI) bleeding and death – summarized by the term NSAID gastropathy. The mechanisms of NSAID-induced GI injury are not fully

understood. Topical damage occurs in acidic NSAIDs such as acetylic-salicylic acid (ASA) and includes the accumulation of ionized NSAID in the gastric epithelial cell called ion trapping effect (Davenport, 1967), the reduction of the hydrophobicity of the gastric mucosal surface (Lichtenberger, 1995) and uncoupling of oxidative phosphorylation (Jorgensen et al., 1976). Disruption of the epithelial barrier allows back-diffusion of acid into the mucosa.

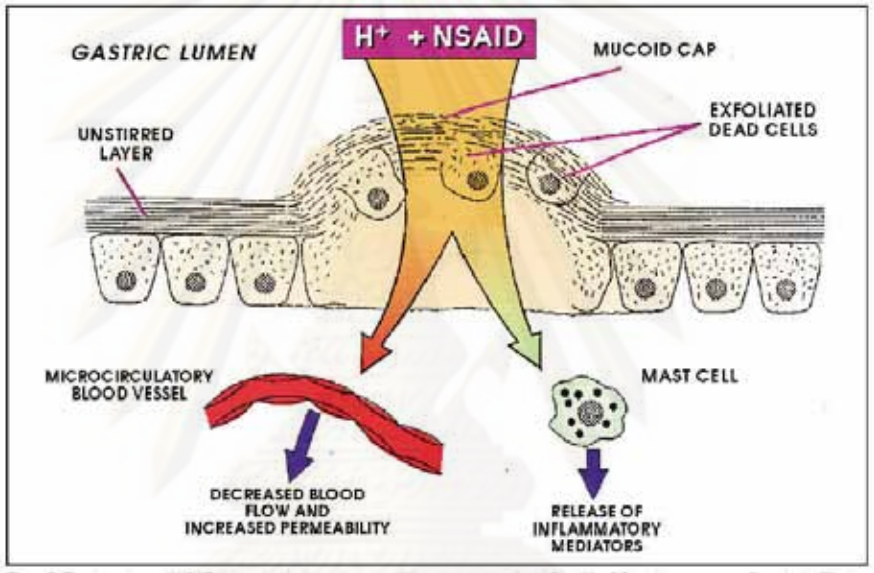

Figure 8 Local effect of NSAIDs induced gastric ulcer.

By inhibiting cyclo-oxygenases (COX) NSAIDs block the formation not only of proinflammatory but also of gastroprotective prostaglandins (Vane, 1971). This is a key element in NSAID gastropathy as prostaglandins maintain gastric mucosal blood flow and increase protective mucus as well as bicarbonate production. The discovery of two different cyclooxygenases led to the development of drugs preferentially inhibiting the COX-2 isoform, on the proposition that prostaglandins produced by the constitutively expressed COX-1 protect gastric mucosa, whereas the inducible isoform COX-2 is responsible for inflammation and pain. Inhibition of cyclo-oxygenases by NSAIDs is furthermore associated with an altered inflammatory mediator production. As a consequence of COX-inhibition enhanced synthesis of leukotrienes may occur by

shunting the arachidonic acid metabolism towards the 5-lipoxygenase pathway (Hudson et al., 1993; Vaananen et al., 1992; Martel-Pelletier et al., 2003). Leukotrienes are supposed to contribute to gastric mucosal injury by promoting tissue ischaemia and inflammation (Martel-Pelletier et al., 2003; Peskar, 1991). Increased expression of adhesion molecules such as intercellular adhesion molecule-1 (McCafferty et al., 1995; Andrews et al., 1994) by proinflammatory mediators such as tumour necrosis factor-alpha (Santucci et al., 1994) leads to an increased neutrophil endothelial adherence and activation (McCafferty et al., 1995). Wallace (Wallace, 1997) postulated that NSAIDs-induced neutrophil adherence might contribute to the pathogenesis of gastric mucosal damage by two principal mechanism: (i) occlusion of gastric microvessels by microthrombi leading to reduced gastric blood flow and ischaemic cell damage; (ii) increased liberation of oxygen-derived free radicals. Free oxygen radicals react with poly unsaturated fatty acids of the mucosa leading to lipid peroxidation and tissue damage.

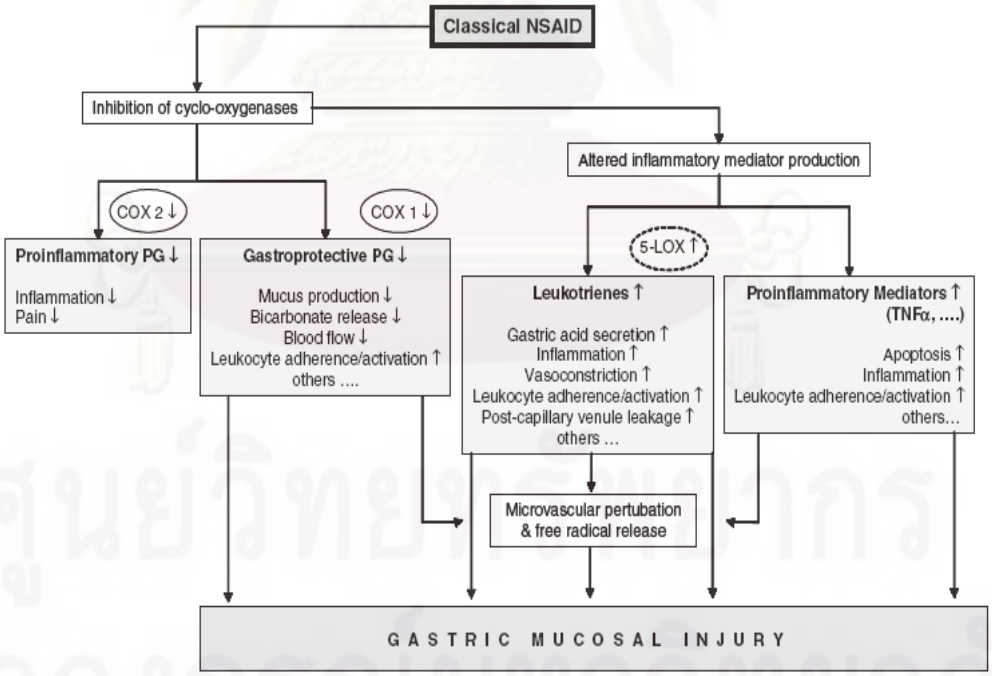

Figure 9 Nonsteroidal anti-inflammatory drugs induced gastric injury (Wallace, 1997).

Leukocyte-endothelial cell adhesion

Leukocyte-endothelial cell adhesion has been implicated in the pathogenesis of a variety of diseases that affect different organ systems. Examples of such diseases include atherosclerosis, gastric ulcers, haemorrhagic shock, myocardial infarction, stroke, and malaria (Korthuis et al., 1994; Panés et al., 1998). The recognition that leukocytes must firmly adhere to vascular endothelial cells in order to mediate the organ dysfunction and tissue injury associated with these diseases has resulted in an intensive effort to define the factors that modulate this cell-cell interaction. A major focal point of this effort has been directed towards identifying and characterizing the adhesion glycoproteins that enable leukocytes to bind to vascular endothelial cells. Data derived from both *in vitro* (isolated leukocytes binding to monolayers of cultured endothelial cells) and *in vivo* (intravital microscopic examination of venules) models of leukocyte-endothelial cell adhesion have revealed the relative contributions of different leukocyte and endothelial cell adhesion molecules (CAMs) to the adhesion responses elicited by various inflammatory stimuli. These studies have also led to an appreciation of the potential cellular and molecular loci that can be targeted to interfere with leukocyte-endothelial cell adhesion. As a result, there is a widely held view that several of these loci also represent novel and potentially powerful therapeutic sites for treatment of acute and chronic inflammatory diseases.

Adhesion molecules

Both leukocyte and endothelial CAMs participate in slowing the leukocyte as it exits the capillary and enters the postcapillary venule, which is the major site of leukocyte-endothelial cell adhesion. The initial low affinity interaction between leukocytes and venular endothelium is manifested as a rolling behaviour. Rolling leukocytes can then become firmly adherent (stationary) on the vessel wall, where the process of transendothelial leukocyte migration can occur if a chemotactic signal is generated in the perivascular compartment. Each of the three stages of leukocyte recruitment), i.e., rolling, firm adhesion (adherence) and transendothelial migration, involves the participation of different families of adhesion molecules, including the selectins, β-integrins and supergene immunoglobulins (Panés et al., 1999).

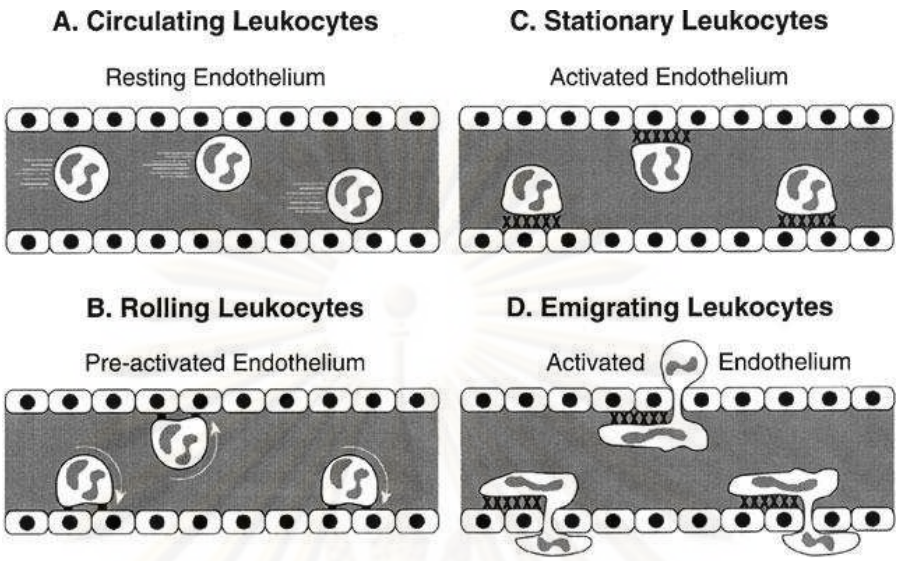

Figure 10 Steps in the recruitment of leukocytes in postcapillary venules. (A) illustrates that in the absence of an inflammatory stimulus, leukocytes are largely flowing in the stream of red cells with no adhesive interactions with venular endothelium. (B) illustrates the low affinity interaction between leukocytes and endothelium that is mediated by selectins and manifested as rolling. (C) illustrates that activation of leukocytes and/or endothelial cells can result in stationary adhesion of leukocytes. (D) illustrates that firmly adherent leukocytes can emigrate from venules into the adjacent interstitial compartment, usually along a chemotactic gradient (Panés et al., 1999).

Cyclooxygenase (COX)

Cyclooxygenases-1 and -2 (COX-1 and-2) convert arachidonic acid, hydrolyzed from cell memcrane phospholipids by a phospholipase A_2, to prostaglandin endoperoxide H_2 (PGH_2), the precursor of the prostanoids-thromboxane A_2 and the prostaglandins (PGD_2, PGE_2, $PGF_{2\alpha}$ และ PGI_2) (Smith, 2000; Rouzer, 2003). Nonsteroidal anti-inflammatory drugs (NSAIDs) are commonly used to treat inflammation, pain and fever, and these actions are generally attributed to inhibition of COX-2 (Masferrer, 1995). Prostanoids are lipid mediators that normally act in a paracrine and autocrine manner to coordinate intercellular events stimulated by a circulating hormone. Their over-

production is associated with pathologies such as tumorigenesis and arthritis whereas artherogenesis is associated with decreasd formation of certain prostanoids.

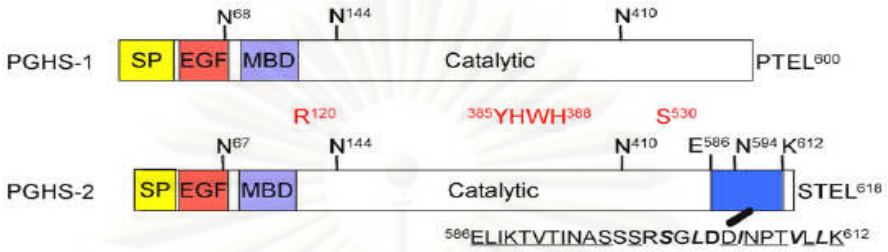

Figure 11 Comparison of the domain structures of PGHS-1/COX-1 and PGHS-2/COX-2 (Yeon-Joo et al., 2007)

COX-1 and COX-2 are the products of different genes (Smith, 2000). COX-1 is present in many but not all cell types and when present is usually expressed constitutively. COX-1 gene expression is developmentally controlled and can be upregulated by tumor-promoting phorbol ester or growth factors as seen with primary megakaryocytes and mekaryoblast cell lines. In contrast to COX-1, COX-2 expression is typically transient. Depending on the cell type COX-2 expression can be rapidly induced by bacterial endotoxin (LPS), cytokines such as IL-1 , IL-2 and TNF-alpha, growth factors and the tumor promoter phorbol myristate acetate (PMA) (Smith, 2000). It should be noted that some cells in lung, brain and kidney, pancreatic beta-cells and gastrointestinal carcinomas exhibit constitutive COX-2 expression.

Regulation of COX-1 and COX-2 gene expression

The human COX-1 gene, located on chromosome 9, is approximately 22kb in length and contains 11 exon. The COX-1 promoter lacks a TATA or CAAT box, has a high GC content, and contains several transcriptional start sites. All of these properties are characteristic of housekeeping genes (Tanabe, 2002). Although COX-1 protein is constitutively expressed in most tissues, COX-1 is upregulated by PMA in some cell types including monocytes, human umbilical vein endothelial cells (HUVEC), and

primary megakaryocytes and mekaryoblasts as they differentiate during development (Tanabe, 2002).

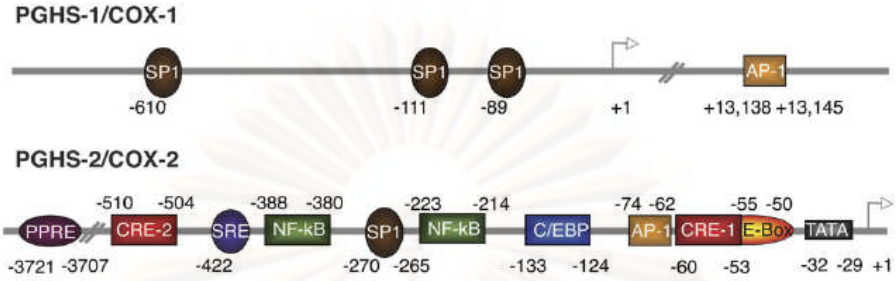

Figure 12 Schematic representation of the functional regulatory elements in the human COX-1 and COX-2 gene promoters (Yeon-Joo et al., 2007).

The human COX-2 gene, located on chromosome 1, is approximately 8.3 kb in long and contains 10 exon. Except for the first exon the intron/exon boundaries of the COX-1 and COX-2 genes are the same. There are two major transcripts of COX-2-a 4.5 kb full length mRNA and a 2.6 kb polyadenylated variant that lacks the terminal 1.9 kb of the 3'- untranslated region (UTR). The 3'-UTR of the human COX-2 gene contains 23 copies of the ATTA RNA instability element that participates in post-transcriptional regulation of COX-2expression (Tanabe, 2002).

Tumor necrosis factor-alpha (TNF- α)

TNF-α is a 17-kDa protein consisting of 157 amino acids that is a homotrimer in solution. In humans, the gene is mapped to chromosome 6. Its bioactivity is mainly regulated by soluble TNF-α binding receptors. TNF-α is mainly produced by activated macrophages, T lymphocytes and nutural killer (NK) cells (Beutler, 1985). Lower expression is known for a variety of other cells, including fibroblasts, smooth muscle cells and tumor cells. In cells, TNF-α is synthesized as pro-TNF (26 kDa), which is membrane bound and is released upon cleavage of its pro domain by TNF-α converting enzyme (TACE) (Beutler et al., 1985; Cerami and Beutler, 1988).

As mentioned above, TNF-α acts via two distinct receptors. Although the affinity for TNF receptor 2 (TNFR-2) is five times higher than that for TNFR-1, latter initiates the majority of the biological activities of TNF-α. TNFR-1 (p60) is expressed on all cell types, while TNFR-2 (p80).

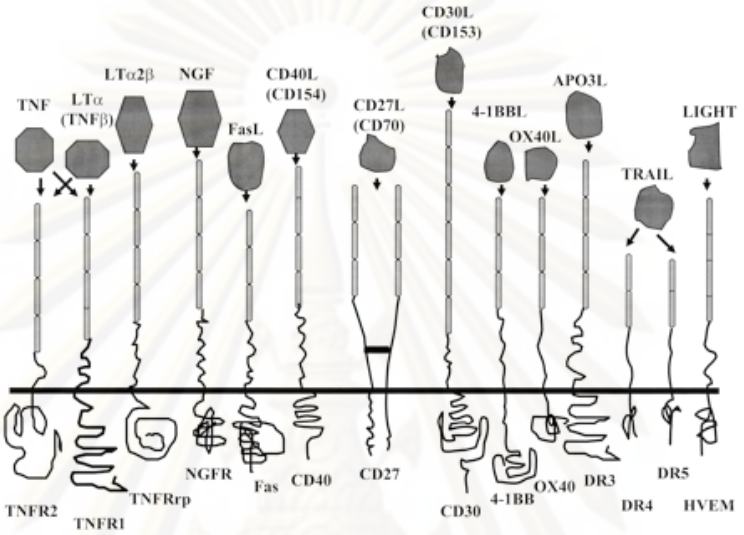

Figure 13 TNF-receptor and ligand (Georges and William, 2000)

Intercellular adhesion molecule-1 (ICAM-1)

Intercellular adhesion molecule-1(ICAM-1), a transmembrane glycoprotein of 505 amino acids, has a molecular mass ranging from 80 to 114 kDa depending on the degree of glycosylation, which varies with cell type. ICAM-1 is a member of the immunoglobulin supergene family and contains five extracellular immunoglobulin-like domains that function in cell-cell and cell-matrix adhesive interactions. In contrast to other cell adhesion molecules, ICAM-1 is expressed in both hematopoietic and non-hematopoietic cells and mediated adhesive interactions by binding to two integrins belonging to the β_2 subfamily i.e., CD11a/CD18 (LFA-1) and CD11b/CD18 (Mac-1). ICAM-1 adhesive interactions are critical for the tranendothelial migration of leukocytes and the activation of T cells where ICAM-1 binding functions as a co-activation signal (Zuckerman, 1998).

ICAM-1 is present constitutively on the cell surface of a wide variety of cell types including fibroblasts, leukocytes, keratinocytes, endothelial cells and epithelial cells, and

is upregulated in response to a number of inflammatory mediators, including retinoic acid, virus infection, oxidant stresses such as H_2O_2 , and the proinflammatory cytokines, interleukin-1β (IL-1β), tumor necrosis factor alpha (TNF-α).

Figure 14 Structure and regulation of the ICAM-1 promoter (Kenneth and Alison, 1999).

The level of ICAM-1 expression on the surface of any given cell type depends on the concentrations of pro- and anti-inflammatory mediators and on the availability of specific receptor-mediated signal transduction pathways and their nuclear transcription factor targets on the ICAM-1 promoter (Van et al., 1996; Shrikant et al., 1994; Bassi et al., 1995). The major intracellular signal transduction pathways involved in the regulation of ICAM-1 expression include protein kinase C (PKC), the mitogen-activated protein (MAP) and NF-κB signaling pathway. Nuclear transcription factors important for the activation of ICAM-1 expression include AP-1, NF-κB, C/EBP, Ets, STAT and Sp1 (Cornelius, 1993).

Mechanisms underlying the expression of adhesion molecules on leukocytes and endothelial cells at the onset of inflammation.

The cellular and molecular basis for the recruitment of leukocytes to sites of inflammation is highly complex and multifactorial, however there is sufficient experimental evidence in the literature to outline the key elements and sequential nature of this process. As illustrated , the inflammatory response involves the participation of multiple cell types, including circulating leukocytes, vascular endothelial cells, and perivascular cells (e.g., mast cells, macrophages), with the latter cells contributing to the initiation and perpetuation of inflammation through the generation of a variety of inflammatory mediators. Following the primary insult (infection, injury, or hypersensitivity

reaction), macrophages and mast cells are stimulated (e.g., by activated complement) to release mediators, such as histamine, oxygen radicals, platelet activating factor, leukotrienes, and cytokines. The engagement of histamine, leukotrienes and certain other mediators with their receptors on endothelial cells results in the rapid mobilization of P-selectin from its preformed pool in Weibel-Palade bodies to the cell surface. Hence, within minutes there is an increased recruitment of rolling leukocytes in postcapillary venules that allows for an enhanced exposure of the previously circulating cells to other mediators liberated from the inflamed tissue. The slowly rolling leukocytes are exposed to PAF, leukotrienes, and other mediators that rapidly activate, and then promote the shedding of, L-selectin on leukocytes. As the L-selectin is shed, there is a corresponding increase in the expression and activation of β_2-integrins on leukocytes. The newly expressed and/or activated CD11/CD18 can then bind to its counter-receptor ICAM-1, which is constitutively expressed on endothelial cells. The β_2-integrin/ICAM-1 adhesive interactions enable the inflamed tissue to recruit firmly adherent and emigrating leukocytes within a few minutes after the initial insult. This intimate interaction also allows PECAM-1, which is constitutively expressed on both endothelial cells and leukocytes, to promote the homophilic adhesion and emigration of leukocytes (Panés et al., 1999).

While the rapid inducers of leukocyte rolling, adherence and emigration are eliciting their actions, mast cell- and macrophage-derived cytokines engage with their receptors on endothelial cells. This ultimately (*via* specific signalling pathways) leads to the activation of nuclear transcription factors that modulate the biosynthesis of endothelial cell adhesion molecules that mediate leukocyte rolling (E-selectin) and adherence (ICAM-1, VCAM-1). Consequently, within a few hours (2–4) after the initial inflammatory insult, there is a profound increase in the density of virtually all endothelial cell adhesion molecules that participate in the trafficking of leukocytes during inflammation. As a result of this increased endothelial CAM expression, the recruitment of leukocytes can be sustained at both a higher level and for a longer duration (Panés et al., 1999).

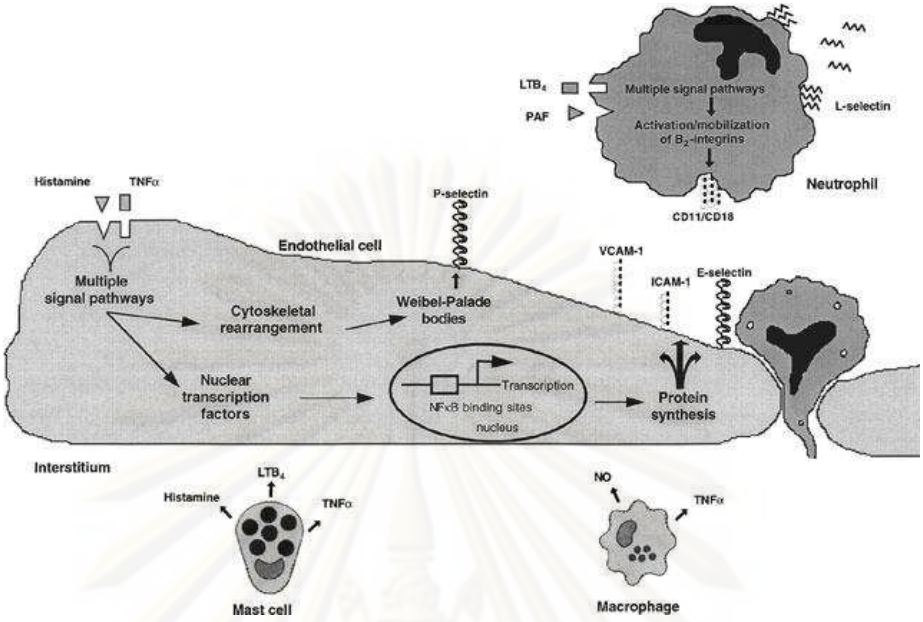

Figure 15 Mechanisms underlying the expression of adhesion molecules on leukocytes and endothelial cells at the onset of inflammation. Perivascular cells such as mast cells and macrophages initiate the response by releasing a variety of inflammatory mediators. Engagement of lipid mediators (LTB_4 and PAF) with receptors on neutrophils results in the activation of β_2-integrins (CD11/CD18). Engagement of histamine with its receptor (H1) on endothelial cells results in the rapid mobilization of preformed P-selectin from its storage site (Weibel-Palade bodies). Engagement of cytokines (e.g., TNF-α) to their receptors on endothelial cells lead to the activation of nuclear transcription factors (e.g., NF-κB) that stimulates the synthesis of adhesion glycoproteins, such as VCAM-1, ICAM-1, and E-selectin, which are subsequently expressed on the cell surface (**Panés et al., 1999**).

A large number of mediators have been implicated in the initiation of leukocyte-endothelial cell adhesion during inflammation. Several experimental strategies have been employed to assess the contribution of specific mediators to this facet of the inflammatory response. These include: (1) detection of the mediator at sites of inflammation characterized by leukocyte adhesion, (2) demonstration that leukocyte-endothelial cell adhesion can be induced by exposure of non-inflamed venules to an exogenous source of mediator, and (3) inhibition of leukocyte adhesion by agents

known to either antagonize or inhibit the production of the mediator. Several inflammatory mediators, including histamine, PAF, LTB_4, cytokines, and chemokines have been shown to promote leukocyte rolling, adherence and/or emigration when applied directly to postcapillary venules (Panés et al., 1998). A role for specific leukocyte and/or endothelial cell adhesion molecules in mediating these actions has been demonstrated for most of the mediators using either monoclonal antibodies directed against the CAMs (Zimmerman et al., 1994) or mice that are genetically deficient in a specific CAM. In some instances (e.g., histamine and cytokines), corroborative *in vivo* evidence of CAM involvement has been obtained from quantitative estimates of endothelial CAM expression in different vascular beds after administration of the inflammatory mediator.

Antagonists to histamine, PAF, leukotrienes, IL-8 and TNF-α (Appleyard et al., 1996) have been shown to prevent or attenuate the leukocyte-endothelial cell adhesion observed in different models of acute or chronic inflammation. For example, the histamine receptor (H_1) antagonist hydroxyzine has been shown to markedly reduce the leukocyte-endothelial cell adhesion and consequent microvascular injury elicited by *Clostridium difficile* toxin A (Kurose et al., 1994). Both PAF- (e.g., WEB 2086) and LTB_4-receptor (SC41930) receptor antagonists have proven effective in reducing the leukocyte adhesion observed in tissues exposed to either ischaemia or reperfusion or to inhibition of nitric oxide biosynthesis. Finally, a role for LTB_4 in mediating the leukocyte-endothelial cell adhesion induced by non-steroidal anti-inflammatory drugs, such as aspirin and indomethacin, has been demonstrated using both an LTB_4-receptor antagonist (SC41930) and a leukotriene biosynthesis inhibitor (L663,536) (Asako et al., 1992).

Curcumin (Diferuloylmethane)

Curcuma, a genus in the plant family of zingiberaceae, is the biological source for curcuminoids, including curcumin. *Curcuma longa*, the yellow tuberous root that is referred to as turmeric, was taken from India to Southeast Asia, China, North Australia, West Indies and South America. Subsequently, its cultivation spread to many African countries. The yellow pigmented fraction of Curcuma longa contains curcuminoids,

which are chemically related to its principal ingredient, curcumin. The three main curcuminoids isolated from turmeric are curcumin, demethoxy curcumin and bisdemethoxy curcumin. Curcuminoids are present in 3-5% of turmeric. Curcumin is the important active ingredient responsible for the biological activity of turmeric. Curcumin, or diferuloyl methane was first isolated in 1815. The crystalline from of curcumin was obtained in 1910, and Lampe solved its structure in 1913. It is insoluble in water, but soluble in ethanol and acetone (Sharma, 2005).

Pharmacokinetic Study and Safety

In animals, the previous study demonstrated that curcumin is poorly absorbed and rapidly metabolized in Sprague-Dawley rats (Wahltrom and Blennow, 1978; Ravindranath and Chandrasekhara, 1980; Pan et al., 1999). Administrating curcumin orally was made by Wahlström and Blennow (Wahltrom and Blennow, 1978). They demonstrated that this compound in a dose of 1 to 5 g/kg BW given to rats apparently did not cause any adverse effects and it was excreted about 75% in the feces, while traces appeared in the urine. In addition, measurements of blood plasma levels and biliary excretion showed that curcumin was poorly absorbed by the gastrointestinal tract. In 1999, Pan et al. investigated the pharmacokinetic properties of curcumin in mice. After intraperitoneal administration of curcumin (0.1 g/kg) in mice, approximately 2.25 μg/ml of curcumin appeared in the plasma within the first 15 min. Curcumin has been demonstrated the safety in human and rats. Oral LD50 of curcumin was found to be 12.2 g/kg BW in rats (Arora et al., 1971). Human appeared to be able to tolerate high doses of curcumin without significant side-effects. A phase 1 study by Cheng et al. (Cheng et al., 2001), found no adverse effects of curcumin ingestion for 3 months of doses up to 8,000 mg/day.

After oral administration of 400 mg curcumin to rats, about 60% of the dose was absorbed. No curcumin was detectable in urine. The urinary excretion of conjugated glucuronides and sulfates significantly increased. No curcumin was present in heart blood. Only traces (less than 5 microgram/ml) in portal blood and negligible quantities in liver and kidney (< 20 micrograms/tissue) were observed from 15 min upto 24 h after administration of curcumin. At the end of 24 h the concentration of curcumin remaining

in the lower part of the gut namely caecum and large intestine amounted to 38% of the quantity administered.

Curcumin alone attained overall moderate serum concentrations over a 4 hr period in rats with peak levels occurring between 0.75 and 1 hr. In humans, when curcumin was given alone only negligible serum concentrations of curcumin were detectable and the serum concentration-time curve was almost flat. This difference may be due to the high oral dose employed in the rat (2 g/kg), whereas the human dose was about 60 times less, approximately 33 mg/kg. Curcumin serum concentrations reached zero at 5 hr in rats and at 3 hr in humans. Furthermore, in rats the addition of piperine resulted in a higher curcumin concentration than in humans (although for a short period) which took a relatively longer time to increase and then decline. In contrast, in humans the maximum concentration was attained earlier and then declined precipitously.

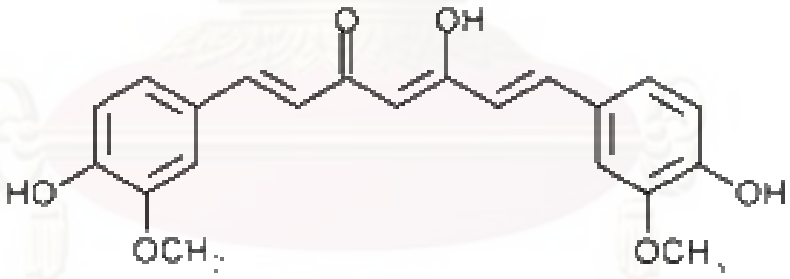

Figure 16 *Curcuma longa Linn* and chemical structure of curcumin
(www.food-info.net/images/curcumin.jpg)

AntiInflammatory Properties of Curcumin

Effect on Cytokines

Macrophages and $CD4^+$ cells, when activated, generate a number of proinflammatory cytokines. The pleiotropic cytokine, tumor necrosis factor-alpha (TNF) induces the production of interleukin-1beta (IL-1), and together, they play significant roles in many acute and chronic inflammatory and autoimmune diseases. *In vitro* studies show that curcumin, at 5 μM, inhibited the lipopolysaccharide (LPS)-induced production TNF-α and IL-1 by a human monocytic macrophage cell line (Chan, 1995). As a consequence, downstream events involving TNF-α and IL-1 are affected. For instance, TNF-α induced expression of leukocyte adhesion proteins, such as intercellular adhesion molecule-1 (ICAM-1) and vascular cell adhesion molecule-1 (VCAM-1). E-selectin is lowered in curcumin treated cells (Gupta,1999). Similarly, IL-1beta stimulated gene expression of a neutrophil chemotactic peptide, interleukin-8 (IL-8), is inhibited by curcumin (Chaudhary, 1996).

All these studies showed that curcumin is an antiinflammatory substance because it can inhibit the activation of the major transcription factor NF-κB. This transcription factors required for the expression of many genes linked with host immune response, such as TNF-α, IL-1β, iNOS, IL-12, MCP-1, MIP-2, and COX-2. Singh and Aggarwal (Singh and Aggarwal, 1995) observed that curcumin inhibited NF-κB activation. Cytoplasmic NF-κB is complexed with its inhibition IkB and therefore is active. The cytokine mediated activation of NF-κB requires activation of various kinases, which ultimately lead to the phosphorylation and degradation of IkB. Several of the beneficial effects of curcumin are consistent with its ability to inhibit the activity of NF-κB (Bierhaus, 1997). Singh and Aggarwal observed that curcumin inhibits NF-κB activation pathway after the convergence of various stimuli mediated by protein tyrosine kinase, protein kinase and ubiquitin conjugation enzymes, but before the phosphorylation and subsequent release of IkB complexed to NF-κB Plummer et al. examined the modulatory potential of curcumin on NF-κB signaling pathways and observed that curcumin prevent phosphorylation of IkB by inhibition the activation of IkB-kinase (IKKs) (Jobin, 1999). Brennan, 1998 found that curcumin inhibits NF-κB by interfering with IkBα degradation and reacts with p50 in the NF-κB complex (Brennan, 1998).

Furthermore, it is reported that curcumin blocks gene expression in intestinal epithelial cells by inhibition the signal leading to IKK activation without directly interfering with NF-κB inducing kinase (NIK) or IKK (Jobin, 1999). This inhibition of the yet unidentified activation signal going to the IKK complex by a signaling system upstream from NIK is in contrast with recent description of the blockade of IKKβ activity by aspirin, the widely used anti-inflammatory compound (Yin, 1998).

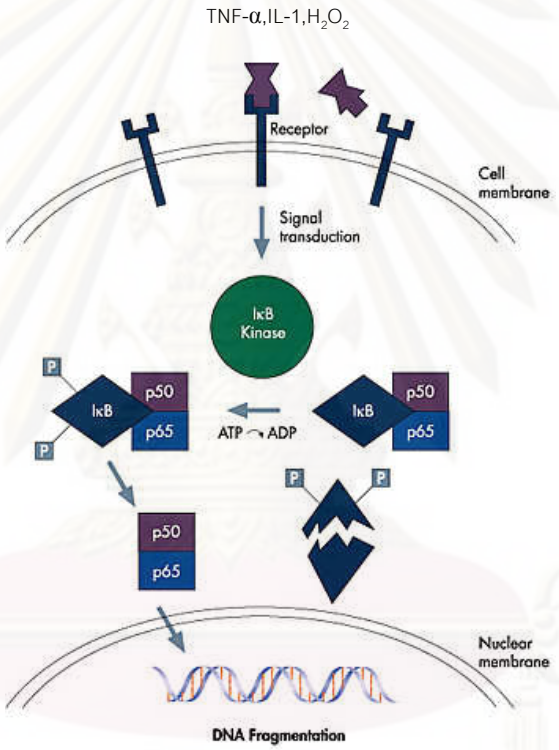

Figure 17 Regulation transcription of NF-κB

IkB=inhibitor I kappa B, IkB kinases =I kappa B kinases

Effect on Lipid Mediators and Eicosanoids

Eicosanoids play an important role in inflammation. Arachidonic acid is an important substrate for pro-inflammatory eicosanoid. The influence of curcumin on the formation and utilization of cellular arachidonic acid for the generation and release of

pro- inflammatory eicosanoids, such as prostaglandins and leukotrienes, have been investigated (Joe,1997a). Curcumin inhibits the cellular uptake of arachidonic acid, but not the release of arachidonic acid in response to phorbol ester treatment of rat peritoneal machophage membranes (Joe, 1997a). Phospholipases are involved in the release of arachidonic acid from membranes. Curcumin inhibits several types of mammalian phospholipases, including phospholipases A_2, C and D. (Yamamoto et al., 1997)

Curcumin is an inhibitor of cyclooxygenases and lipoxygenase and inhibits the production of prostaglandin E_2 and leukotrienes, B_4 and C_4 (Huang, 1997). Molecular mechanisms for the inhibition of lipoxygenses are beginning to be understood. Two independent studies suggest that curcumin, or a degradation product of curcumin, mat bind to the centrai cavity of the active site of lipoxygenases (Began, 1998). Based on spectroscopic measurements, Began et al concluded that the curcumin, after binding to phosphatidyl choline micelles, binds to iron, which is present in the active center of LOX-1 and acts as a competitive inhibitor of lipoxygenase 1 (LOX 1). On the other hand, using X-ray diffraction and mass spectrometry, Skrzypezak-Jankun et al. suggest that curcumin is a substrate for LOX1. They demonstrated that 4-hydroxyperoxy-2 methoxyphenol, a degradation product of curcumin, inhibits lipoxygenase by binding to the central cavity of its active site.

Antioxidant Property of Curcumin

The discovery of the antioxidant properties of curcumin explains many of its wide ranging pharmacological activities. The phenolic and the methoxy groups on the benzene rings are important structural features that contribute to its antioxidant properties. Curcumin is an effective antioxidant and scavenges O_2^-, H_2O_2, and nitric oxide from activated macrophages (Joe and Lokesh, 1994). Interestingly, curcumn not only exhibits antioxidative and free radical scavenging properties, but also enhances the activities of other antioxidants, such as superoxide dismutase, catalase and glutathione peroxidase (Kunchandy, 1990).

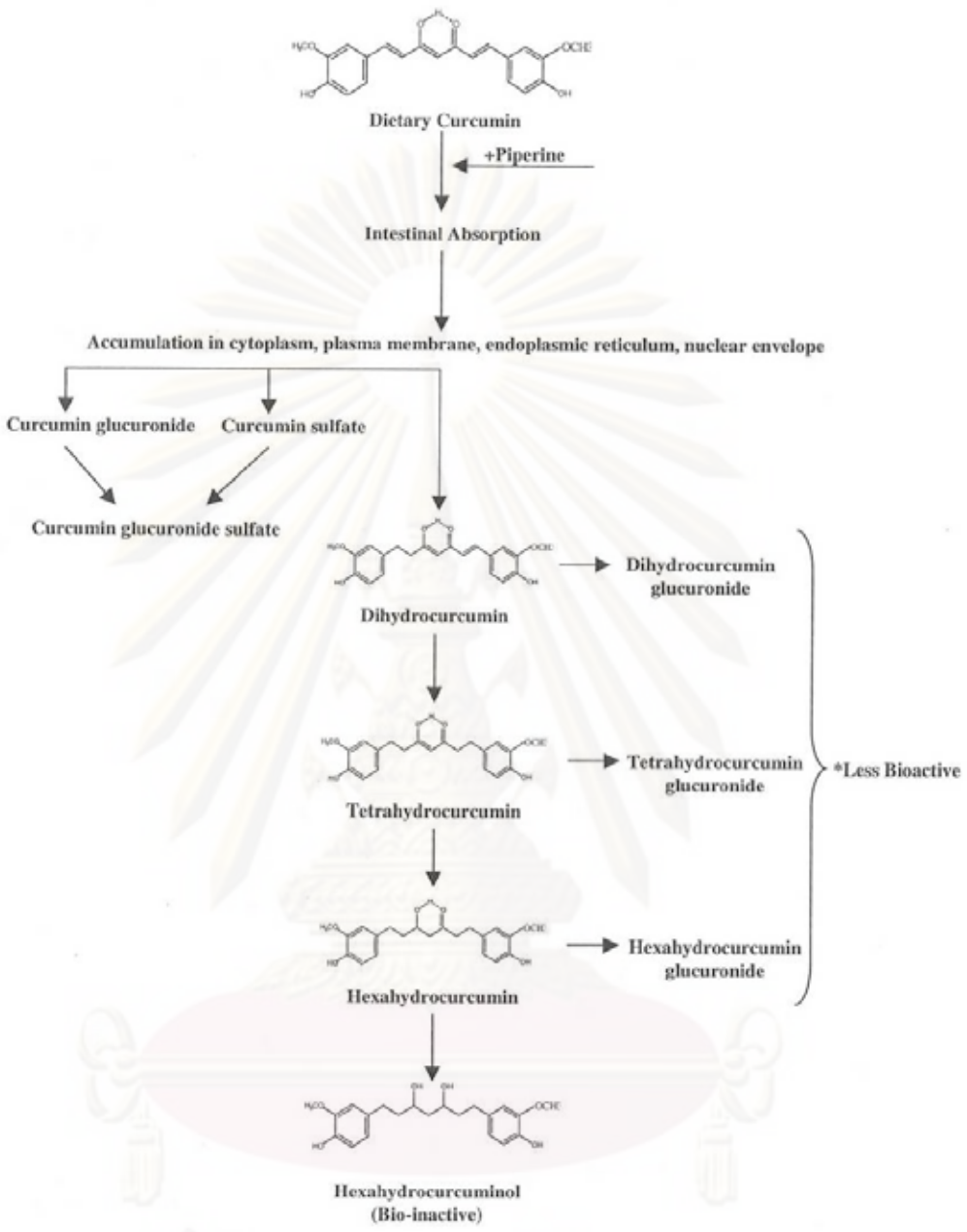

Figure 18 Absorption and metabolism of curcumin (Joe, 2004)

Animal Model used in Pre Study of Nonsteroidal Anti-Inflammatory Drugs-Induced Gastric Injury

1. Hideo and Co-Worker Model

Protocols, all rats were fasted, with free access to water ad libitum, for 22-24 hours before the experiment and deprived of water one hour before each experiment. Rats were fed indomethacin 30 mg/kg BW in 5% $NaHCO^-_3$ 1 ml. After 1 hour, Stomach showed gastric ulcer and increased reactive oxygen species (Hideo, 2006).

2. Murakami and Co-Worker Model

Protocols, all rats were fasted, with free access to water ad libitum, for 18-20 hours before the experiment. Rats were fed indomethacin 30 mg/kg BW in 5% $NaHCO^-_3$ After 3 hour, Stomach showed gastric mucosal lesion and increased infiltration of leukocytes (Murakami, 1999).

3. Ishita and Co-Worker Model

Protocols, all rats were fasted, with free access to water ad libitum, for 24 hours before the experiment and deprived of water before each experiment. Rats were fed indomethacin 48 mg/kg BW. After 4 hour, Stomach showed gastric ulcer and increased reactive oxygen species such as lipid peroxidation, hydroxyl radical (Ishita, 2006).

4. Swarnakar and Co-Worker Model

Protocols, all rats were fasted, with free access to water ad libitum, for 24 hours before the experiment and deprived of water before each experiment. Rats were fed indomethacin 48 mg/kg BW. After 4 hour, Stomach showed gastric ulcer and exhibit significant up-regulation of pro-MMP-9 (92 kDa) activity (Swarnakar, 2005).

5. Santucci and Co-Worker Model

Protocols, all rats were fasted, with free access to water ad libitum, for 20-22 hours before the experiment and deprived of water two to four hours before each experiment. Rats were fed indomethacin 20 mg/kg BW dissolved in 5% $NaHCO^-_3$. After 3 hour, Stomach showed gastric ulcer (Santucci, 1994).

Preliminary Study of Nonsteroidal Anti-Inflammatory Drugs Model Trial Before in This Thesis

Model 1 Rats were fed indomethacin at dose 60, 100 and 200 mg/kg BW in normal saline 1 ml (Ishita, 2006).

Table 1 Summary of infiltration of inflammatory cells and erosion in all groups. Data are expressed as the number of rats exhibiting the grade of infiltration of inflammatory cells and erosion indicated.

Group	Number	Neutrophil infiltration[a]				Pathology[b]		
		0	1	2	3	no erosion	erosion	ulcer
IMN 60 mg/kg in normal saline	1	1	-	-	-	1	-	-
IMN 100 mg/kg in normal saline	3	1	2	-	-	1	2	-
IMN 200 mg/kg in normal saline	1	1	-	-	-	1	-	-

[a]The severity neutrophil infiltration of was grade by:

0 = none

1 = neutrophil infiltration found 1/3 of gastric mucosal layer (mild)

2 = neutrophil infiltration found 2/3 of gastric mucosal layer (moderate)

3 = neutrophil infiltration found in the muscularis mucosae of gastric mucosal layer (severe)

[b]Pathology

Gastric erosions are superficial lesions involving the gastric mucosa; gastric ulcers extend through the mucosa and into the muscularis mucosa.

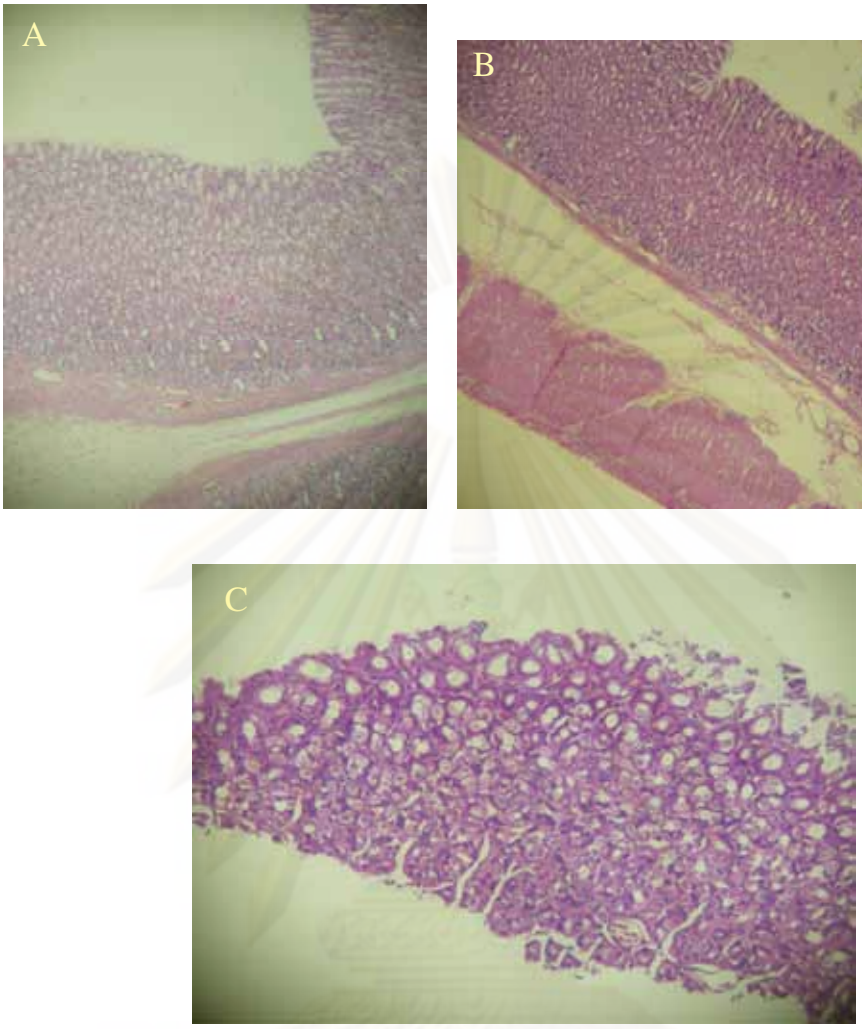

Figure 19 Hematoxylin-eosin stained stomach sections. (A) NSAIDs group in rats were fed indomethacin at dose 60 mg/kg BW in normal saline. Stomach showed no erosion and no infiltration of inflammatory cells inflammation. (B) NSAIDs group in rats were fed indomethacin at dose 100 mg/kg BW in normal saline. Stomach showed gastric erosion and showed mild infiltration of inflammatory cells inflammation. (C) NSAIDs group in rats were fed indomethacin at dose 200 mg/kg BW in normal saline. Stomach showed no erosion and no infiltration of inflammatory cells inflammation.

Model 2 Rats were fed indomethacin at dose 30, 60 and 100 mg/kg BW in 5% sodium bicarbonate 1 ml (Murakami, 1999).

Table 2 Summary of infiltration of inflammatory cells and erosion in all groups. Data are expressed as the number of rats exhibiting the grade of infiltration of inflammatory cells and erosion indicated.

Group	Number	Neutrophil infiltration[a]				pathology[b]		
		0	1	2	3	no erosion	erosion	ulcer
IMN 30 mg/kg in 5% sodium bicarbonate	2	-	2	-	-	-	2	-
IMN 60 mg/kg in 5% sodium bicarbonate	2	1	1	-	-	1	1	-
IMN 100 mg/kg in 5% sodium bicarbonate	2	-	1	1	-	-	2	-

[a]The severity of neutrophil infiltration was grade by:

0 = none

1 = neutrophil infiltration found 1/3 of gastric mucosal layer (mild)

2 = neutrophil infiltration found 2/3 of gastric mucosal layer (moderate)

3 = neutrophil infiltration found in the muscularis mucosae of gastric mucosal layer (severe)

[b]Pathology

Gastric erosions are superficial lesions involving the gastric mucosa; gastric ulcers extend through the mucosa and into the muscularis mucosa.

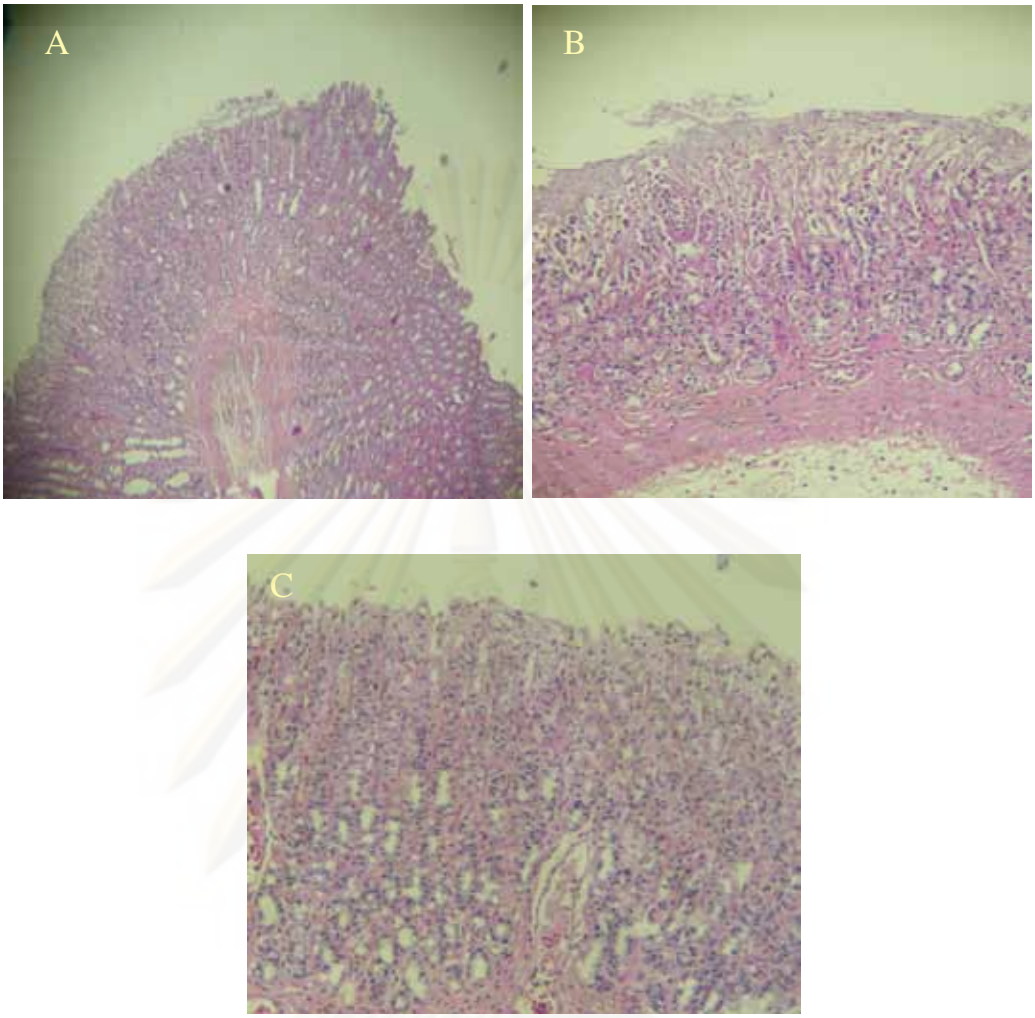

Figure 20 Hematoxylin-eosin stained stomach sections. (A) NSAIDs group in rats were fed indomethacin at dose 30 mg/kg BW in 5% sodium bicarbonate. Stomach showed erosion and showed mild infiltration of inflammatory cells inflammation. (B) NSAIDs group in rats were fed indomethacin at dose 60 mg/kg BW in 5% sodium bicarbonate. Stomach showed gastric erosion and showed mild infiltration of inflammatory cells inflammation. (C) NSAIDs group in rats were fed indomethacin at dose 100 mg/kg BW in 5% sodium bicarbonate. Stomach showed gastric erosion and showed mild to moderate infiltration of inflammatory cells inflammation.

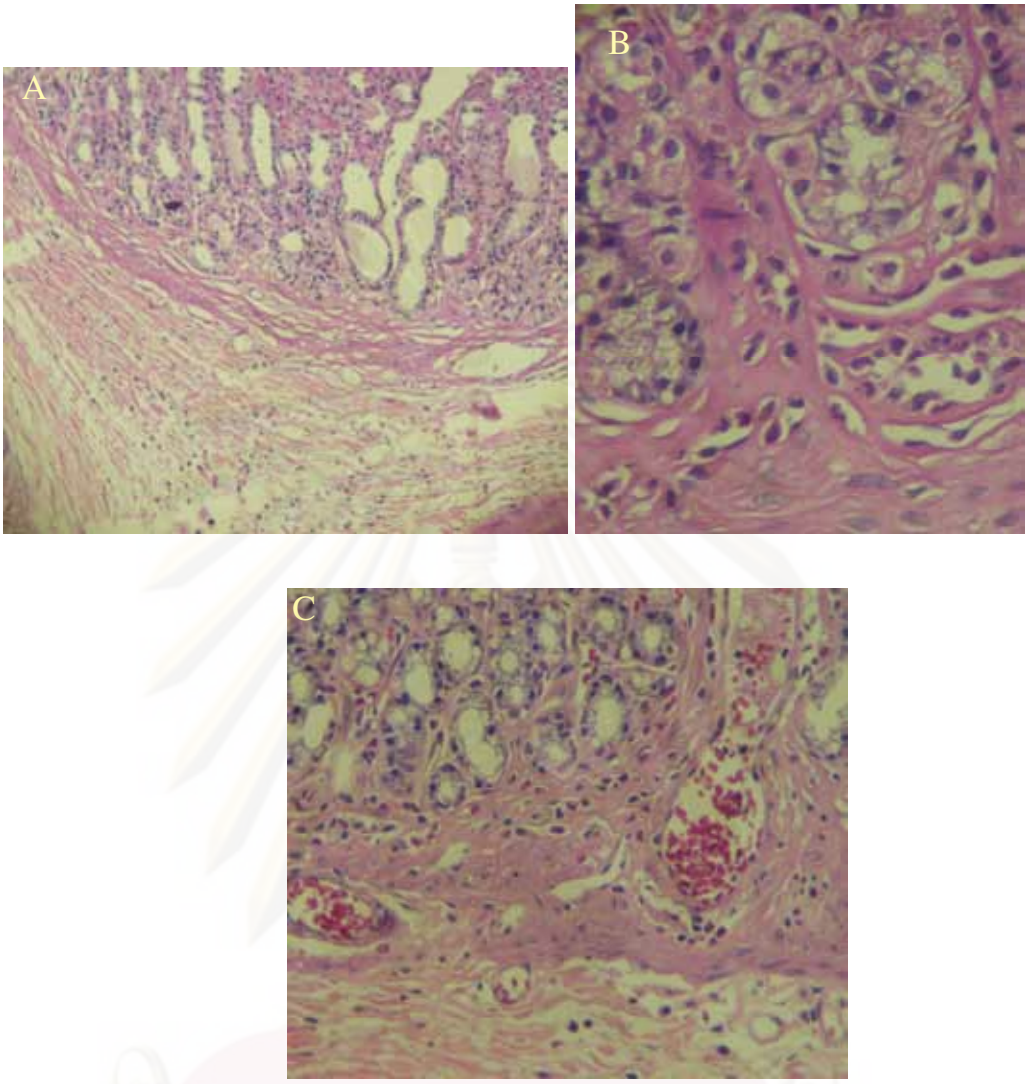

Figure 21 Hematoxylin-eosin stained stomach sections. (A) NSAIDs group in rats were fed indomethacin at dose 30 mg/kg BW in 5% sodium bicarbonate. Stomach showed mild infiltration of inflammatory cells inflammation. (B) NSAIDs group in rats were fed indomethacin at dose 60 mg/kg BW in 5% sodium bicarbonate. Stomach showed mild infiltration of inflammatory cells inflammation. (C) NSAIDs group in rats were fed indomethacin at dose 100 mg/kg BW in 5% sodium bicarbonate. Stomach showed mild to moderate infiltration of inflammatory cells inflammation.

Model 3 Rats were fed indomethacin at dose 100 and 150 mg/kg BW in 5% sodium bicarbonate 1 ml twice day (Ishita, 2006; Murakami, 1999; Hideo, 2006).

Table 3 Summary of infiltration of inflammatory cells and erosion in all groups. Data are expressed as the number of rats exhibiting the grade of infiltration of inflammatory cells and erosion indicated.

Group	Number	Neutrophil infiltration[a]				pathology[b]		
		0	1	2	3	no erosion	erosion	ulcer
IMN 100 mg/kg in 5% sodium bicarbonate	2	-	2	-	-	-	2	-
IMN 150 mg/kg in 5% sodium bicarbonate	2	-	-	1	1	-	2	-

[a]The severity of neutrophil infiltration was grade by:

0 = none

1 = neutrophil infiltration found 1/3 of gastric mucosal layer (mild)

2 = neutrophil infiltration found 2/3 of gastric mucosal layer (moderate)

3 = neutrophil infiltration found in the muscularis mucosae of gastric mucosal layer (severe)

[b]Pathology

Gastric erosions are superficial lesions involving the gastric mucosa; gastric ulcers extend through the mucosa and into the muscularis mucosa.

Nonsteroidal Anti-Inflammatory Drugs Model in This Thesis (Model 3)

All rats were fasted, with free access to water ad libitum, for 22-24 hours before the experiment and deprived of water one hour before each experiment. Rats were fed indomethacin 150 mg/kg BW in 5% $NaHCO^-_3$ 1 ml twice day. After 8 hour, stomach showed gastric ulcer and increased infiltration of inflammatory cells. Model 3 was selected in the experiment.

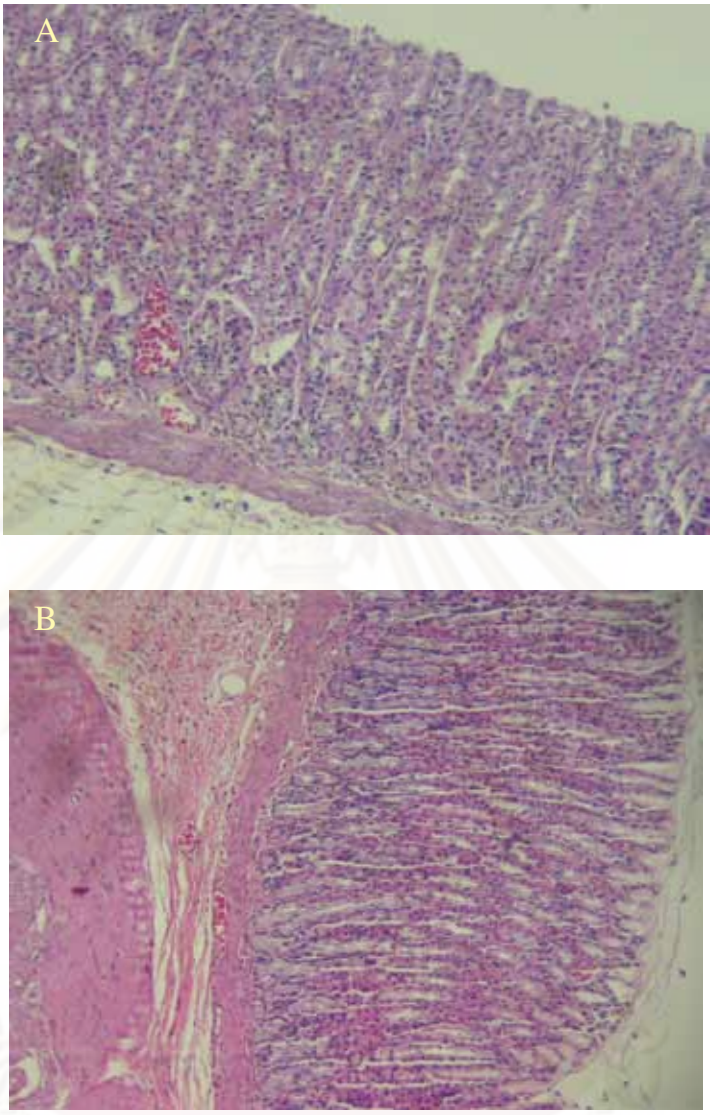

Figure 22 Hematoxylin-eosin stained stomach sections. (A and B) NSAIDs group in rats were fed indomethacin at dose 100 mg/kg BW in 5% sodium bicarbonate twice day. Stomach showed erosion and showed mild infiltration of inflammatory cells inflammation.

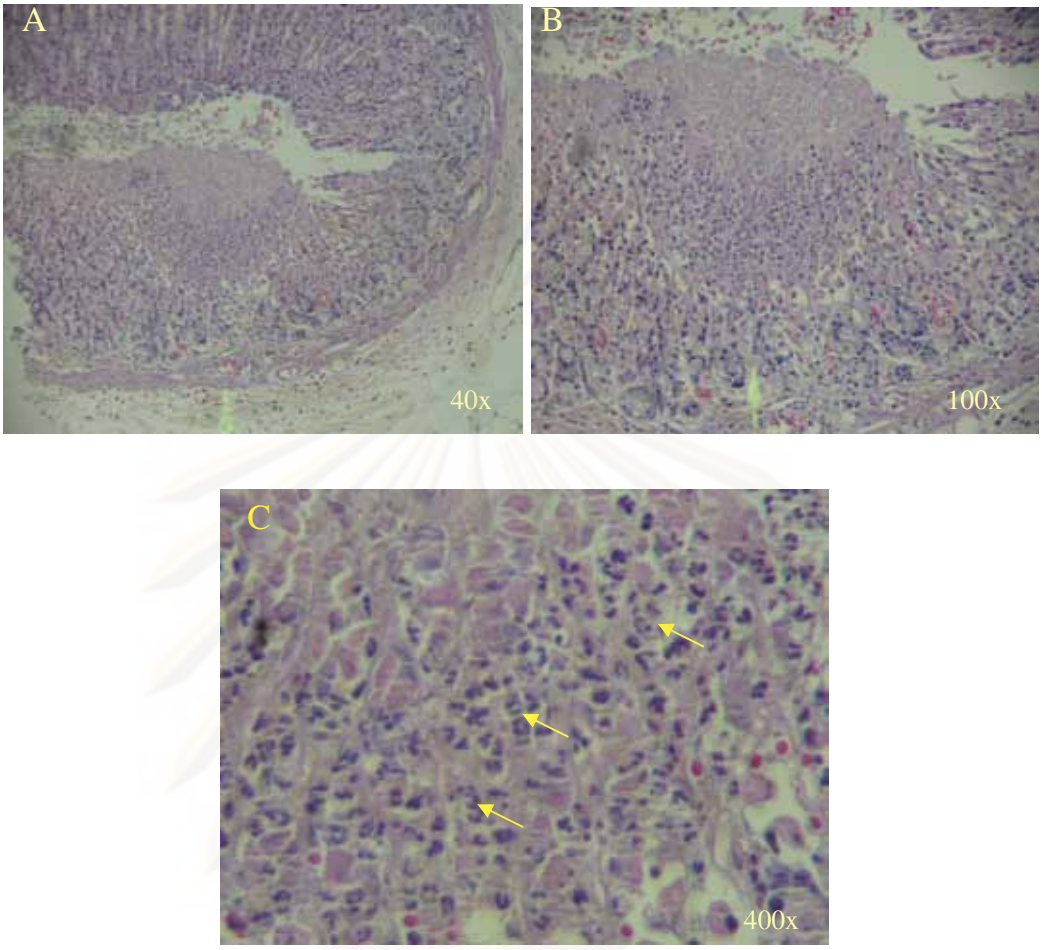

Figure 23 Hematoxylin-eosin stained stomach sections. (A and B) NSAIDs group in rats were fed indomethacin at dose 150 mg/kg BW in 5% sodium bicarbonate 1 ml at twice day. Stomach showed gastric ulcer and (C) showed moderate to severe infiltration of inflammatory cells inflammation.

Conceptual framework

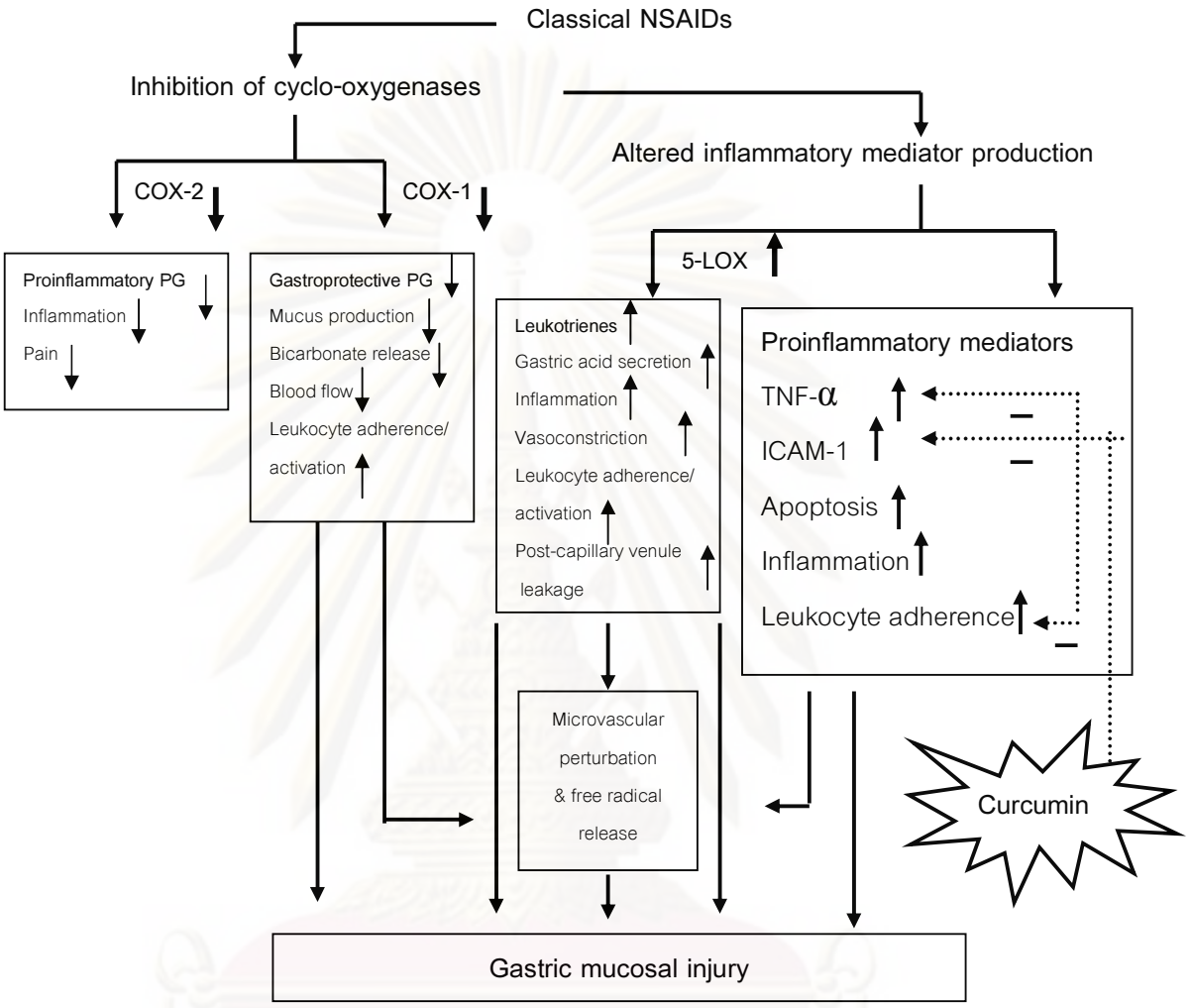

CHAPTER III

MATERIALS AND METHODS

This research was animal experimental design to study effects of curcumin on leukocyte-endothelium interaction of gastric microcirculation, serum TNF-α level, serum ICAM-1 level and change of histopathology with nonsteroidal anti-inflammatory drugs induced gastric injury in rats. Male Sprague-Dawley rats were fed with nonsteroidal anti-inflammatory drugs to induce gastric injury and pretreated with curcumin. Leukocyte-endothelium interaction at postcapillary venule were record, After the end of experiment, blood samples were collected for measure TNF-α and ICAM-1 levels using ELISA and stomach samples were analyzed for histopathology.

Reagents

Acridine orange (Sigma Chemical CO., USA)

95% alcohol

Curcumin (Cayman Chemical Company, USA)

Distilled water

Formalin solution

Heparin (Leo Pharmaceutical Products, Denmark)

ICAM-1 ELISA kit (R&D systems, Inc., USA)

Indomethacin (Chulalongkorn Hospital,Thailand)

Krebs's solution

NaCl (Merck, Germany)

$NaHCO^{-}_{3}$ (Merck, Germany)

Olive oil

4% Para-formaldehyde in phosphate buffer

Sterile normal saline solution

Thiopental (Abbott, Italy)

TNF-α ELISA kit (R&D systems, Inc., USA)

Animal Preparation

Male Sprague-Dawley rats, weighing 180-220 g, were purchased from the National Laboratory Animal Center, Mahidol University, Salaya, Nakorn Pathom. The rats were kept in a controlled temperature room at 25±1ºC under standard conditions (12 hour light:dark) and had freely access to food and tap water. All rats were received well care in accordance with the Ethical Committee, Faculty of Medicine, Chulalongkorn University, Thailand (approval No.21/2551).

Curcumin Preparation

Curcumin in powder form (Cayman Chemical Company, USA) was suspended in olive oil.

Experimental Protocols

All rats were weighed before experiment. Rats were fasted, with free access to water ad libitum, for 22-24 hours before the experiment. They were randomly divided into three experimental groups.

Group 1 (Control, n=6): Rats were fed olive oil 30 minute prior to 5% $NaHCO^-_3$ 1 ml orally via an intragastric tube at time 0^{th},4^{th} hr.

Group 2 (NSAIDs, n=6): Rats were fed olive oil 30 minute prior to indomethacin 150 mg/kg BW dissolved in 5% $NaHCO^-_3$ 1 ml orally via an intragastric tube at time 0^{th},4^{th} hr.

Group 3 (NSAIDs+cur, n=6): Rats were fed curcumin 200 mg/kg BW dissolved in olive oil 0.5 ml 30 minute prior to indomethacin 150 mg/kg BW dissolved in 5% $NaHCO^-_3$ 1 ml orally via an intragastric tube at time 0^{th},4^{th} hr.

After 8^{th} hours 30 min, the animals were anesthetised with intraperitoneal injection of thiopental (50 mg/kg body weight). After tracheostomy, carotid artery and jugular vein were canulated for blood pressure measurement using polygraph and administration of fluorescent marker. The abdominal wall was incised and the stomach was extended and fixed. Then the leukocyte adherence in stomach was observed by Intravital fluorescence microscopy. After the end of experiment, blood samples were collected for TNF-α and ICAM-1 levels was observed by ELISA. The stomach was cut

and fixed in 10% formalin solution to determine histopathology. The study design was summarized in the diagram below (Figure 24).

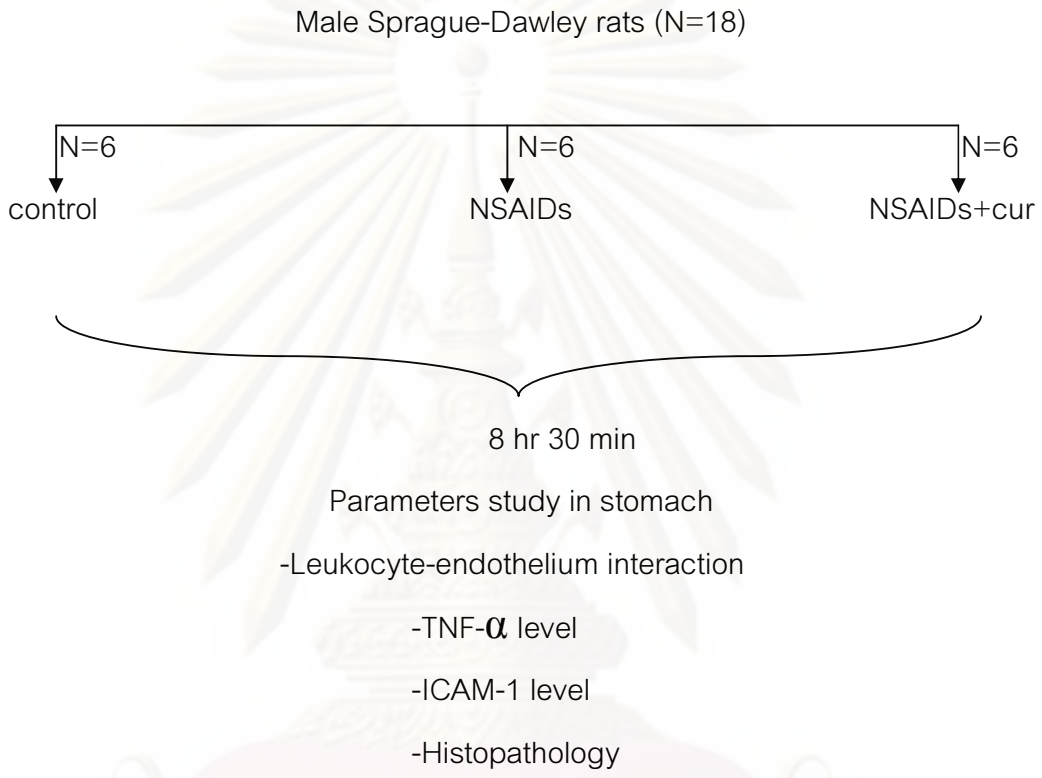

Figure 24 Diagram of experimental design

Data Collection

1. Histopathological Examination

Stomach samples were fixed in 10% formaldehyde in 0.2 M sodium phosphate buffer, pH 7.4 at room temperature. Stomach was processed by standard methods. Briefly, gastric tissues were embedded in paraffin, sectioned at 5 μm thickness. Then tissues were stained with H&E and picked up on glass slides for light microscopy. All samples were evaluated by an experienced pathologist who was blinded to the

experiment. Histopathological were examined for grading of infiltration of inflammatory cells according to Dixon et al.'s criteria and erosion indicated.

neutrophil infiltration was scored of neutrophil infiltration found in gastric mucosa.

0 = none

1 = neutrophil infiltration found 1/3 of gastric mucosal layer (mild)

2 = neutrophil infiltration found 2/3 of gastric mucosal layer (moderate)

3 = neutrophil infiltration found in the muscularis mucosae of gastric mucosal layer (severe)

Pathology

Gastric erosions are superficial lesions involving the gastric mucosa; gastric ulcers extend through the mucosa and into the muscularis mucosa.

2. Experimental for leukocyte-endothelium interaction on gastric microcirculation by intravital fluorescent microscopy

After 8^{th} hours, the animals were anesthetised with intraperitoneal injection of thiopental (50 mg/kg body weight). A tracheotomy was performed. Then, a fine polyethylene catheter (PE 10, inner diameter 0.28 mm) was inserted into the left common carotid artery (inserted 1.0 cm). The carotid catheter was maintained with heparinized saline. The mean arterial pressure (MAP) was monitored via this catheter by using pressure transducer (Nihon Kohden). The another catheter was inserted into jugular vein for injection of fluorescence (acridine orange, 0.3 mg/kg BW).

After laparotomy, a 1.0 cm incision was made by scissors in the anterior wall of the exteriorized stomach parallel to the limiting ridge. Observations were made from the glandular portion of stomach. Care was taken to avoid injurious through blood vessels, the stomach was gently extended and held in place by a stay suture. During the surgery, the area was kept by allowing drops of the warmed normal saline to fall on the incision. The body temperature of the animal was kept constant at 36-37 ºC by mean of heating pad. After preparing the stomach for fluorescent *in vivo* microscopy the animal was places on microscopic stage of the fluorescent microscopy equipped with transillumination and epiilumination optics (Nikon Optiphol-2). After intravenous application of acridine orange, epillumination was achieved with a 50 W, mercury lamp

with a 488 nm attached to excitation filter and 515 emission barrier filters. An intravital microscopy with a 40x long working distance objective (CF Achromat) were to observe microvessels in the stomach. A video camera mounted on the microscope projected the image onto a black-white monitor. The images of microvessels were stored on videotape (Sony, SLV-X311) for playback analysis using a video cassette recorder. A videotape connected to a video timer (UTG-33) for time later recorder. During the experiment, microvessels images could be printed by using video graphic printer (Sony,UP-890 CE). All instruments used for quantitive studies of hemodynamic and the morphologic parameters in microcirculation were shown in Figure 26.

Study of leukocyte-endothelium interaction at postcapillary venule

To observe the leukocyte adhesion in postcapillary venule, the intravital microscope with a 40x long working distance objective (CF Achromat) were used to observe the microvessels in muscle layer at the body region of the stomach. Anatomical of blood vessel that supply the body region of stomach were observed for a landmark in every animals. After 15 minutes of equilibration period, the fluorescent marker, acridine orange was infused intravenously (Sigma chemical Co., USA, 0.5 mg/kg BW) for 10-15 minutes for visualized the leukocyte adhesion. During experiment, leukocytes were recored on videotape for further observation of leukocyte adhesion.

Videotape of each experiment was played back and then leukocyte adhesion on postcapillary venules (diameter=15-30 μm) were counted at 10-15 min after arcridine orange injection by Image proplus program. Leukocyte adhesion were defined as cells which did not move or detach from the endothelial lining within the entire observation for a period equal to or greater than 30 seconds whereas rolling leukocytes were defined as nonadherent leukocytes passing through the observed vessel segment within the observation period (Gabour and kubes, 1994). The image analysis that used to count number of leukocyte adhesion was show in Figure 27. All samples were evaluated by person who was blinded to the experiment.

Figure 25 Study of leukocyte- endothelium interaction on gastric microcirculation at body region of the stomach in rats.

The PCVs were selected to study including:

1. Diameters of PCVs are 15-30 μm.
2. Blood flow in PCVs must collect from branches of capillary end and flow directed to the collecting venule.
3. PCVs are located at the body region of stomach.

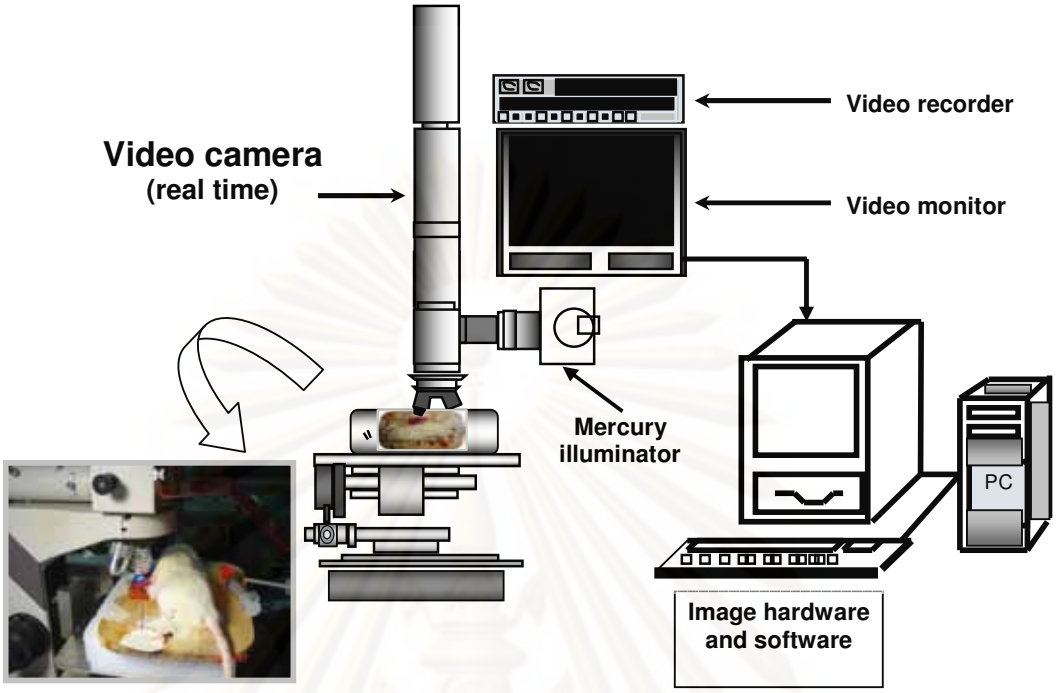

Figure 26 Intravital fluorescent microscopy and instruments are used for studying of leukocyte adhesion of gastric microcirculation.

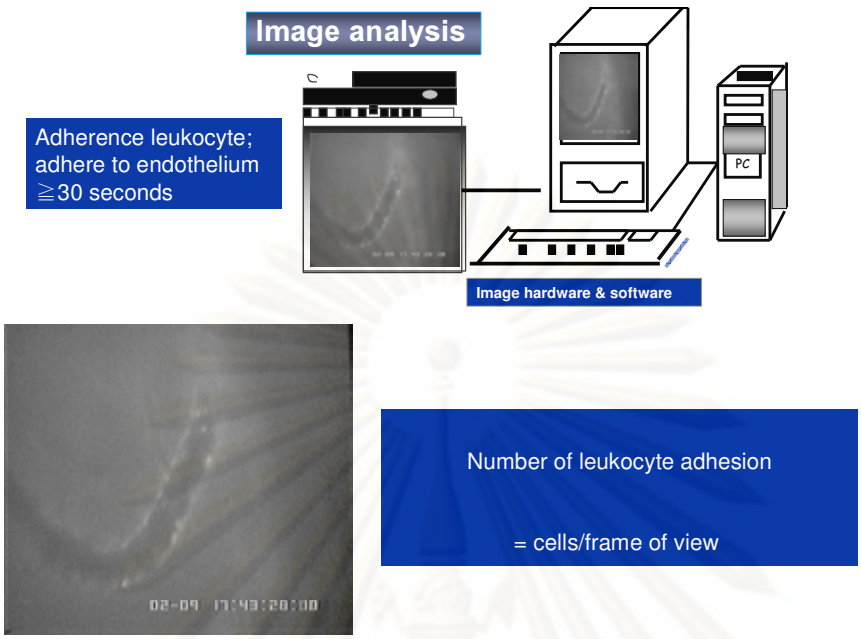

Figure 27 Image analysis for determined number of leukocyte adhesion using by image proplus program. Number of leukocyte adhesion (cells/frame of view)

3. Enzyme-linked immunosorbent assay (ELISA)

ELISA is a useful method in evaluating the concentration of proteins in a sample such as cell culture supernatant, serum, or plasma. ELISA kit is performed in 96 well plates which allow high throughput results. A monoclonal antibody has been pre-coated onto a microplate. Standards, control, and samples are pipetted into the wells and any antigen present is bound by the immobilized antibody. After washing away any unbound substances, an enzyme-linked polyclonal antibody is added to the wells. Following a wash to remove any unbound antibody-enzyme reagent, a substrate solution is added to the wells. The enzyme reaction yields a blue product that turns yellow when the stop solution is added. The intensity of color measured is in proportion to the amount of antigen bound in the initial step. The sample values are then read off the standard curve.

TNF-α assay

This assay employs the quantitative sandwich enzyme immunoassay technique. A monoclonal antibody specific for rat TNF-α has been pre-coated onto a microplate. Standards, Control, and samples are pipetted into the wells and any rat TNF-α present is bound by the immobilized antibody. After washing away any unbound substances, an enzyme-linked polyclonal antibody specific for rat TNF-α is added to the wells. Following a wash to remove any unbound antibody-enzyme reagent, a substrate solution is added to the wells. The enzyme reaction yields a blue product that turns yellow when the Stop Solution is added. The intensity of the color measured is in proportion to the amount of rat TNF-α bound in the initial step. The sample values are then read off the standard curve.

Procedure

1. Prepare reagents, working standards, control, and samples as directed in the previous sections.

2. Remove excess microplate strips from the plate frame, return them to the foil pouch containing the desiccant pack, reseal.

3. Add 50 µL of Assay Diluent RD1-41 to each well.

4. Add 50 µL of Standard, Control, or sample* to each well. Mix by gently tapping the plate frame for 1 minute. Cover with the adhesive strip provided. Incubate for 2 hours at room temperature. A plate layout is provided to record standards and samples assayed.

5. Aspirate each well and wash, repeating the process four times for a total of five washes. Wash by filling each well with Wash Buffer (400 µL) using a squirt bottle, manifold dispenser, or autowasher. Complete removal of liquid at each step is essential to good performance. After the last wash, remove any remaining Wash Buffer by aspirating or by inverting the plate and blotting it against clean paper towels.

6. Add 100 µL of rat TNF-α Conjugate to each well. Cover with a new adhesive strip. Incubate for 2 hours at room temperature.

7. Repeat the aspiration/wash as in step 5.

8. Add 100 µL of Substrate Solution to each well. Incubate for 30 minutes at room temperature, protect from light.

9. Add 100 µL of Stop Solution to each well. Gently tap the plate to ensure thorough mixing.

10.Determine the optical density of each well within 30 minutes, using a microplate reader set to 450 nm. If wavelength correction is available, set to 540 nm or 570 nm. If wavelength correction is not available, subtract readings at 540 nm or 570 nm from the readings at 450 nm. This subtraction will correct for optical imperfections in the plate. Readings made directly at 450 nm without correction may be higher and less accurate.

To calculate results, the duplicated readings for each standard, control, and samples were averaged and subtracted the average of zero standard optical density. Then, the standard curve was created by using computer software of generating a linear curve-fit. The measured O.D. of each unknown was converted to its corresponding concentration by standard curve. The below table and figure showed the calculation of results.

Standard TNF-α (pg/ml)	Obtical density (O.D.) (450 nm-540 nm)		Average O.D.	Corrected O.D.
	Data 1	Data 2		
0	0.034	0.034	0.034	-
12.5	0.085	0.080	0.082	0.048
25	0.128	0.127	0.128	0.094
50	0.214	0.216	0.215	0.181
100	0.383	0.372	0.378	0.344
200	0.692	0.698	0.695	0.661
400	1.218	1.222	1.220	1.186
800	2.023	1.988	2.006	1.972

Table 4 The corrected O.D. plotted on y-axis of standard curve was calculated from the mean subtract the average of zero standard O.D. Note: pg/ml = picogram per milliliter; nm = nanometer

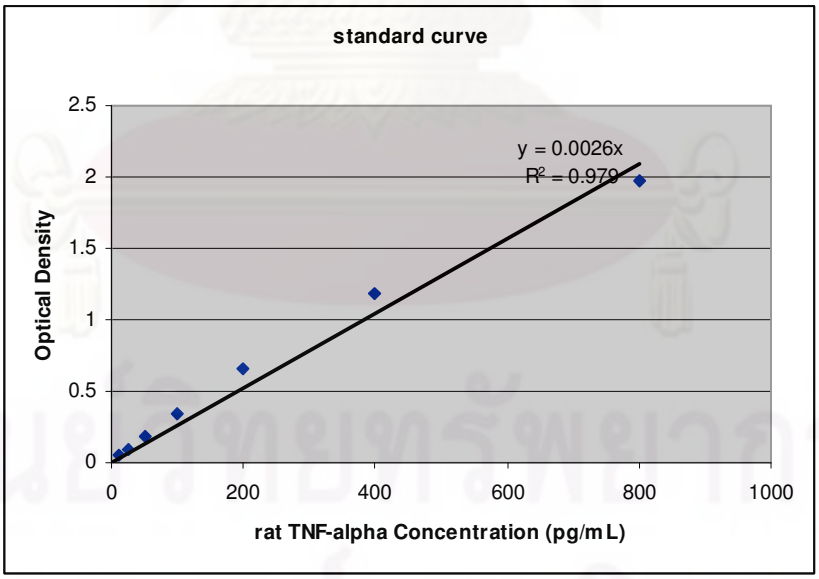

Figure 28 Standard curve of TNF-α: The x-axis and y-axis of the standard curve represented standard TNF-α concentrations (pg/ml) and O.D., respectively

The data were linearized with computer software and the best fit line can be determined by regression analysis. From the linear equation of standard curve, the sample concentration will be calculated. If samples have been diluted prior to assay, the concentration read from the standard curve must be multiplied by the dilution factor.

ICAM-1 assay

This assay employs the quantitative sandwich enzyme immunoassay technique. A monoclonal antibody specific for rat sICAM-1 has been pre-coated onto a microplate. Standards, controls, and samples are pipetted into the wells and any rat sICAM-1 present is bound by the immobilized antibody. After washing away any unbound substances, an enzyme-linked polyclonal antibody specific for rat sICAM-1 is added to the wells. Following a wash to remove any unbound antibody-enzyme reagent, a substrate solution is added to the wells. The enzyme reaction yields a blue product that turns yellow when the Stop Solution is added. The intensity of the color measured is in proportion to the amount of rat sICAM-1 bound in the initial step.

The sample values are then read off the standard curve.

Procedure

1. Prepare reagents, standard dilutions, controls and samples as directed in the previous sections.

2. Remove excess microplate strips from the plate frame, return them to the foil pouch containing the desiccant pack, reseal.

3. Add 50 µL of Assay Diluent RD1-21 to each well.

4. Add 50 µL of Standard, Control or sample* per well. Cover with the adhesive strip provided. Incubate for 2 hours at room temperature on a horizontal orbital microplate shaker (0.12" orbit) set at 500 50 rpm. A plate layout is provided to record the standards and samples assayed.

5. Aspirate each well and wash, repeating the process four times for a total of five washes. Wash by filling each well with Wash Buffer (400 µL) using a squirt bottle, multi-channel pipette, manifold dispenser or autowasher. Complete removal of liquid at each step is essential to good performance. After the last wash, remove any remaining

Wash Buffer by aspirating or decanting. Invert the plate and blot it against clean paper towels.

6. Add 100 µL of diluted rat sICAM-1 Conjugate to each well. Cover with a new adhesive strip. Incubate for 2 hours at room temperature on the shaker.

7. Repeat the aspiration/wash as in step 5.

8. Add 100 µL of Substrate Solution to each well. Incubate for 30 minutes at room temperature on the benchtop, protect from light.

9. Add 100 µL of Stop Solution to each well. Gently tap the plate to ensure thorough mixing.

10. Determine the optical density of each well within 30 minutes, using a microplate reader set to 450 nm. If wavelength correction is available, set to 540 nm or 570 nm. If wavelength correction is not available, subtract readings at 540 nm or 570 nm from the readings at 450 nm. This subtraction will correct for optical imperfections in the plate. Readings made directly at 450 nm without correction may be higher and less accurate.

To calculate results, the duplicated readings for each standard, control, and samples were averaged and subtracted the average of zero standard optical density. Then, the standard curve was created by using computer software of generating a linear curve-fit. The measured O.D. of each unknown was converted to its corresponding concentration by standard curve. The below table and figure showed the calculation of results.

Standard ICAM-1 (pg/ml)	Obtical density (O.D.) (450 nm-540 nm)		Average O.D.	Corrected O.D.
	Data 1	Data 2		
0	0.068	0.072	0.070	-
31.2	0.125	0.126	0.126	0.056
62.5	0.183	0.188	0.186	0.116
125	0.295	0.297	0.296	0.226
250	0.527	0.531	0.529	0.459
500	0.926	0.963	0.943	0.873
1000	1.627	1.686	1.656	1.586
2000	2.733	2.783	2.758	2.688

Table 5 The corrected O.D. plotted on y-axis of standard curve was calculated from the mean subtract the average of zero standard O.D. Note: pg/ml = picogram per milliliter; nm = nanometer

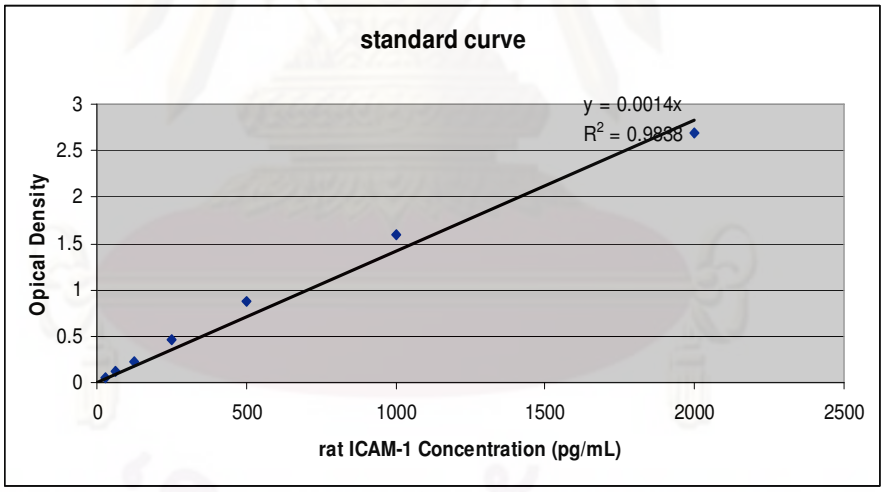

Figure 29 Standard curve of ICAM-1: The x-axis and y-axis of the standard curve represented standard ICAM-1 concentrations (pg/ml) and O.D., respectively

The data were linearized with computer software and the best fit line can be determined by regression analysis. From the linear equation of standard curve, the

sample concentration will be calculated. If samples have been diluted prior to assay, the concentration read from the standard curve must be multiplied by the dilution factor.

Data Analysis

Data were expressed and analyzed as means ± standard deviation (SD). Each parameter was compare among groups with One-way analysis of variance (One-way ANOVA), LSD, and Duncan ($p<0.05$) with SPSS program for window version 11.0.

CHAPTER IV

RESULTS

1. Histopathological examination

The histologic appearance of the stomach in the control group was normal. In the indomethacin treated group, the histologic features showed mild to moderate gastric mucosal injury. Gastric lesions were erosive and ulcerative. In rats treated with indomethacin and curcumin improved the stomach histopathology that showed only mild gastric mucosal injury and erosive lesion in gastric mucosa. The summary of infiltration of inflammatory cells and gastric lesion were shown in Table 6.

2. Interaction between leukocytes and endothelial cells

After gastric injury was induced by administration of indomethacin, leukocyte adherence to endothelial cells of postcapillary venules (15-30 μm in diameter) was observed under intravital fluorescence microscopy at 10-15 min after acridine orange injection. The number of leukocytes adhered to postcapillary venules for 30 s or longer was counted of observation. The mean number of leukocyte adherences in the NSAIDs group without treatment was significantly increased compared to the control group (6.40 ± 2.30 vs 1.20 ± 0.83 cells/frame, p=0.000).

The number of leukocyte adherences was significantly decreased in the pretreatment with curcumin compared to the NSAIDs group (3.00 ± 0.81 vs 6.40 ± 2.30 cells/frame, p=0.007).

3. Changes of TNF-α level

The level of TNF-α increased in indomethacin treated group as compared with control group (154.66 ± 166.03 vs. 73.85± 83.00 pg/mL, p=0.258). Pretreatment with curcumin decreased the elevation of TNF-α level when compared with indomethacin treated group (78.40 ± 83.00 vs. 154.66± 166.03 pg/mL, p=0.284).

4. Changes of ICAM-1 level

The level of ICAM-1 increased significantly in indomethacin treated group as compared with control group (1106.50 ± 504.22 vs. 336.93 ± 224.82 pg/mL, p=0.001). Pretreatment with curcumin decreased the elevation of ICAM-1 level significantly when compared with indomethacin treated group (413.66 ± 147.74 vs. 1106.50 ± 504.22 pg/mL, p=0.002).

5. Hemodynamic

The changes of hemodynamic characters of animals were recorded. The animals were monitored systolic blood pressure (SBP), diastolic blood pressure (DBP), and heart rate (HR) via catheter (PE 10, inner diameter 0.28 mm) by using the pressure transducer (Nihon Kohden). Mean arterial blood pressure (MAP) was calculated with this formula: MAP = 1/3 (SBP+2DBP). The mean and standard deviation (SD) of these parameters were shown in the table 10. There is no significant difference of these hemodynamic parameters among experimental groups.

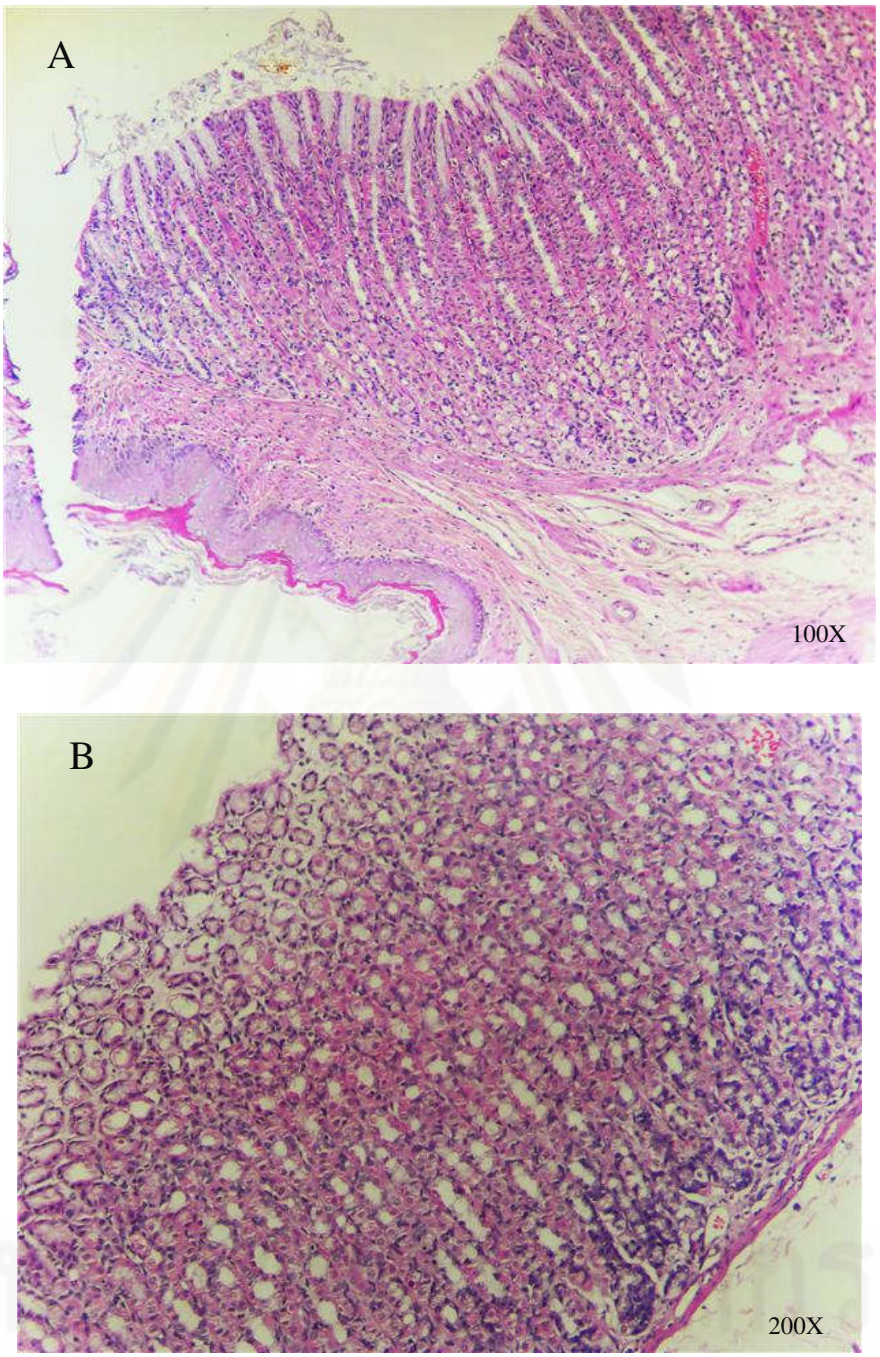

Figure 30 Hematoxylin-eosin stained stomach sections (100X, 200X).
Control group (A and B) showed normal stomach histopathology.

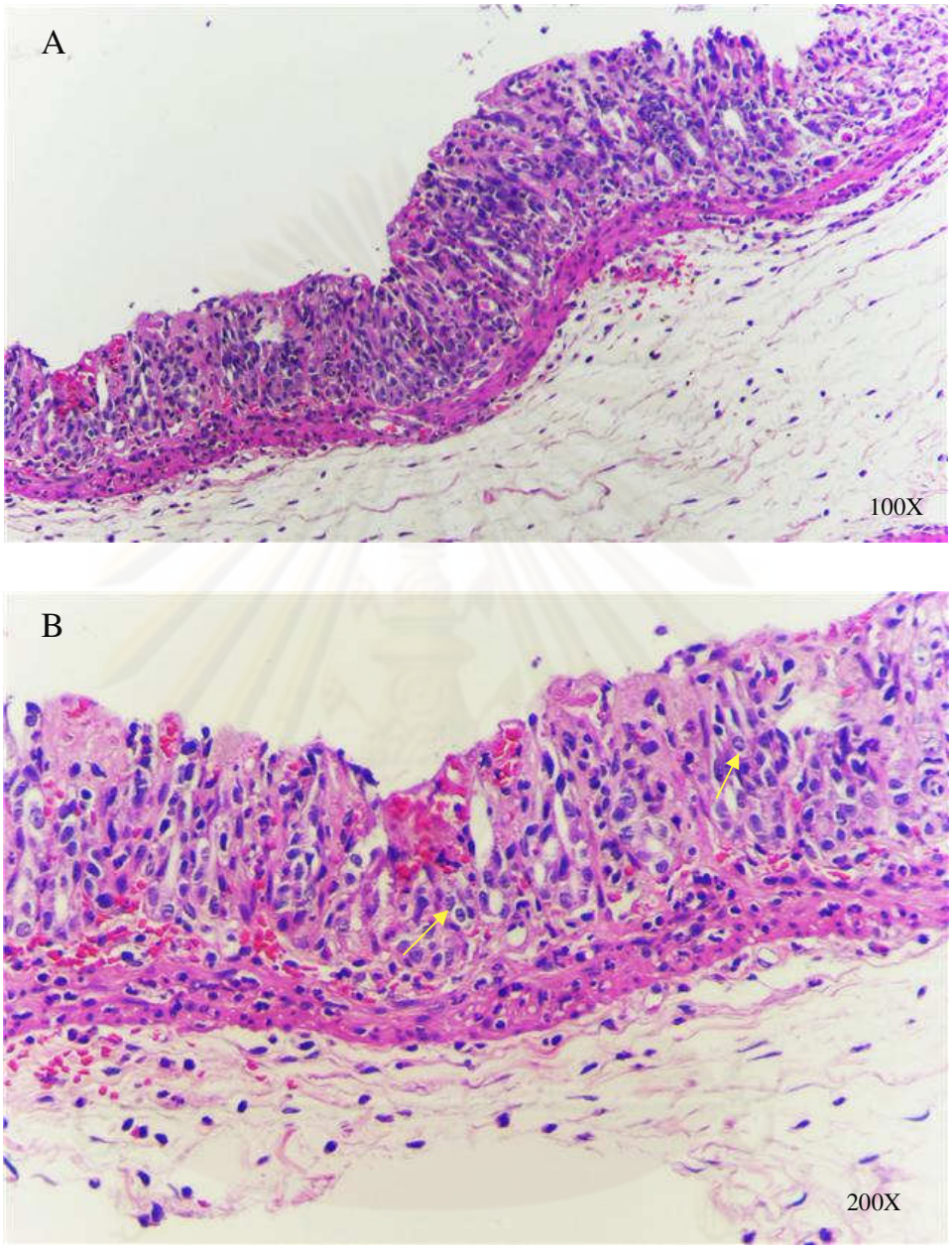

Figure 31 Hematoxylin-eosin stained stomach sections (100X and 200X). Indomethacin treated group (A and B) showed gastric ulcer and mild to moderate infiltration of inflammatory cells.

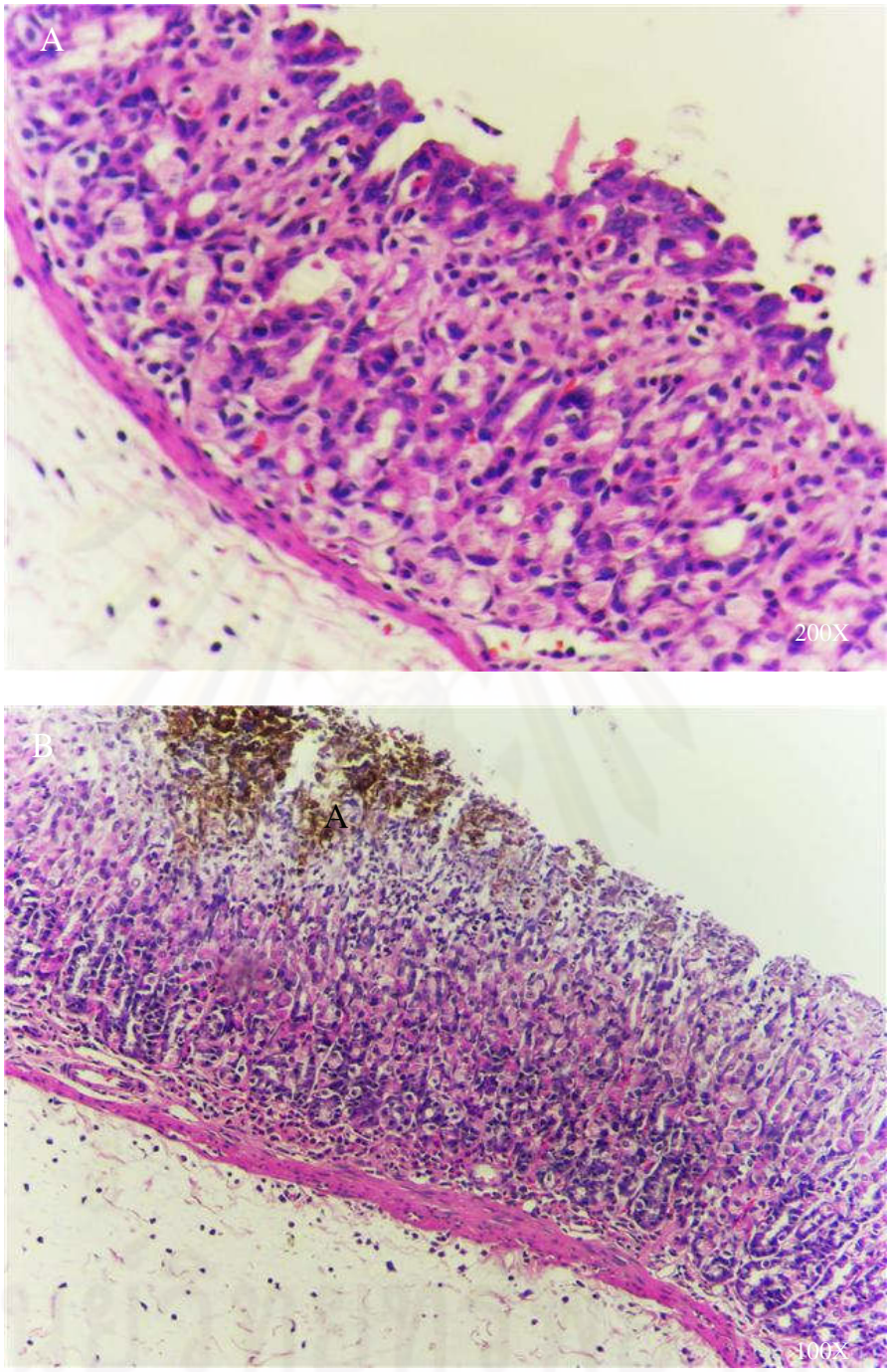

Figure 32 Hematoxylin-eosin stained stomach sections (200X and 100X). Indomethacin treated group (A and B) showed gastric ulcer and mild to moderate infiltration of inflammatory cells.

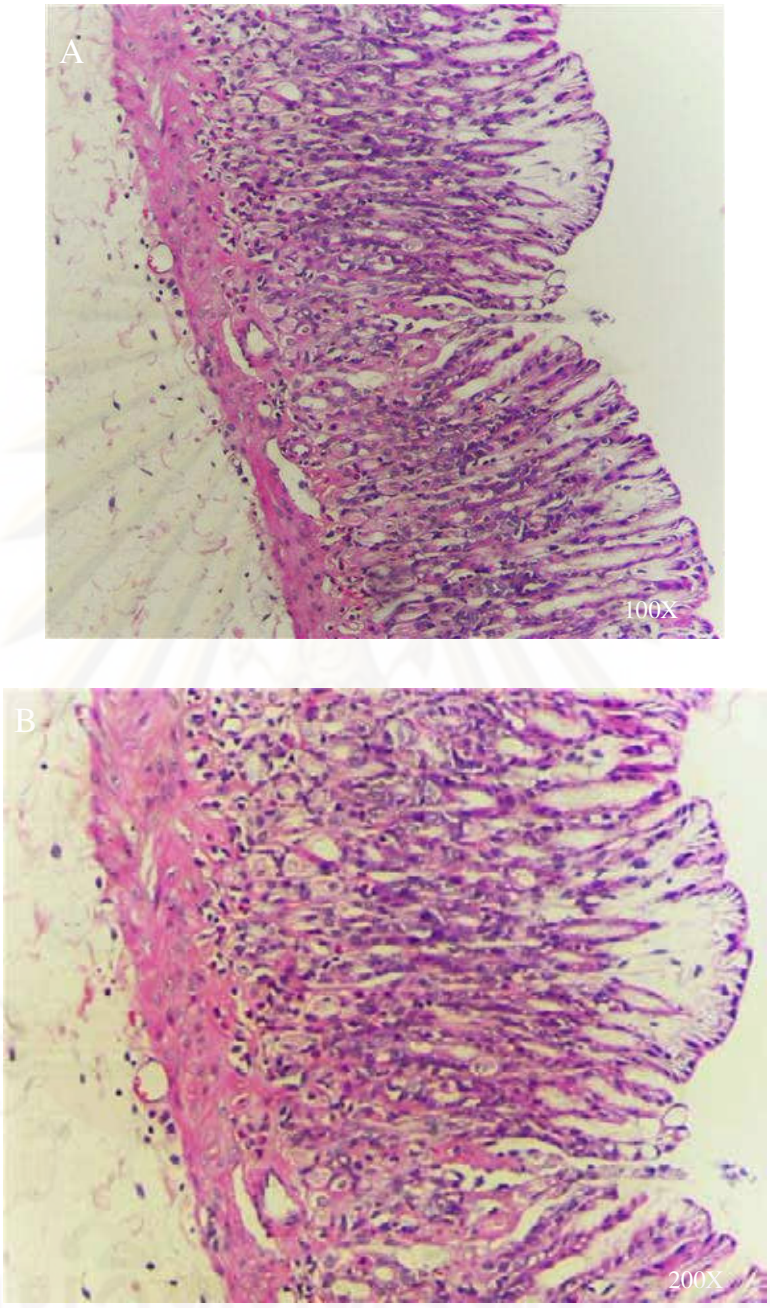

Figure 33 Hematoxylin-eosin stained stomach sections (100X and 200X). Pretreatment with curcumin group (A and B) showed examples of improvement in ulcer and inflammation.

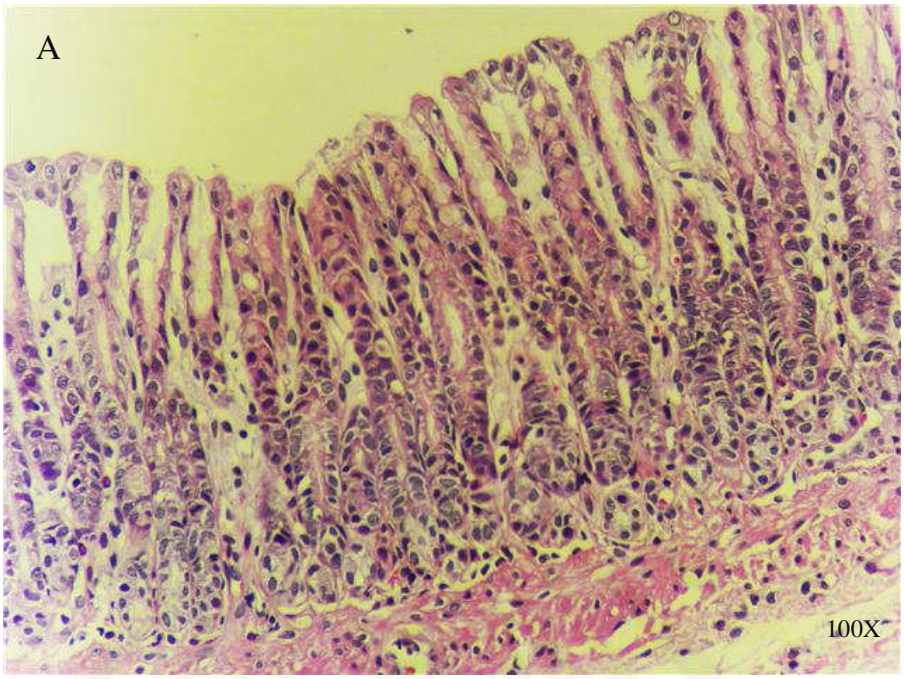

Figure 34 Hematoxylin-eosin stained stomach sections (100X). Pretreatmen with curcumin group (A) showed examples of protection in ulcer and inflammation.

Table 6 Summary of infiltration of inflammatory cells and erosion in all groups. Data are expressed as the number of rats exhibiting the grade of infiltration of inflammatory cells and erosion indicated.

Group	Number	Neutrophil infiltration[a]				pathology[b]		
		0	1	2	3	no erosion	erosion	ulcer
control	6	6	-	-	-	6	-	-
indomethacin	6	-	3	3	-	-	2	4
indomethacin+cur	6	4	2	-	-	4	2	-

[a]The severity of infiltration of inflammatory cells were grade by:

0 = no gastric mucosal injury

1 = neutrophil infiltration found 1/3 of gastric mucosal layer (mild)

2 = neutrophil infiltration found 2/3 of gastric mucosal layer (moderate)

3 = neutrophil infiltration found in the muscularis mucosae of gastric mucosal layer (severe)

[b]Pathology

Gastric erosions are superficial lesions involving the gastric mucosa; gastric ulcers extend through the mucosa and into the muscularis mucosa.

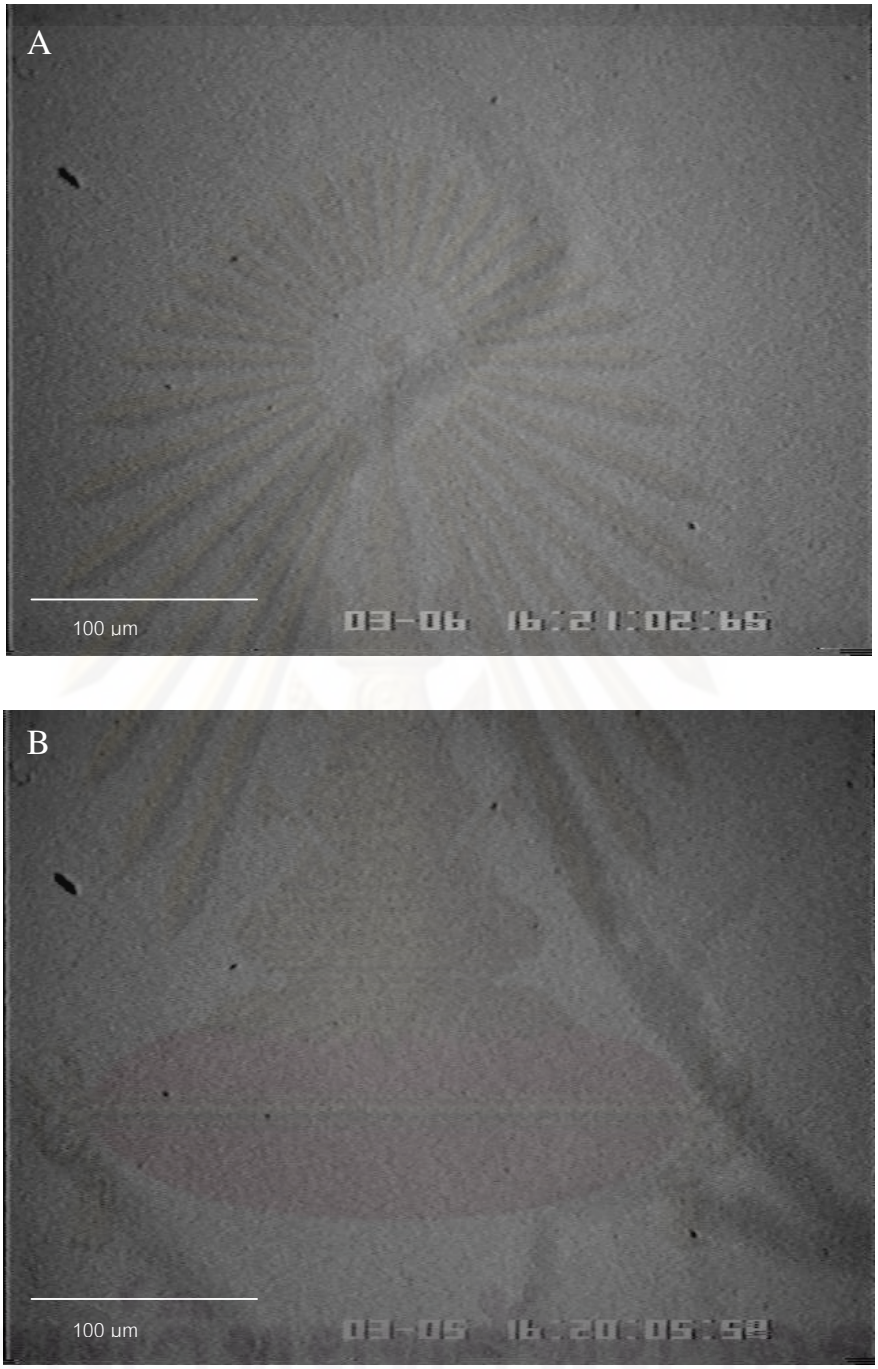

Figure 35 Sample of intravital microscopic (40X) images of leukocyte adherence on vascular endothelium of postcapillary venules by the time 10-15 minute after acridine orange injection in control group (A and B).

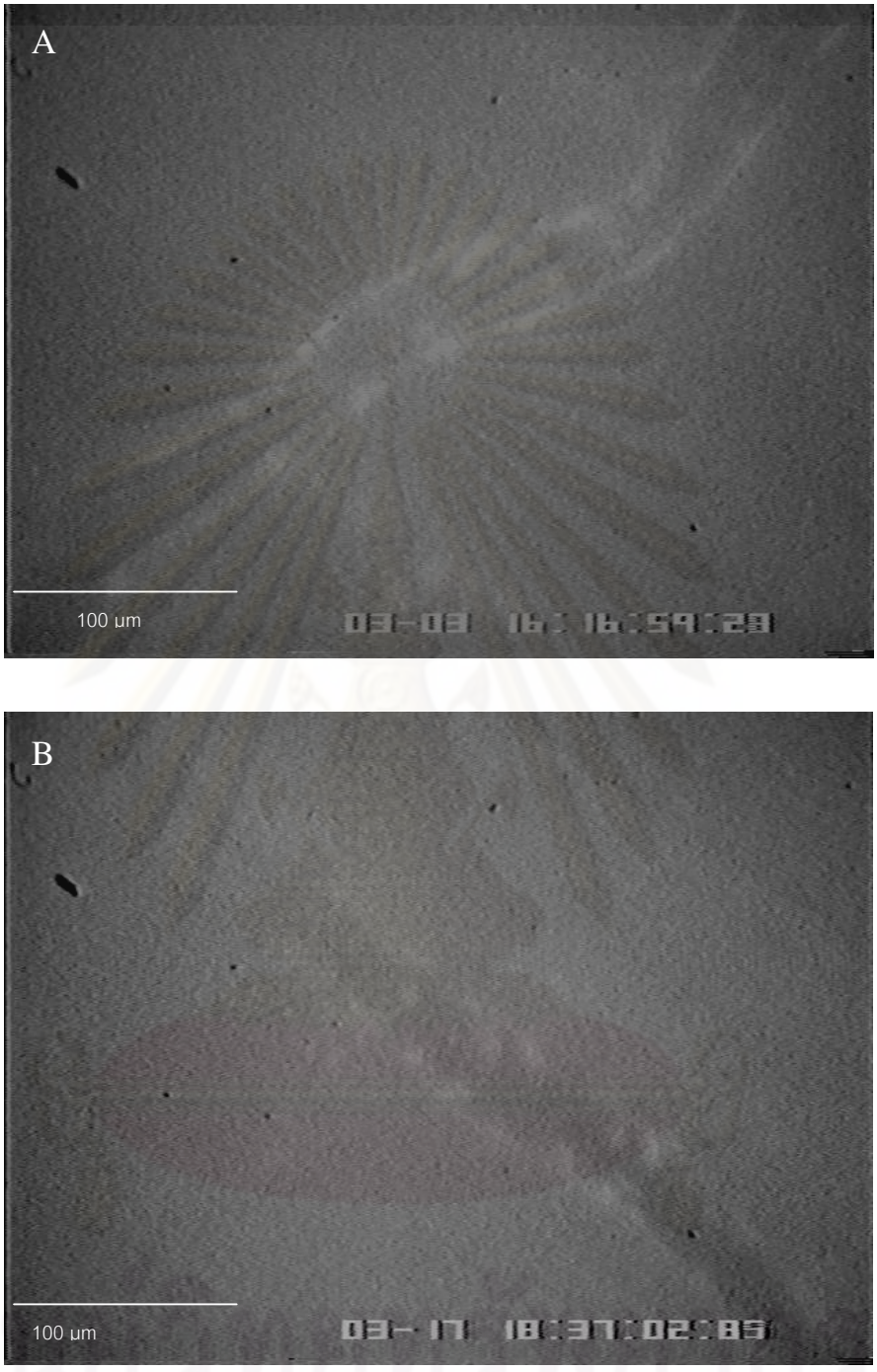

Figure 36 Sample of intravital microscopic (40X) images of leukocyte adherence on vascular endothelium of postcapillary venules by the time 10-15 minute after acridine orange injection in indomethacin group (A and B) (increased number of leukocyte adherence when compared control group).

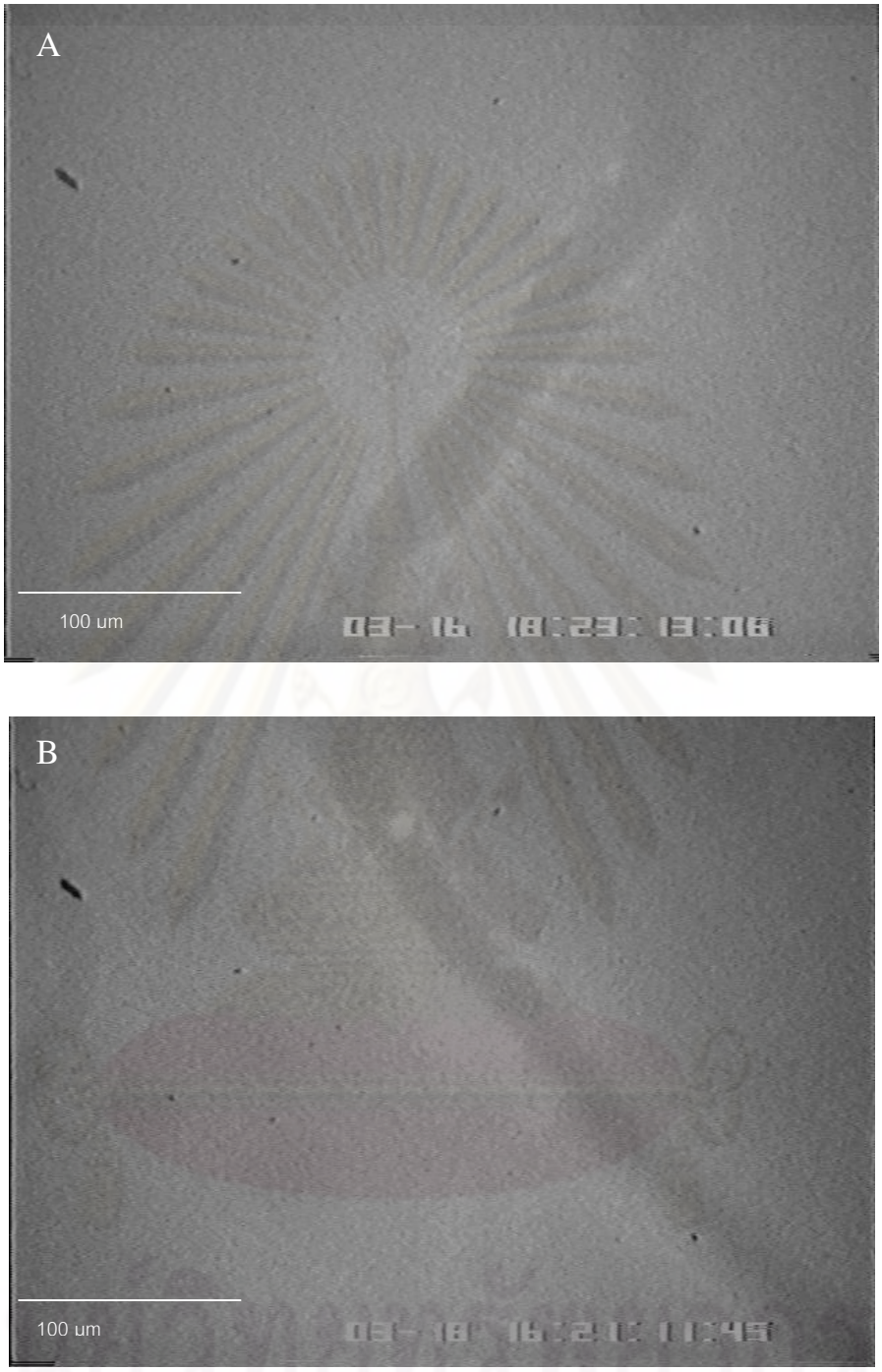

Figure 37 Sample of intravital microscopic (40X) images of leukocyte adherence on vascular endothelium of postcapillary venules by the time 10-15 minute after acridine orange injection in pretreatment with curcumin group (A and B) (decreased number of leukocyte adherence when compared indomethacin group).

Table 7 Summary of leukocyte adherence (cells/frame) in all groups at 10-15 min after acridine orange injection and Leukocyte adherence (cells/frame) by persons who was blinded to the experiment.

	Leukocyte adherence (cells/frame)	Leukocyte adherence (cells/frame) by persons who was blinded to the experiment.
Control group		
No 1	0	1
No 2	1	0
No 3	2	2
No 4	1	2
No 5	2	3
NSAIDs group		
No1	7	5
No 2	9	3
No 3	4	2
No 4	8	5
No 5	4	4
Curcumin+NSAIDs group		
No1	4	2
No2	3	1
No3	2	2
No4	3	1

Table 8 Summary of mean leukocyte adhesion (cells/frame) in all groups at 10-15 min after acridine orange injection. All data are expressed as mean±SD. The mean leukocyte adhesion were significantly higher in the indomethacin treated group when compared with control group (*p=0.000). Pretreatment with curcumin group decreased significantly mean leukocyte adhesion when compared with indomethacin (+p=0.007).

Group	Mean of leukocyte adhesion at 10-15 min (cells/frame)
Control (N=5)	1.20 ± 0.83
NSAIDs (N=5)	6.40± 2.30 *
NSAIDs+curcumin (N=4)	3.00±0.81 +

* p=0.000, significant difference as compared to control group

+ p=0.007, significant difference as compared to NSAIDs group.

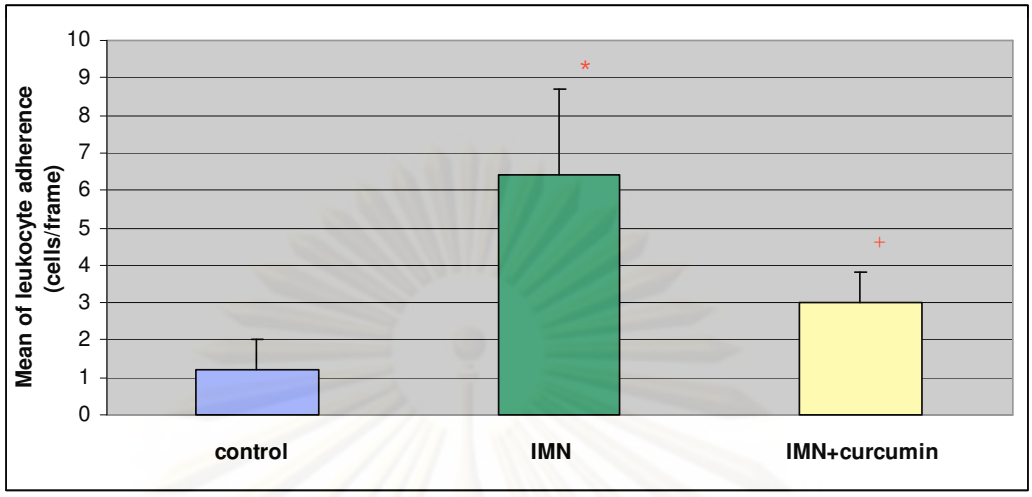

Figure 38 Mean leukocyte adhesion in all groups at 10-15 min after acridine orange injection. All data are expressed as mean±SD. The mean leukocyte adhesion were significantly higher in the indomethacin treated group when compared with control group (*p=0.000). Pretreatment with curcumin group decreased significantly mean leukocyte adhesion when compared with indomethacin (+p=0.007).

Table 9 Summary of mean leukocyte adhesion (cells/frame) in all groups at 10-15 min after acridine orange injection. All data are expressed as mean±SD. The mean leukocyte adhesion were significantly higher in the indomethacin treated group when compared with control group (*p=0.008). Pretreatment with curcumin group decreased significantly mean leukocyte adhesion when compared with indomethacin (+p=0.009). All images were evaluated by persons who was blinded to the experiment.

Group	Mean leukocyte adhesion at 10-15 min (cells/frame)
Control (N=5)	1.60±1.14
NSAIDs (N=5)	3.80±1.30 *
NSAIDs+curcumin (N=4)	1.50±0.57 +

* p=0.008, significant difference as compared to control group

+ p=0.009, significant difference as compared to NSAIDs group.

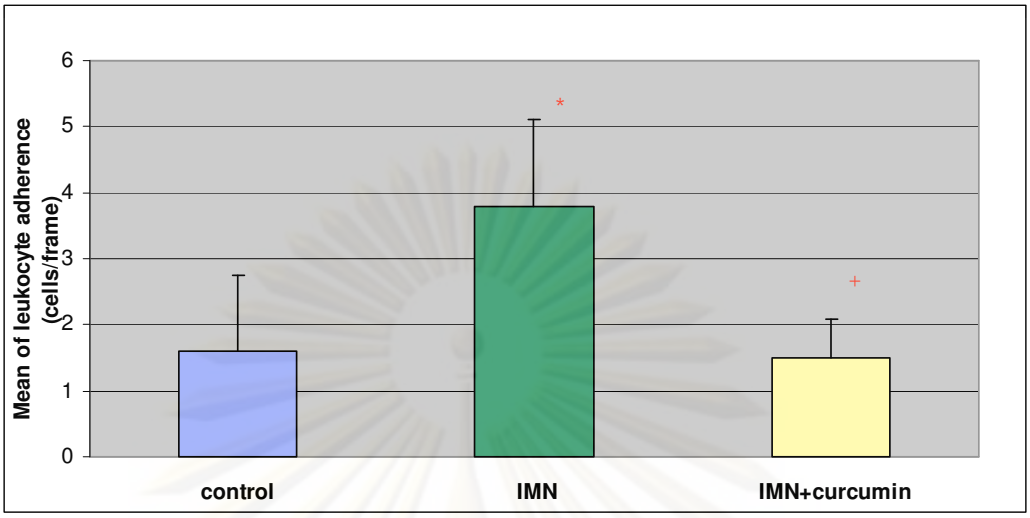

Figure 39 Mean leukocyte adhesion in all groups at 10-15 min after acridine orange injection. All data are expressed as mean±SD. The mean leukocyte adhesion were significantly higher in the indomethacin treated group when compared with control group (*p=0.008). Pretreatment with curcumin group decreased significantly mean leukocyte adhesion when compared with indomethacin (+p=0.009). All images were evaluated by persons who was blinded to the experiment.

Table 10 Mean ± SD of hemodynamic parameters, systolic blood pressure (SBP), diastolic blood pressure (DBP), mean arterial pressure (MAP), and heart rate (HR) of all experimental groups.

Group	DBP (mmHg)	SBP (mmHg)	MAP (mmHg)	HR (beats/min)
Control (N=3)	113.33 ±12.58	141.66± 24.66	122.77± 16.01	340.00 ± 34.64
NSAIDs (N=3)	114.33 ± 21.12 ^{ns}	131.66± 28.43 ^{ns}	118.86± 22.19 ^{ns}	380.00 ± 34.64 ^{ns}
NSAIDs+curcumin (N=3)	128.33± 23.62 $^{\#ns}$	145± 26.45 $^{\#ns}$	131.6 ± 16.7 $^{\#ns}$	380.00 ± 34.64 $^{\#ns}$

^{ns} p>0.05, No significant difference as compared to control group

$^{\#ns}$ p>0.05, No significant difference as compared to NSAIDs group

Standard TNF-α (pg/ml)	Obtical density (O.D.) (450 nm-540 nm)		Average O.D.	Corrected O.D.
	Data 1	Data 2		
0	0.050	0.054	0.052	-
12.5	0.097	0.099	0.098	0.046
25	0.135	0.132	0.133	0.081
50	0.206	0.210	0.208	0.156
100	0.388	0.398	0.393	0.341
200	0.740	0.720	0.730	0.678
400	1.298	1.224	1.261	1.209
800	2.050	2.063	2.056	2.004

Table 11 The corrected O.D. plotted on y-axis of standard curve was calculated from the mean subtract the average of zero standard O.D. Note: pg/ml = picogram per milliliter; nm = nanometer

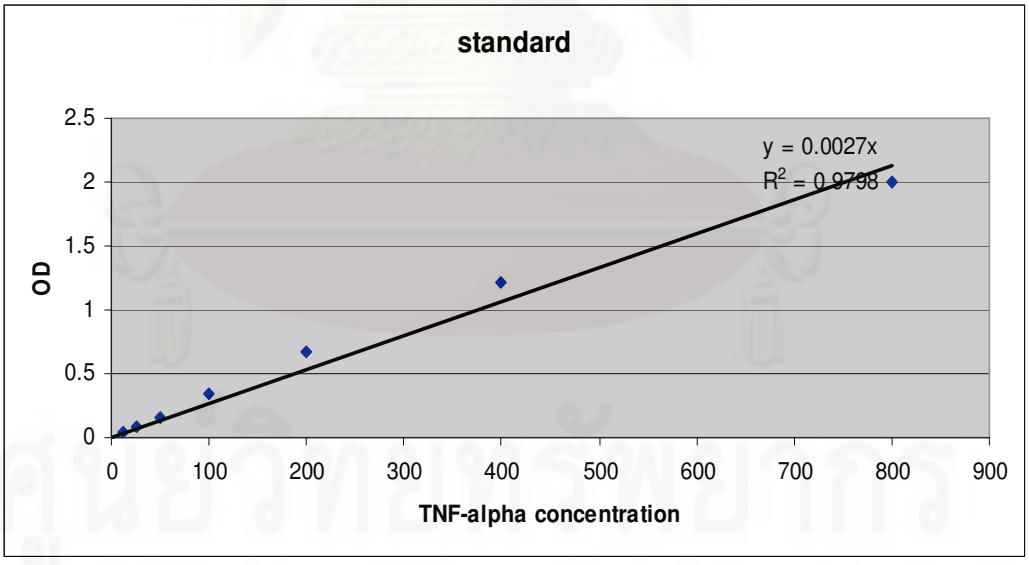

Figure 40 Standard curve of TNF-α: The x-axis and y-axis of the standard curve represented standard TNF-α concentrations (pg/ml) and O.D., respectively.

Table 12 Summary of serum of TNF-α. All data are expressed as mean±SD. The serum of TNF-α were increased in the indomethacin treated group when compared with control group. Pretreatment with curcumin decreased serum of TNF-α when compared with indomethacin.

Group	serum of TNF-α (pg/ml)
Control (N=6)	73.85± 83.00
NSAIDs (N=6)	154.66 ± 166.03 [ns]
NSAIDs+curcumin (N=6)	78.4± 89.55 [#ns]

[ns] p=0.258, No significant difference as compared to control group

[#ns] p=0.284, No significant difference as compared to NSAIDs group

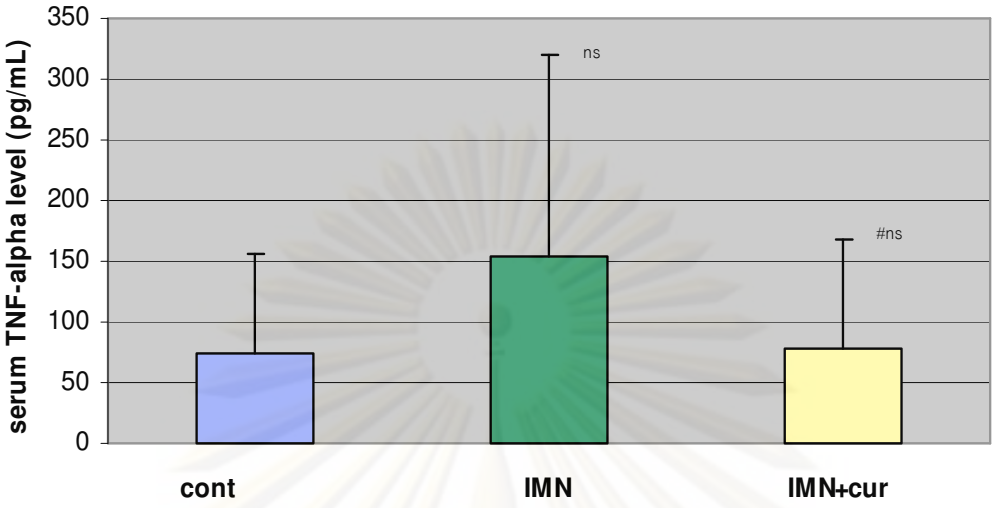

Figure 41 Serum TNF-α level in all groups. All data are expressed as mean±SD. The mean of TNF-α were increased in the indomethacin treated group when compared with control group. Pretreatment with curcumin decreased serum of TNF-α when compared with indomethacin.

[ns] p=0.258, No significant difference as compared to control group

[#ns] p=0.284, No significant difference as compared to NSAIDs group.

Standard ICAM-1 (pg/ml)	Obtical density (O.D.) (450 nm-540 nm)		Average O.D.	Corrected O.D.
	Data 1	Data 2		
0	0.073	0.057	0.065	-
31.2	0.136	0.119	0.127	0.062
62.5	0.191	0.189	0.190	0.125
125	0.307	0.294	0.300	0.235
250	0.585	0.550	0.567	0.502
500	0.677	0.646	0.661	0.596
1000	1.785	1.713	1.749	1.684
2000	2.215	2.395	2.305	2.24

Table 13 The corrected O.D. plotted on y-axis of standard curve was calculated from the mean subtract the average of zero standard O.D. Note: pg/ml = picogram per milliliter; nm = nanometer

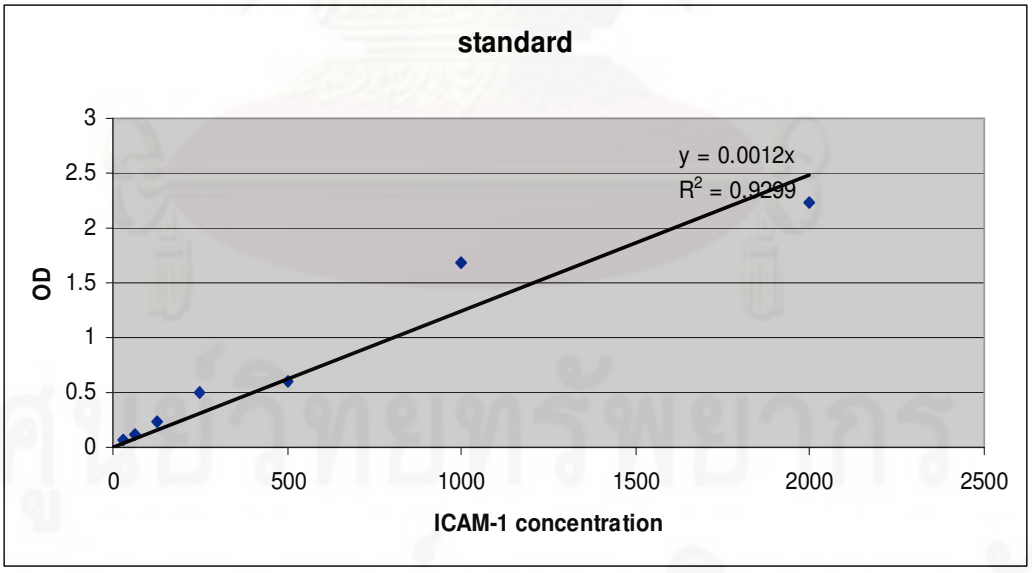

Figure 42 Standard curve of ICAM-1: The x-axis and y-axis of the standard curve represented standard ICAM-1 concentrations (pg/ml) and O.D., respectively

Table 14 Summary of serum of ICAM-1. All data are expressed as mean±SD. The serum of ICAM-1 were significantly higher in the indomethacin treated group when compared with control group (*p=0.001). Pretreatment with curcumin decreased significantly serum of ICAM-1 when compared with indomethacin ($^{+}$p=0.002).

Group	Serum of ICAM-1 (pg/ml)
Control (N=6)	336.93 ± 224.82
NSAIDs (N=6)	1106.50 ± 504.22 *
NSAIDs+curcumin (N=6)	413.66 ± 147.74 +

* p=0.001, significant difference as compared to control group

+ p=0.002, significant difference as compared to NSAIDs group

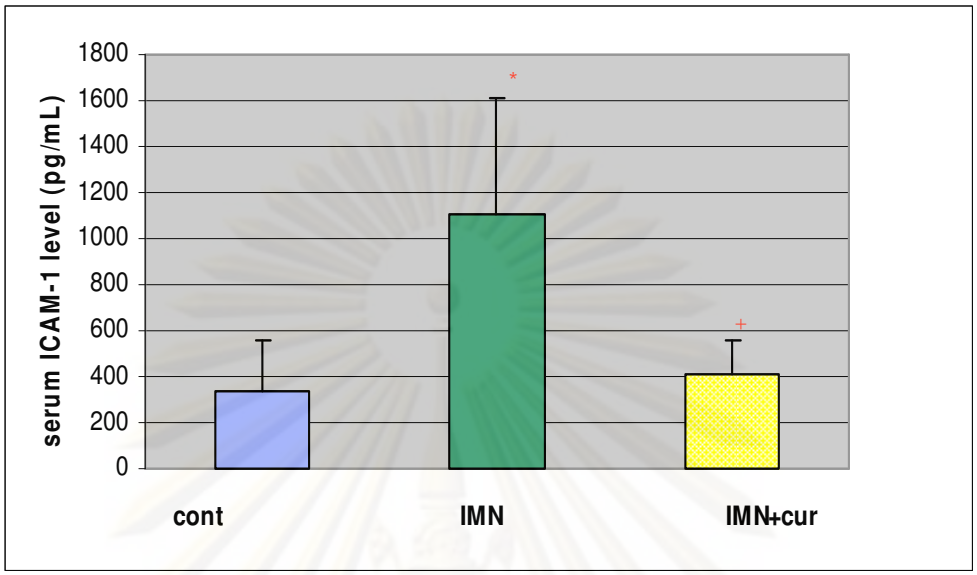

Figure 43 Serum ICAM-1 level in all groups. All data are expressed as mean±SD. The mean ICAM-1 level were significantly increased in the indomethacin treated group (NSAIDs) when compared with control group (*p=0.001). Pretreatment with curcumin decreased significantly ICAM-1 level when compared with indomethacin ($^{+}$p=0.002).

CHAPTER V

DISCUSSION AND CONCLUSION

The present study found that the stomach pathology in NSAIDs group revealed mild to moderate inflammation as well as showed gastric ulcer and leukocyte endothelium interaction. Pretreatment with curcumin treatments resulted in improving stomach pathology, decreasing ICAM-1 and leukocyte endothelium interaction.

Effect of NSAIDs on leukocyte-endothelium interaction in gastric microcirculation in rats

We investigated the effects of curcumin on indomethacin-induced gastric injury in rats. The results clearly demonstrate that pretreatment of curcumin prevents the ulcerogenic effect of indomethacin. In this study, after gastric injury was induced by NSAIDs, gastric inflammation increased leukocyte adherence to the endothelial surface of postcapillary venules and was characterized by the migration of macrophages and PMNs in the ulcer area. The migrated macrophages then released proinflammatory cytokines can up-regulate adhesion molecule expression on endothelial cells and leukocytes (Pober, 1989) and cause leukocyte recruitment. Adhesion molecules on endothelial cells and leukocytes involve rolling, adhesion, and transmigration of leukocytes in gastric inflamed areas. Neutrophils play an important role in the development of inflammation and tissue injury by releasing a variety of inflammatory mediators, including neutrophil elastase and reactive oxygen species. Since these inflammatory mediators are capable of producing tissue injury, they may be involved in the pathogenesis of indomethacin-induced gastric mucosal injury. Among these mediators, neutrophil elastase has been demonstrated to play an important role in neutrophil infiltration and neutrophil-induced tissue injury.

A limitation of leukocyte endothelium interaction in this study was deserved discussion. It had to consider important number of rat that NSAIDs differ from many parameter including: 1) technical of leukocyte endothelium interaction study made a difficult in other parameter. ; 2) leukocyte adherence in stomach was observed by *in vivo* microscopy.

Our study showed the increase of leukocyte-endothelium interaction at 10-15 min after acridine orange injection in indomethacin group and was decreased in the pretreatment with curcumin group.

Effect of NSAIDs on stomach histopathology in rats

The pathological changes of gastric injury range from NSAIDs to inflammation and gastric ulcer. In the present study, the stomach in NSAIDs group showed gastric ulcer and moderate infiltration of inflammatory cells inflammation.

Gastric mucosal damage as a result of treatment with nonsteroidal anti-inflammatory drugs (NSAID) is recognized as the most serious adverse reaction to this class of compounds and has been the stimulus behind much of the research in the past decade aimed at developing more effective gastroprotective compounds. Parenteral administration of a variety of NSAID, including indomethacin and acetylsalicylic acid, represents a very simple and effective animal model for studying the mechanisms underlying NSAID-induced gastropathy (Schoen et al., 1989).

The literature indicates that NSAID induce gastric damage by at least two separate mechanisms. One is the well-characterized effect of NSAID to block cyclooxygenase and there by inhibit endogenous prostaglandin production. The second mechanism is called ion trapping and results from the acid dissociation of NSAID (pKa=3.5-4.0) in the comparatively neutral (pH=7.0) intracellular environment of mucosal cells. In the ionized state, NSAID are water soluble and become trapped inside the cell, creating a concentration gradient that favors the movement of dissociated ions of weak organic acids (NSAID) into the gastric mucosa. Cell permeability alterations and damage result as hydrogen ions influx while sodium and potassium ions move into the gastric lumen. Buffering intraluminal pH to 6.0-7.0 diminishes NSAID- induced gastric damage and this property has been exploited in the manufacture of various buffered NSAID (Schoen et al., 1989).

Although it has been proposed that the mechanism by which NSAIDs induce this gastric mucosal injury is via ability to inhibit cyclooxygenase (COX)- mediated produation of protective prostaglandins, several lines of evidence suggest that the mechanism may be more complex than originally thought. For example, Ligumsky et al.

have shown that inhibition of prostaglandin production by >95% via rectal administration of certain NSAIDs did not induce gastric ulcer (Ligumsky et al., 1990). In addition, recent studies by Langenbach et al. demonstrate that homologous recombination to disrupt the *Ptgs 1* gene encoding for COX-1 in mice does not result in spontaneous gastric ulcers (Langenbach et al., 1995). In fact, these COX-1 deficient animals are less sensitive to NSAID- induced gastropathy than their age- matched wild- type controls.

A limitation of NSAIDs model in this study was deserved discussion. It had to consider important high dose that NSAIDs differ from many experiments including: 1) strain of rat made a difference in NSAIDs-induced gastric injury; 2) this study employed NSAIDs a like of patient in hospital.

Effect of NSAIDs on TNF-α level of rats

Ulcerative lesions of the gastrointestinal tract of the gastrointestinal tract are one of the major side effects of nonsteroidal anti-inflammatory drugs (NSAIDs) (Ivey, 1988). Although the mechanism of NSAID-induced gastric injury generally believed to be related to the ability of these agents to inhibit gastric prostaglandin generation, evidence that polymorphonuclear neutrophil leukocyte (PMNs) adherence to the vascular endothelium is one of the early and pivotal events in the process of NSAID- induced mucosal injury is accumulating, at least in experimental models.

Tumor necrosis factor (TNF) α is a pleiotropic cytokine with potent proinflammatory activity. TNF has been show to up-regulate the expression of cell surface adhesion molecules on both circulating PMN and endothelial cells and so to favor the binding of PMN to the vessel at sites of inflammation. Because previous investigations have shown that indomethacin administration to rats causes a marked increase in TNF plasma levels that correlates with the extent of the gastric PMN margination and mucosal damage, we postulated that substances that regulate either the synthesis or the release of TNF could influence the effect that indomethacin exert on the gastric mucosa (Bevilacqua,1987).

NF-ĸB plays an important role in the expression of a large number of inducible genes, many of which contribute to the cellular responses to stress, injury and inflammation. Consequently, NF-ĸB can be activated by signals that are associated with

such states, including cytokines (such as IL-1 and TNF-α), bacterial endotoxins, and pro-apoptotic and necrotic stimuli such as oxygen free radicals, u.v. light and gamma-irradiation. When cells are exposed to these pathogenic stimuli, a cascade of events leads to the phosphorylation and subsequent degradation of IκB, resulting in NF-κB liberation and its entry into the nucleus, where it activates gene expression. NF-κB activation is triggered by the phosphorylation and subsequent conjugation of IκB with ubiquitin, which makes IκB a substrate for degradation by the proteasome proteolytic pathway. Peptide aldehyde inhibitors of the proteasome such as calpain inhibitor 1 and MG-132 (Brown et al., 1995) have been shown to block the degradation of IκB and consequent activation of NF-κB that is elicited by TNF-α.

A limitation of TNF-α study in this study was deserved discussion. It had to consider important no significant that study differ from many experiments including: 1) low number of rat made a difference in TNF-α study; 2) this study employed serum of rat.

Our study showed the increase of serum TNF-α level in indomethacin group and decrease in the pretreatment with curcumin group.

Effect of NSAIDs on ICAM-1 level in rats

Increasing evidence implicates a role for vascular mechanisms in gastric mucosal injury. Recent attention has particularly focused on the importance of polymorphonuclear leukocytes (PMNs) in the pathogenesis of acute gastric mucosal injury induced by a variety of factors, including ethanol, ischemia- reperfusion and particularly nonsteroidal anti-inflammatory drugs (NSAIDs) (Jacobson, 1992) . Wallace et al. (Wallace et al.,1990) demonstrated that depletion of PMN by pretreatment with antineutrophil antiserum significantly reduced macroscopic injury and completely prevented vascular injury induced by indomethacin or naproxen in rats. Aspirin induced injury has also been shown to be associated with PMN. This study found that depletion of PMN in rats with antineutrophil antiserum or methotrexate significantly reduced macroscopic mucosal injury induced by aspirin (Lee et al., 1992).

It is becoming increasingly apparent that neutrophilic polymorphonuclear leukocytes (PMNs) may play an important role in the pathogenesis of NSAIDs-induced

gastropathy. Wallace and colleagues (Wallace et al.,1993) have demonstrated that NSAID-induced gastric ulcerations may be attenuated by rendering animals neutropenic or by infusing blocking antibodies directed against CD18, intercellular adhesion molecule 1 (ICAM-1), P- selectin, and to a lesser extent E- selectin. The latter findings suggest that NSAIDs may enhance the expression of cell adhesion molecules on the surface of endothelial cells. Qualitative data that support this possibility were provided by immunohistochemical experiments that demonstrate an increased staining of gastric venules for ICAM-1 30 min after oral administration of indomethacin (Andrews et al., 1994). The mechanisms by which adhesion of PMNs to postcapillary venules induces gastric epithelial cell injury are not at all clear. There has been some suggestion that leukocyte adhesion and aggregation occludes the microvasculature, resulting in ischemic mucosal injury.

Our study showed the increase of serum ICAM-1 level in indomethacin group and decrease in the pretreatment with curcumin group.

Anti-oxidant and anti-inflammation effect of curcumin in rats with NSAIDs

Curcuma, a genus in the plant family of Zingiberacea,is the biological source for curcuminoids, including curcumin. *Curcuma longa*, the yellow tuberous root that is referred to as turmeric, was taken from India to Southeast Asia, China, North Australia, West Indies and South America. Subsequently, its cultivation spread to many African countries. The yellow pigmented fraction of *Curcuma longa* contains curcuminoids, which are chemically related to its principal ingredient, curcumin. The three main curcuminoids isolated from turmeric are curcumin, demethoxy curcumin and bisdemethoxy curcumin.

Curcumin is very rich in phenolics, they are known to possess antioxidant properties. Curcumin could reduce gastric injury was induced by NSAIDs. It has been reported that curcumin can decrease gastric injury that indomethacin inactivates gastric peroxidase to induce reactive-oxygen-mediated gastric damage and curcumin protects it by preventing peroxidase inactivation and scavenging reactive oxygen (Ishita et al., 2006). According to NF-κB involving inflammation, NF-κB has been showed to be inhibited by curcumin *in vitro* and *in vivo* studies. Curcumin has been observed to

suppress TNF-α induced NF-κB activation in human myeloid ML-1a cells (Singh and Aggarwal, 1995). The data exhibited that curcumin can directly inhibit NF-κB activation. Reyes-Gordillo and co-workers also reported that curcumin was able to avoid NF-κB translocation to the nucleus induced by CCl_4 administration as a result of decreased inflammatory cytokines such as TNF-α, IL-1β (Reyes-Gordillo et al., 2007). All these studies showed that curcumin is an anti-inflammation substance because it can inhibit the activation of the major transcription factor NF-κB. This transcription factors required for the expression of many proinflammatory genes, such as TNF-α, IL-1β, iNOS and COX-2 (Singh et al., 1995). There are currently limited studies investigatiog the effect of curcumin on anti-inflammation action in the gastric microcirculation on NSAIDs-induced gastric injury in rats.

Conclusion, in this study, we found that curcumin could attenuate gastric injury induced by indomethacin through improved gastric injury, ICAM-1 level, TNF-α level and decrease leukocyte-endothelium interaction.

In conclusion, this study proved that curcumin had an anti-inflammatory property. We found that curcumin could attenuate gastric injury induced by indomethacin through the decrease of ICAM-1 level, decrease leukocyte-endothelium interaction, reduction gastric inflammation and peptic ulcer. The usefulness of curcumin might be applied for the prevention of NSAIDs induced peptic ulcer in clinical practice.

REFERENCES

Andrews FJ, Malcontenti-Wilson C, O' Brien PE. Effect of nonsteroidal anti-inflammatory drugs on LFA-1 and ICAM-1 expression in gastric mucosa. Am J Physiol 266 (1994) : G657-64.

Appleyard CB, McCafferty DM, Tigley AW, Swain MG, Wallace JL. Tumor necrosis factor mediation of NSAIDs induced gastric damage: role of leukocyte adherence. Am J Physiol 270 (1996) : 42-48.

Asako H, Kubes P, Wallace J, Gaginella T, Wolf RE, Granger DN. Indomethacin-induced leukocyte adhesion in mesenteric venules: role of lipoxygenase products. Am J Physiol 262 (1992) : G903–G908.

Armstrong CP, Blower AL. Non-steroidal anti-inflammatory drugs and life threatening complications of peptic ulceration. Gut 28 (1987) : 527-32.

Bassi V, Vitale M, Feliciello A, De Riu S, Rossi G, Fenzi G. Retinoic acid induces intercellular adhesion molecule-1 hyperexpression in human thyroid carcinoma cell lines. J Clin Endocrinol Metab 80 (1995) : 1129-1135.

Beutler B, Greenwald D, Hulmes JD, Chang M, Pan YC, Mathison J, Ulevitch R, Cerami A. Identify of tumor necrosis factor and the macrophage-secreted factor cachectin. Nature 316 (1985) : 552-554.

Bevilacqua MP, Pober JS, Mendick DL, Cotran RS,Gimbrone MA. identification of an inducible endothelial-leukocyte adhesion molecule. Proc Natl Acad Sci USA 84 (1987) : 9238-9242.

Bharti AC, Donato N, Singh S, Aggarwal BB. Curcumin (diferuloylmethane) down-regulates the constitutive activation of nuclear factor-kappa B and Ikappa Balpha kinase in human multiple myeloma cells, leading to suppression of proliferation and induction of apoptosis. Blood 101 (2003) : 1053-1062.

Bierhaus A, Zhang Y, Quehenberger P, Luther T, Haase N, Muller M, Mackman N, Ziegler R, and Nawroth PP. The dietary pigment curcumin reduced endothelial tissue factor gene expression by inhibition binding of AP-1 to the DNA and activation of NF-kappa B. Thromb Haemost 77 (1997) : 772-782.

Bjorkman DJ. Current status of nonsteroidal anti-inflammatory drugs (NSAID) use in the United States: risk factors and frequency of complication. Am J Med 107 (1999) : 3S-8S.

Brendan, JR. Gastrointestinal effects of nonsteroidal anti-inflammatory drugs. Fundamental & Clinical Pharmacology 17 (2003) : 301-313.

Burdan F, Szumilo J, Klepacz R, Dudka J, Korobowicz A, Tokarska E, Cendrowska-Pinkosz M. Gastrointestinal and hepatic toxicity of selective and non-selective cyclooxygenase-2 inhibitors in pregnant and non-pregnant rats. Pharmacol Res 50 (2004) : 533-543.

Cerami A, Beutler B. The role of cachectin/TNF in endotoxic shock and cachexia. Immunol Today 9 (1988) : 28-31.

Chan, MM. Inhibition of tumor necrosis factor by curcumin, a phytochemical. Biochem Pharmacol 49 (1995) : 1551-1556.

Cornelius LA, Taylor JT, Degitz K, Li LJ, Lawley TJ, Caughman SW. A 5' portion of the ICAM-1 gene confers tissue-specific differential expression levels and cytokine responsiveness. J Invest Dermatol 100 (1993) : 753-758.

Davenport HW. Salicylate damage to the gastric mucosal barrier. N Engl J Med 276 (1967) : 1307-12.

Ding SZ, Lam SK, Yuen ST, Wong BC, Hui WM, Ho J, Guo X, Cho CH. Prostaglandin, tumor necrosis factor-alpha and neutrophils : causative relationship in indomethacin-induced stomach injuries. Eur J Pharmacol 348 (1998) : 257-263.

Dixon MF, Genta RM, Yardley JH, Correa P. Classification and grading of gastritis: the update Sydney system. Am J Surg Pathol 20 (1994) : 1161-1181.

Douthwaite AH, Lintott GAM. Gastroscopic observation of effect of aspirin and certain other substances on stomach. Lancet 2 (1983) : 1222-5.

Elliott SN, McKniqht W, Cirino G, Wallace JL. A nitric oxide-releasing nonsteroidal anti-inflammatory drug accelerates gastric ulcer healing in rats. Gastroenterology 109 (1995) : 524-30.

Ferreira SH. Peripheral analgesic sites of action of anti-inflammatory drugs. Int J Clin Pract 128 (2002) : 2-10.

Fries J.F, Miller SR, Spitz PW, Williams CA, Hubert HB, Bloch DA. Toward an epidemiology of gastropathy associated with non- steroidal anti-inflammatory drug use. Gastroenterology 96 (1989) : 647-655.

Fromm D. How do non-steroidal anti-inflammatory drugs affect gastric mucosal defenses? Clin Invest Med 10 (1987) : 251-58.

Gaboury JP, Kubes P. Reductions in physiological shear stress lead to CD11/CD18-dependent, selectin- independent leukocyte rolling *in vivo*. Blood 83 (1994) : 345-350.

Gabriella C, Nicola Venturi, Silvana Spaggiari. Gastrointestinal safety of novel nonsteroidal antiinflammatory drugs: selective COX-2 inhibitors and beyond. Acta Biomed 78 (2007) : 96-110.

Georges H, William A. Tumor necrosis factor (TNF)-α and TNF receptors in viral pathogenesis. PSEBM 223 (2000) : 241-257.

Gupta B, Ghosh B. Curcuma longa inhibits TNF-alpha induced expression of adhesion molecules on human umbifical vein endothelial cell. Int J Immunopharmacol 21 (1999) : 745-77.

Hideo U, Keiji Y, Tetsuhiro S, Ken-ichi Y, Ryota S, Takashi Y, Masazumi T. Noninvasive mapping of reactive oxygen species by in vivo electron spin resonance spectroscopy in indomethacin induced gastric ulcers in rats. J Pharmacol Exp Ther 317 (2006) : 228-235.

Hudson N, Balsitis M, Everitt S, Hawkey CJ. Enhanced gastric mucosal leukotriene B4 synthesis in patients taking non- steroidal anti-inflammatory drugs. Gut 34 (1993) : 742-7.

Ishita C, Uday B, Kaushik B, Pallab M, Ranajit KB. Indomethacin inactivates gastric peroxidase to induce reactive-oxygen-mediated gastric mucosal injury and curcumin protects it by preventing peroxidae inactivation and scavenging reactive oxygen. Free Radic Biol Med 40 (2006) : 1397-1408.

Ivey KJ. Mechanism of NSAID-induced gastric damage: actions of the therapeutic agents. Am J Med 84 (1988) : 41-48.

Jacobson, ED. Circulatory mechanisms of gastric mucosal damage and protection. Gastroenterology 102 (1992) : 1788-1800.

Jaruga E, Salvioli S, Dobrucki J, Chru S, Bandorowicz- Pikula, Sickora E, Franceschi C, Cossarizza A, Bartosz G. Apoptosis- like, reverible changes in plasma membrane asymmetry and permeability, and transient modifications in mitochondrial membrane potential induced by curcumin in rat thymocytes. FEBS Lett 433 (1998) : 287-293.

Joe B, Lokesh B R. Effect of curcumin and capsaicin on arachidonic acid metabolism and lysosomal enzyme secretion by rat peritoneal macrophages. Lipids 32 (1997) : 1173-1180.

Johnson, L. R. 1997. Gastrointestinal physiology. Fifth edition: Mosby-year Book.

Jorgensen TG, Weis- Fogh US, Nielsen HH, Olesen HP. Salicylate and aspirin- induced uncoupling of oxidative phosphorylation in mitochondria isolated from the mucosal membrane of the stomach. Scand J Clin Lab Invest 36 (1976) : 649-54.

Kelly JP, Kaufman DW, Jurgelon JM, Sheehan J, Koff RS, Shapiro S. Risk of aspirin-associated major upper-gastrointestinal bleeding with enteric-coated or buffered product. Lancet 348 (1996) : 1413-16.

Kenneth A, Alison F. Regulation of intercellular adhesion molecule-1 (CD54) gene expression. J Leukoc Biol 66 (1999) : 876-888.

Klinkenberg-Knol EC, Nelis F, Dent J, Snel P, Mitchell B, Prichard P, Lloyd D, Havu N, Frame MH, Roman J, Walan A. Long-term omeprazole treatment in resistant gastroesophageal reflux disease: Efficacy, safety, and influence on gastric mucosa. Gastroenterology 118 (2000) : 661-669.

Korthuis RJ, Anderson DC, Granger DN. Role of neutrophil-endothelial cell adhesion in inflammatory disorders. J Crit. Care 9 (1994) : 47–71.

Kunchandy E, Rao MNA. Oxygen radical scavenging activity of curcumin. Int J Pharmaceut 58 (1990) : 237-240.

Kurose I, Pothoulakis C, La Mont JT, Anderson DC, Paulson JC, Miyasaka M, Wolf R, Granger DN. Clostridium difficile toxin A-induced microvascular dysfunction: Role of histamine. J Clin Invest 94 (1994) : 1919–1926.

Laine L. Approaches to nonsteroidal anti- inflammatory drug use in the high- risk patient. Gastroenterology 120 (2001) : 594-606.

Langenbach R, Morham SG, Tiano HF,et al. Prostaglandin synthase 1 gene disruption in mice reduces arachidonic acid-induced inflammatory and indomethacin-induced gastric ulceration. Cell 83 (1995) : 483-92.

Langman MJ, Weil J, Wainwright P, Lawson DH, Rawlins MD, Logan RF, Murphy M, Vessey MP, Colin-Jones DG. Risks of bleeding peptic ulcer associated with individual to nonsteroidal anti- inflammatory drugs. Lancet 343 (1994) : 1075-1078.

Langtry HD, Wilde MI. Omeprazole. A review of its use in Helicobacter pylori infection, gastro- oesophageal reflux disease and peptic ulcers induced by nonsteroidal anti- inflammatory drugs. Drugs 56 (1998) : 447-486.

Lee M, Aldred K, Lee E, Feldman M. A. Aspirin-induced acute gastric mucosal injury is a neutrophil-dependent process in rats. Am J Physiol Gastrointest Liver Physiol 263 (1992) : G920-G926.

Lehr HA, Guhlmann A, Nolte D, Keppler D, Messmer K. Leukotrienes as mediators in ischemia-reperfusion injury in a microcirculation model in the hamster. J Clin Inves 87 (1991) : 2036-2041.

Levy M. Aspirin use in patients with major upper gastrointestinal bleeding and peptic-ulcer disease: a report from the Boston Collaborative Drug Surveillance Program, Boston University Medical Center. N Engl J 290 (1974) : 1158-62.

Lichtenberger LM. The hydrophobic barrier properties of gastrointestinal mucus. Annu Rev Physiol 57 (1995) : 565-83.

Lichtenberger LM,Wang ZM, Romero JJ, et al. Non-steroidal anti-inflammatory drugs associate with zwitterionic phospholipids: insight into the mechanism and reversal of NSAIDs- induced gastrointestinal injury. Nat Med 1 (1995) : 154-58.

Ligumsky M, Sestieri M, Karmeli F, Zimmerman J, Okon E, Rachmilewitz D. Rectal administration of nonsteroidal anti-inflammatory drugs. Gastroenterology 98 (1990) : 1245-1249.

Martel-Pelletier J, Lajeunesse D, Reboul P, Pelletier JP. Therapeutic role of dual inhibitors of 5-LOX and COX, selective and non-selective non- steroidal anti-inflammatory drugs. Ann Rheum Dis 62 (2003) : 501-9.

Masferrer JL, Zweifel BS, Colburn SM, Ornberg RL, Salvemini D, Isakson P, Seibert K. The role of cyclooxygenase-2 in inflammation. Am J Ther 2 (1995) : 607-10.

McCafferty DM, Granger DN, Wallace JL. Indomethacin- induced gastric injury and leukocyte adherence in arthritic versus healthy rats. Gastroenterology 109 (1995) : 1173-80.

Mitchell JA, Warner TD. Cyclooxygenase-2: pharmacology,physiology, biochemistry and relevance to NSAID therapy. Br J Pharmacol 128 (1999) : 1121-1132.

Morise Z, Komatsu S, Fuseler JW, Granger DN, Perry M, Issekutz AC, Grisham MB. ICAM-1 and P-selectin expression in a model of NSAID-induced gastropathy. Am J Physiol 274 (1998) : G246-52.

Murakami K, Okajima K, Harada N, Isobe H, Liu W, Johno M, Okabe H. Plaunotol prevents indomethacin-induced gastric mucosal injury in rats by inhibiting neutrophil activation. Aliment Pharmacol Ther 13 (1999) : 521-530.

Panes J, Perry MA, Anderson DC, Manning A, Leone B, et al. Regional differences in constitutive and induced ICAM-1 expression *in vivo*. Am J Physiol 269 (1995) : H1955-64.

Panes J, Granger DN. Leukocyte-endothelial cell interactions: molecular mechanisms and implications in gastrointestinal disease. Gastroenterology 114 (1998) : 1066–1090.

Panés J, Perry M, Granger DN. Leukocyte-endothelial cell adhesion: avenues for therapeutic intervention. Br J Pharmacol 126 (1999) : 537–550.

Patrignani P. Nonsteroidal anti-inflammatory drugs, COX-2 and colorectal cancer. Toxicol Let 112 (2000) : 493-498.

Perry MA, Phillipson M, Holm L. Transmural gradient of leukocyte-endothelial interaction in the rat gastrointestinal tract. Am J physiol Gastrointest Liver Physiol 289 (2005) : G852- G859.

Peskar BM. Role of leukotriene C4 in mucosal damage caused by necrotizing agents and indomethacin in the rat stomach. Gastroenterology 100 (1991) : 619-26.

Peti-Peterdi, J., G. Kovacs, P. Hamar, and L. Rosivall. 1998. Hemodynamics of gastric microcirculation in rats. Am J Physiol Heart Circ Physiol 275 (1998) : 1404-1410.

Pober JS, Bevilacqua MP, Mendrick DL, Lapierre LA, Fiers W, Gimbrone MA Jr. Two distinct monokines, interleukin 1 and tumor necrosis factor, each independently induce biosynthesis and transient expression of the same antigen on the surface of cultured human vascular endothelial cells. J Immunol 136 (1986) : 1680-1687

Pohlman TH, Stanness KA, Beatty PG, Ochs HD, Harlan JM. An endothelial cell surface factor(s) induced in vitro by lipopolysaccharide, interleukin 1, and tumor necrosis factor-alpha increases neutrophil adherence by a CDw18-dependent mechanism. J Immunol 136 (1986) : 4548-4553.

Rainsford KD, Willis C. Relationship of gastric mucosal damage induced in pigs by anti- inflammatory drugs to their effects on prostaglandin production. Dig Dis Sci 27 (1982) : 624-35.

Rainsford KD. Microvascular injury during gastric damage by anti- inflammatory drugs in pigs and rats. Agents Actions 13 (1983) : 457-60.

Rouzer C, Marnett L. Mechanism of free radical oxygenation of polyunsaturated fatty acids by cyclooxygenases. Chem Rev 103 (2003) : 2239-304.

Ruby AJ, Kuttan G, Babu KD, Rajasekharan KN, Kuttan R. Anti- tumour and antioxidant activity of natural curcuminoids. Cancer Lett 94 (1995) : 79-83.

Santucci L, Fiorucci S, Giansanti M, Brunori PM, Di Matteo FM, Morelli A. Penoxifylline prevents indomethacin induced acute gastric mucosal damage in rats: role of tumor necrosis factor alpha. Gut 35 (1994) : 909-15.

Satoskar PR, Shah SJ, Shenoy SG. Evaluation of anti-inflammatory property of curcumin (diferuloyl methane) in pateients with postoperative inflammation. Int J Clin Pharmacol Ther Toxicol 24 (1986) : 651-4.

Schoen RT, Vender RJ. Mechanisms of nonsteroidal anti-inflammatory drug- induced gastric damage. Am J Med 86 (1989) : 449-58.

Shrikant P, Chung IY, Ballestas ME, Benveniste EN. Regulation of intercellular adhesion molecule-1 gene expression by tumor necrosis factor-alpha, interleukin-1, and interferon-gamma in astrocytes. J Neuroimmunol 51 (1994) : 209-220.

Silvoso GR, Ivey KJ, Butt JH, Lockard OO, Holt SD, Sisk C, Baskin WN, Mackercher PA, Hewett J. Incidence of gastric lesion in patients with rheumatic disease on chronic aspirin therapy. Ann Intern Med 91 (1979) : 517-20.

Singh G, Ramey DR, Terry R, Khraishi M, Triadafilopoulos G. NSAID-related effects on the GI tract: an ever widening spectrum. Arthritis Rheum 40 (1997): Suppl: S93.

Singh G. Recent considerations in nonsteroidal anti- inflammatory drug gaastropathy. Am J Med 105 (1998) : 31S- 38S.

Singh G, Triadafilopoulus G. Epidemiology of NSAID-induced GI complications. J Rheumatol 26 (1999) : 18-24.

Singh S, Aggarwal BB. Activation of transcription factor NF-ΚB is suppressed by curcumin (Diferuloylmethane). J Biol Chem 270 (1995) : 24995-5000.

Smith W, DeWitt D, Garavito R. Cyclooxygenases: structural, cellular, and molecular biology. Annu Rev Biochem 69 (2000) : 145-82.

Snehasikta S, Krishnendu G, et al. Curcumin regulates expression and activity of matrix metalloproteinases 9 and 2 during prevention and healing of indomethacin-induced gastric ulcer. JBC 280 (2005) : 9409-9415.

Somboonwong J, Thanamitramanee S, Jariyapongskul A, Patumraj S. Therapeutic effects of *aloe vera* on cutaneous microcirculation and wound healing in second degree burn model in rat. J Med Assoc Thai 83 (2000) : 417-25.

Srimal RC, Dhawan BN. Pharmacology of diferuloyl methane (curcumin), a non-steroidal anti-inflammatory agent. J Pharm Pharamacol 52 (1973) : 519-25.

Sun DC, Roth SH, Mitchell CS, Englund DW. Upper gastrointestinal disease in rheumatoid arthritis. Am J Dig Dis 19 (1974) : 405-10.

Surh YJ. Anti-tumor promoting potential of selected spice ingredients with antioxidative and anti- inflammatory activities: a short review. Food Chem Toxicol 40 (2002) : 1091-1097.

Swarnakar S, Ganguly K, Kundu P, Banerjee A ,Maity P, Sharma AV. Curcumin regulates expression and activity of matrix metalloproteinases 9 and 2 during prevention and healing of indomethacin-induced gastric ulcer. J Biologic Chemistry 280 (2005) : 9409-15.

Tanabe T, Tohnai N. Cyclooxygenase isozymes and their gene structures and expression. Prostaglandin Other Lipid Mediat 68 (2002) : 95-114.

Tartaglia LA, Weber RF, Figari IS, Reynolds C, Palladino MAJ, Goeddel DV. The two different receptors for tumor necrosis factor mediate distinct cellular responses. Proc Natl Acad Sci USA 88 (1991) : 9292-9296.

Thomson, A. B. R., and E. A. Shaffer. 1992 First principles of gastroenterology. In A.B.R. Thomson (ed.), The basis of disease and an approach to management. Canada: University of Toronto Press (1992) : 133-136.

Toda S, Miyase T, Arichi H, et al. Natural antioxidants. III. Antioxidative components isolated from rhizome of Curcuma longa L. Chemic Pharmaceutic Bull 33 (1985) : 1725-8.

Towbin, H., Staehelin, T., and Gordon, J. Electrophoretic transfer of proteins from polyacrylamide gels to nitrocellulose sheets: procedure and some applications. P. Natl. Acad. Sci USA 76(1979) : 4350-4354.

Watanabe T, Higuchi K, Hamaguchi M, Shiba M, Tominaga K, Fujiwara Y, Matsumoto T, Arakawa T. Monocyte chemotactic protein-1 regulates leukocyte recruitment during gastric ulcer recurrence induced by tumor necrosis factor-alpha. Am J Physiol Gastrointest Liver Physiol 287 (2004) : G919-G928.

Tytgat GN. Shortcomings of the first- generation proton pump inhibitors. Eur J Gastroenterol Hepatol 1 (2001) : S29-S33.

Vaananen PM, Keenan CM, Grisham MB, Wallace JL. Pharmacological investigation of the role of leukotrienes in the pathogenesis of experimental NSAID gastropathy. Inflammation 16 (1992) : 227-40.

Van de Stolpe A, Van der Saag PT. Intercellular adhesion molecule-1. J Mol Med 74 (1996) : 13-33.

Vane JR. Inhibition of prostaglandin synthesis as a mechanism of action for aspirin- like drug. Nat New Biol 231 (1971) : 232-35.

Vane JR, Flower RJ, Botting RM. History of aspirin and its mechanism of action. Stroke 21 (1990) : IV-12- IV-23.

Wada K, Kamisaki Y, Kitano M, Kishimoto Y, Nakamoto K, Itoh T. A new gastric ulcer model induced by ischemia-reperfusion in the rat: role of leukocytes on ulceration in rat stomach. Life Sci 59 (1996) : PL295-PL301.

Wahltrom B, Blennow G. A study on the fate of curcumin in the rat. Pharmacol Toxicol 43 (1978) : 86-92.

Wallace JL, Whittle BJR. Role of mucus in the repair of gastric epithelial damage in the rat. Inhibition of epithelial recovery by mucolytic agents. Gastroenterology 91 (1986) : 603-611.

Wallace JL. Gastric resistance to acid: is the mucus-bicarbonate barrier functionally redundant. Am J Physiol 256 (1989) : G31-G38.

Wallace JL, Keenan CM, Granger DN. Gastric ulceration induced by nonsteroidal anti-inflammatory drugs is a neutrophil-dependent process. Am J Physiol 259 (1990) : G462-67.

Wallace JL, Arfors KE, McKnight GW. A monoclonal an-tibody against the CD18 leukocyte adhesion molecule pre-vents indomethacin-induced gastric damage in the rabbit. Gastroenterology 100 (1991): 878-883

Wallace JL, McKnight W, Miyasaka M, Tamatani T, Paulson J, Anderson DC, Granger DN, Kubes P. Role of endothelial adhesion molecules in NSAID-induced gastric mucosal injury. Am J Physiol 265 (1993) : G993-G998.

Wallace JL, Granger DN. The cellular and molecular basis for gastroduodenal mucosal desense. FASEB J 10 (1996) : 731-740.

Wallace JL. Nonsteroidal anti-inflammatory drugs and gastroenteropathy: the second hundred years. Gastroenterology 112 (1997) : 1000-16.

Wallace JL. Nonsteroidal anti- inflammatory drugs and the gastrointestinal tract. Mechanisms of protection and healing: current knowledge and future research. Am J Med 10 (2001) : 19S-23S.

Warner TD, Giluliano F, Vojnovic I, Bukasa A, Mitchell JA, Vane JR. Nonsteroidal drug selectivities for cyclooxygenase-1 rather than cyclooxygenase-2 are associated with human gastrointestinal toxicity: a full *in vivto* analysis. Proc Natl Acad Sci USA 96 (1999) : 7563-7568.

Watanabe T, Arakawa T, Fukuda T, Higuchi K, Kobayashi K. Role of neutrophils in a rat model of gastric ulcer recurrence caused by interleukin-1 beta. Am J Pathol 150 (1997) : 971-979

Whittle BJ. Temporal relationship between cyclooxygenase inhibition, as measured by prostacyclin biosynthesis, and the gastrointestinal damage induced by indomethacin in the rat. Gastroenterology 80 (1981) : 94-98.

Wolfe MM, Soll AH. The physiology of gastric acid secretion. N Engl J Med 319 (1988) : 1707-15.

Xie W, Chipman JG, Robertson DL, Erikson RL, Simmons DL. Expression of a mitogen-responsive gene encoding prostaglandin synthase is regulated by mRNA splicing. Proc Natl Acad Sci USA 88 (1991) : 2692-2696.

Yeon-Joo K, Uri R, et al. Regulation of intracellular cyclooxygenase levels by gene transcription and protein degradation. Prog Lipid Res 46 (2007) : 108-125.

Zimmerman BJ, Holt JW, Paulson JC, Anderson DC, Miyasaka M, Tamatani T, Todd RFR, Rusche JR, Granger DN. Molecular determinants of lipid mediator-induced leukocyte adherence and emigration in rat mesenteric venules. Am J Physiol 266 (1994) : H847–H853.

Zuckerman LA, Pullen L, Miller J. Functional consequences of costimulation by ICAM-1 on IL-2 gene expression and T cell activation. J Immunol 16 (1998) : 3259-3268.

http://www.food-info.net/images/curcumin.jpg [2010, April 11]

http://missinglink.ucsf.edu/lm/IDS_106_UpperGI/Upper%20GI/stomach.htm [2010, April 11]

http://www.mybodyindex.com/m-stomach.php [2010, April 11]

APPENDICES

APPENDIX A

ANOVA

TNF-α

	Sum of Squares	df	Mean Square	F	Sig.
Between Groups	24738.328	2	12369.164	.874	.438
Within Groups	212382.849	15	14158.857		
Total	237121.178	17			

Descriptives

	N	Mean	Std. Deviation	Std. Error	95% Confidence Interval for Mean		Minimum	Maximum
					Lower Bound	Upper Bound		
1	6	73.8500	83.00804	33.88789	-13.2616	160.9616	18.10	181.00
2	6	154.6683	166.03301	67.78269	-19.5726	328.9093	19.60	461.85
3	6	78.4000	89.55041	36.55880	-15.5774	172.3774	20.00	200.00
Total	18	102.3061	118.10294	27.83713	43.5749	161.0373	18.10	461.85

1=Control, 2=NSAIDs, 3=NSAIDs+cur

Test of Homogeneity of Variances

TNF-α

Levene Statistic	df1	df2	Sig.
.792	2	15	.471

Multiple Comparisons

Dependent Variable: TNF-α

	(I) group	(J) group	Mean Difference (I-J)	Std. Error	Sig.	95% Confidence Interval	
						Lower Bound	Upper Bound
LSD	1	2	-80.8183	68.69948	.258	-227.2478	65.6111
		3	-4.5500	68.69948	.948	-150.9795	141.8795
	2	1	80.8183	68.69948	.258	-65.6111	227.2478
		3	76.2683	68.69948	.284	-70.1611	222.6978
	3	1	4.5500	68.69948	.948	-141.8795	150.9795
		2	-76.2683	68.69948	.284	-222.6978	70.1611

1=Control, 2=NSAIDs, 3=NSAIDs+cur

Homogeneous Subsets

TNF-alpha

	Group	N	Subset for alpha = .05
			1
Duncan(a)	1	6	73.8500
	3	6	78.4000
	2	6	154.6683
	Sig.		.282

Means for groups in homogeneous subsets are displayed.

a Uses Harmonic Mean Sample Size = 6.000.

1=Control, 2=NSAIDs, 3=NSAIDs+cur

Descriptives

	Group	N	Mean	Std. Deviation	Std. Error	95% Confidence Interval for Mean		Minimum	Maximum
						Lower Bound	Upper Bound		
ICAM-1	1.00	6	336.9333	224.82710	91.78528	100.9918	572.8749	104.10	545.00
	2.00	6	1106.5167	504.22247	205.84796	577.3676	1635.6657	497.50	1880.00
	3.00	6	413.6600	147.74444	60.31641	258.6117	568.7083	232.50	593.33
	Total	18	619.0367	472.13355	111.28294	384.2502	853.8232	104.10	1880.00

1=Control, 2=NSAIDs, 3=NSAIDs+cur

Test of Homogeneity of Variances

	Levene Statistic	df1	df2	Sig.
ICAM-1	7.256	2	15	.006

ANOVA

		Sum of Squares	df	Mean Square	F	Sig.
ICAM-1	Between Groups	2156391.698	2	1078195.849	9.903	.002
	Within Groups	1633079.736	15	108871.982		
	Total	3789471.434	17			

Multiple Comparisons

Dependent Variable		(I) Group	(J) Group	Mean Difference (I-J)	Std. Error	Sig.	95% Confidence Interval	
							Lower Bound	Upper Bound
ICAM-1	LSD	1.00	2.00	-769.5833(*)	190.50108	.001	-1175.6268	-363.5399
			3.00	-76.7267	190.50108	.693	-482.7701	329.3168
		2.00	1.00	769.5833(*)	190.50108	.001	363.5399	1175.6268
			3.00	692.8567(*)	190.50108	.002	286.8132	1098.9001
		3.00	1.00	76.7267	190.50108	.693	-329.3168	482.7701
			2.00	-692.8567(*)	190.50108	.002	-1098.9001	-286.8132

* The mean difference is significant at the .05 level.

1=Control, 2=NSAIDs, 3=NSAIDs+cur

Homogeneous Subsets

ICAM-1

	Group	N	Subset for alpha = .05	
			1	2
Duncan(a)	1.00	6	336.9333	
	3.00	6	413.6600	
	2.00	6		1106.5167
	Sig.		.693	1.000

Means for groups in homogeneous subsets are displayed.

a Uses Harmonic Mean Sample Size = 6.000.

Oneway

Descriptives

leukocyte adhesion

	N	Mean	Std. Deviation	Std. Error	95% Confidence Interval for Mean		Minimum	Maximum
					Lower Bound	Upper Bound		
1.00	5	1.2000	.83666	.37417	.1611	2.2389	.00	2.00
2.00	5	6.4000	2.30217	1.02956	3.5415	9.2585	4.00	9.00
3.00	4	3.0000	.81650	.40825	1.7008	4.2992	2.00	4.00
Total	14	3.5714	2.70937	.72411	2.0071	5.1358	.00	9.00

1=Control, 2=NSAIDs, 3=NSAIDs+cur

by person who was blinded to the experiment.

	N	Mean	Std. Deviation	Std. Error	95% Confidence Interval for Mean		Minimum	Maximum
					Lower Bound	Upper Bound		
1.00	5	1.6000	1.14018	.50990	.1843	3.0157	.00	3.00
2.00	5	3.8000	1.30384	.58310	2.1811	5.4189	2.00	5.00
3.00	4	1.5000	.57735	.28868	.5813	2.4187	1.00	2.00
Total	14	2.3571	1.49908	.40065	1.4916	3.2227	.00	5.00

1=Control, 2=NSAIDs, 3=NSAIDs+cur

ANOVA

leukocyte adhesion

	Sum of Squares	df	Mean Square	F	Sig.
Between Groups	69.429	2	34.714	14.687	.001
Within Groups	26.000	11	2.364		
Total	95.429	13			

by person who was blinded to the experiment.

	Sum of Squares	df	Mean Square	F	Sig.
Between Groups	16.214	2	8.107	6.860	.012
Within Groups	13.000	11	1.182		
Total	29.214	13			

Post Hoc Tests

Multiple Comparisons

Dependent Variable: leukocyte adhesion

	(I) VAR00001	(J) VAR00001	Mean Difference (I-J)	Std. Error	Sig.	95% Confidence Interval	
						Lower Bound	Upper Bound
LSD	1.00	2.00	-5.2000(*)	.97234	.000	-7.3401	-3.0599
		3.00	-1.8000	1.03133	.109	-4.0699	.4699
	2.00	1.00	5.2000(*)	.97234	.000	3.0599	7.3401
		3.00	3.4000(*)	1.03133	.007	1.1301	5.6699
	3.00	1.00	1.8000	1.03133	.109	-.4699	4.0699
		2.00	-3.4000(*)	1.03133	.007	-5.6699	-1.1301

by person who was blinded to the experiment

	(I) VAR00001	(J) VAR00001	Mean Difference (I-J)	Std. Error	Sig.	95% Confidence Interval	
						Lower Bound	Upper Bound
LSD	1.00	2.00	-2.2000(*)	.68755	.008	-3.7133	-.6867
		3.00	.1000	.72926	.893	-1.5051	1.7051
	2.00	1.00	2.2000(*)	.68755	.008	.6867	3.7133
		3.00	2.3000(*)	.72926	.009	.6949	3.9051
	3.00	1.00	-.1000	.72926	.893	-1.7051	1.5051
		2.00	-2.3000(*)	.72926	.009	-3.9051	-.6949

Correlations

		TNF-α	ICAM-1
TNF-α	Pearson Correlation	1	.124
	Sig. (2-tailed)	.	.624
	N	18	18
ICAM-1	Pearson Correlation	.124	1
	Sig. (2-tailed)	.624	.
	N	18	18

BIOGRAPHY

Miss Sakonwan Chuchuai was born on 2nd May, 1983, in Nakhon Si Thammarat, Thailand. She graduated Bachelor degree of Science in Physical Therapy from Mahidol University, Bangkok, Thailand in 2006.